

AD

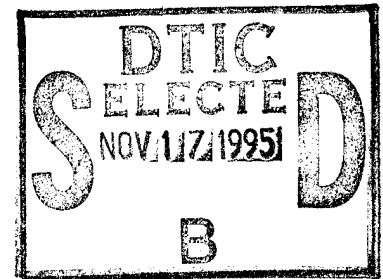
AD-E402 692

Contractor Report ARFSD-CR-95008

## EFFECT OF LONG-TERM STORAGE ON ELECTRONIC DEVICES

Pecht Associates, Inc.  
7027 Hunter Lane  
Hyattsville, MD 20782

Joseph Martinelli  
Project Engineer  
ARDEC



November 1995



US ARMY  
TANK AUTOMOTIVE AND  
ARMAMENTS COMMAND  
ARMAMENT RDE CENTER

### U.S. ARMY ARMAMENT RESEARCH, DEVELOPMENT AND ENGINEERING CENTER

Fire Support Armaments Center

Picatinny Arsenal, New Jersey

Approved for public release; distribution is unlimited.

19951116 001

DTIC QUALITY INSPECTED B

The views, opinions, and/or findings contained in this report are those of the author(s) and should not be construed as an official Department of the Army position, policy, or decision, unless so designated by other documentation.

The citation in this report of the names of commercial firms or commercially available products or services does not constitute official endorsement by or approval of the U.S. Government.

Destroy this report when no longer needed by any method that will prevent disclosure of its contents or reconstruction of the document. Do not return to the originator.

# REPORT DOCUMENTATION PAGE

Form Approved  
OMB No. 0704-0188

Public reporting burden for this collection of information is estimated to average 1 hour per response, including the time for reviewing instructions, searching existing data sources, gathering and maintaining the data needed, and completing and reviewing the collection of information. Send comments regarding this burden estimate or any other aspect of this collection of information, including suggestions for reducing this burden, to Washington Headquarters Services, Directorate for Information Operations and Reports, 1215 Jefferson Davis Highway, Suite 1204, Arlington, VA 22202-4302, and to the Office of Management and Budget, Paperwork Reduction Project (0704-0188), Washington, DC 20503.

<b>1. AGENCY USE ONLY (Leave blank)</b>	<b>2. REPORT DATE</b> November, 1995	<b>3. REPORT TYPE AND DATES COVERED</b> Final Scientific & Technical, 8/93 to 7/95
---	---	---

<b>4. TITLE AND SUBTITLE</b> EFFECT OF LONG TERM-STORAGE ON ELECTRONIC DEVICES	<b>5. FUNDING NUMBERS</b> DAAA21-93-C-0065
---	---

**6. AUTHOR(S)**  
Pecht Associates, Inc.  
Joseph Martinelli, Project Engineer, ARDEC

<b>7. PERFORMING ORGANIZATION NAME(S) AND ADDRESS(ES)</b> Pecht Associates, Inc. ARDEC, FSAC 7027 Hunter Lane Precision Munitions/Mine and Demolitions Division Hyattsville, Md 20782 (AMSTA-AR-FSP) Picatinny Arsenal, NJ 07806-5000	<b>8. PERFORMING ORGANIZATION REPORT NUMBER</b>
---	---

<b>9. SPONSORING/MONITORING AGENCY NAME(S) AND ADDRESS(ES)</b> ARDEC, DOIM Information Research Center (AMSTA-AR-IMC) Picatinny Arsenal, NJ 07806-5000	<b>10. SPONSORING/MONITORING AGENCY REPORT NUMBER</b>  Contractor Report ARFSD-CR-95008
---	--

**11. SUPPLEMENTARY NOTES**

<b>12a. DISTRIBUTION / AVAILABILITY STATEMENT</b>  Approved for public release; distribution is unlimited.	<b>12b. DISTRIBUTION CODE</b>
--	-------------------------------

**13. ABSTRACT (Maximum 200 words)**

This Phase II project identifies physics-of-failure based models for the dominant failure mechanisms in microelectronic packages subject to long-term storage; provides a user-friendly interactive software tool to assess the reliability of infrared (IR) and millimeter wave (MMW) sensors and associated smart munition electronic packages; and, provides a software tool to aid in defining tests for long term reliability and identifying failure mechanisms in electronic packaging methods, technologies, materials and designs.

Through a questionnaire and literature search, failure mechanisms and models were identified. The questionnaire, requesting failure mechanisms, accelerated test and field reliability information for IR and MMW devices, was sent to experts from many organizations. The responses and literature search provided background for the engineering reference text titled, "Long-term Non-operating Reliability of Electronic Devices."

Another part of this project was the development of CADMP-IIe, a software tool which facilitates the physics-of-failure reliability analysis for microcircuits subject to long-term storage. Inputs to the software include geometric, material, and mounting characteristics of the device. Many storage environments are part of the software's environment database. CADMP-IIe can analyze MMW and IR package architectures using failure models and material properties that were added. The software provides a useful design aid to assess storage reliability allowing the user to determine time-to-failure and to rank the dominance of each potential failure mechanism.

<b>14. SUBJECT TERMS</b> Reliability Storage Life cycle failure mechanisms Reliability software Physics of failure	<b>15. NUMBER OF PAGES</b> 123
	<b>16. PRICE CODE</b>

<b>17. SECURITY CLASSIFICATION OF REPORT</b> UNCLASSIFIED	<b>18. SECURITY CLASSIFICATION OF THIS PAGE</b> UNCLASSIFIED	<b>19. SECURITY CLASSIFICATION OF ABSTRACT</b> UNCLASSIFIED	<b>20. LIMITATION OF ABSTRACT</b> SAR
--	---	--	--

# CONTENTS

SUMMARY .....	1
INTRODUCTION .....	2
Motivation .....	2
Prior Work .....	4
Scope of the Present Study .....	5
DEFINING PHYSICS OF FAILURE MODELS .....	7
Questionnaire .....	7
Storage Reliability Reference Book .....	8
CADMP-IIe: PHYSICS-BASED RELIABILITY SOFTWARE .....	9
Introduction .....	9
CADMP-IIe Functionality .....	12
Storage Environments .....	15
IR and MMW Devices .....	41
Failure Mechanisms in CADMP-IIe .....	62
Material Properties .....	79
CADMP-IIe Reliability Analysis .....	85
CONCLUSIONS .....	88
RECOMMENDATIONS .....	89
UNIX-based CADMP-IIe .....	89
Enhance Plastic Encapsulated Microcircuit Capability .....	90
Integrate CADMP-IIe with Higher-level Reliability Tools .....	90
REFERENCES .....	91
APPENDIX A: QUESTIONNAIRE AND RESPONSE SUMMARY .....	95
APPENDIX B: CADMP-IIe MODELS AND ATTRIBUTES .....	115
DISTRIBUTION LIST .....	123

Accession For	
ENIS ORA&I	<input checked="" type="checkbox"/>
DTIC TAB	<input type="checkbox"/>
Unannounced	<input type="checkbox"/>
Justification	
By _____	
Distribution/	
Availability Codes	
Dist	Avail and/or
A-1	Spec

## FIGURES

1 The physics-of-failure process. . . . .	6
2 CADMP-IIe in the design process. . . . .	10
3 Hierarchy and ownership of CADMP-II software. . . . .	12
4 Storage environments in CADMP-IIe . . . . .	19
5 Example parameters of the storage environment . . . . .	20
6 Example descriptive text and reference source for storage environment . . . . .	20
7 Detector mechanisms [Georgia Tech 1994] . . . . .	43
8 Schematic of a typical detector package [Cincinnati] . . . . .	44
9 Detector, cold shield and filter mounting configuration for multiple-element array [Cincinnati] . . . . .	45
10 Monolithic array [Georgia Tech 1994] . . . . .	45
11 Hybrid array [Georgia Tech 1994] . . . . .	46
12 Schematic of a detector Dewar [Georgia Tech] . . . . .	47
13 Schematic cross-section of a Peltier Cooler [Sim 1993] . . . . .	48
14 Effects of degradation on characteristics of a Peltier cooler [Sim 1993] . . . . .	48
15 Dewar design options . . . . .	53
16 Cross sectional view of Dewar . . . . .	53
17 Top view of Dewar . . . . .	54
18 Window (Lid) parameters . . . . .	54
19 Dewar (case) parameters . . . . .	55
20 Two elements, detector and processor die. . . . .	56
21 Defining <b>Stacked on Top of Die</b> attribute . . . . .	56
22 Zoomed-in view showing hybrid FPA stack . . . . .	57
23 Activating and deactivating leads . . . . .	58
24 Three leaded device in the package designer . . . . .	58
25 Metallic can package . . . . .	59
26 Top view of metallic can package . . . . .	59
27 Cross-sectional view of metallic can package . . . . .	60
28 The Gunn diode package . . . . .	60
29 Top view of Gunn diode . . . . .	61
30 Cross-sectional view of Gunn diode package . . . . .	61
31 Cracking of Windows failure mechanism . . . . .	65
32 Comments on Cracking of Windows . . . . .	65
33 User input of window parameters . . . . .	66
34 Window Shatter failure mechanism . . . . .	68
35 Comments on Window Shatter . . . . .	69
36 Dewar Mission Time failure mechanism . . . . .	70
37 Comments on Dewar Mission Time . . . . .	71
38 User input of Dewar parameters . . . . .	72
39 Dewar Outgassing failure mechanism . . . . .	73

## FIGURES (Continued)

40	Comments on Dewar Outgassing	74
41	User input of Dewar parameters	75
42	Flip Chip Solder Fatigue failure model	77
43	Comments on Flip Chip Solder Fatigue	77
44	User input of flip-chip parameters	79
45	Infrared Window Materials	84
46	Cryogenic Materials	84
47	IR Optical Materials (numbered 400 and above)	85
48	Ranked results of the reliability assessment	86
49	Example of the CADMP-IIe derating function	87
50	The Accelerated Test Results window	88

## TABLES

1 CADMP-IIe material types . . . . .	13
2 CADMP-IIe failure mechanisms . . . . .	14
3 Desert, Outdoor environmental parameters . . . . .	21
4 Arctic, Outdoor environmental parameters . . . . .	22
5 Tropical Rainforest, Outdoor environmental parameters. . . . .	23
6 Tropical Marine, Outdoor environmental parameters . . . . .	24
7 Tropical Monsoon, Outdoor environmental parameters . . . . .	25
8 Tropical Monsoon, Outdoor environmental parameters . . . . .	26
9 Hot-humid, Indoor environment parameters . . . . .	27
10 Hot-humid, Outdoor environment parameters . . . . .	28
11 Severe Cold, Indoor environment parameters . . . . .	29
12 Severe Cold, Outdoor environment parameters . . . . .	30
13 Cold, Indoor environmental conditions . . . . .	31
14 Cold, Outdoor environmental conditions . . . . .	32
15 Basic Cold, Indoor environmental parameters . . . . .	33
16 Basic Cold, Outdoor environmental parameters . . . . .	34
17 Basic Hot, Indoor environmental conditions . . . . .	35
18 Basic Hot, Outdoor environmental conditions . . . . .	36
19 Constant High Humidity, Indoor environmental conditions . . . . .	37
20 Constant High Humidity, Outdoor environmental conditions . . . . .	38
21 Variable High Humidity, Indoor environmental conditions . . . . .	39
22 Variable High Humidity, Outdoor environmental conditions . . . . .	40
23 Density and Young's modulus data for selected mirror blank materials . . . . .	50
24 Crack growth exponent and coefficient for ZnSe and ZnS . . . . .	64

## SUMMARY

A scientifically based understanding of the effect of environmental stresses on electronics allows effective design trade-offs, accelerated test tailoring, shelf life determination and root cause failure analysis. This methodology, known as the physics-of-failure (PoF) approach, is gaining an increased acceptance by the military and electronics industry. This Phase II SBIR final report discusses the theory, development, and use of a physics-of-failure based software tool, CADMP-IIe, that assesses the long-term storage reliability of microelectronic devices and packaging.

The specific objectives of this project were to:

- Define physics-of-failure based models for the dominant failure mechanisms in microelectronic packages subject to long term storage.
- Modify the University of Maryland CADMP-II software tool to allow storage reliability assessment of infrared (IR) and millimeter wave (MMW) devices, and associated smart munition electronic packages.
- Provide a software tool to aid in defining tests for long term reliability, and to point out potential failure mechanisms in the electronic packaging methods, technologies, materials, and designs.

The effort to identify failure mechanisms and PoF models consisted of questionnaires, conversations with industrial experts, and a literature search. A questionnaire requesting failure mechanisms, accelerated test and field reliability information for IR and MMW devices, was developed and sent to experts from a variety of organizations: device suppliers, systems houses, major contractors, universities, and government agencies. The responses, conversations with respondents, and literature search provided background for the engineering reference book titled, "Long-term Non-operating Reliability of Electronic Devices," CRC Press, Boca Raton, Florida, 1995. This book provides a documented investigation into the area of electronic storage reliability, and outlines key electrical, corrosion, radiation and mechanical failure mechanisms.

The second objective of this project was the development of CADMP-IIe software that addresses storage environments with an emphasis on IR and MMW device architectures, failure mechanism models, and material properties. First, a storage environment library was added to the software database. Each storage environment includes the necessary model inputs: maximum, minimum, and average temperature; magnitude and number of temperature cycles per year; maximum, minimum and average relative humidity. Next, IR and MMW package architectures were added to CADMP-IIe, including: infrared Dewar, hybrid focal plane array, beam lead diodes, three leaded devices, metal cans, and Gunn diodes. Failure mechanism models were then included to accommodate the new packages and failure sites, such as: window and filter shattering, stress corrosion cracking of windows, fatigue of flip-chip hybrid detector bumps, Dewar heat leakage, and Dewar outgassing. New materials and material properties were then collected and assembled in the CADMP-IIe database to support the modeling of IR and MMW



devices; including materials for IR windows, cryogenics, IR detectors and microwave monolithic integrated circuits.

CADMP-IIe fills an important role in the design process. With the software, a package designer or system engineer has a tool with which to quantitatively optimize storage (as well as operational) reliability, perform design trade-offs, and design accelerated tests. The software allows the capability to:

- Evaluate reliability in terms of average time-to-failure,
- Analyze and rank each failure mechanism, and
- Highlight the dominant failure mechanisms.

In order to further enhance CADMP-IIe, three items would make the software even more valuable to the packaging design community: first, the development of a UNIX version; second, the addition of capability for plastic encapsulated microcircuits reliability assessment, and finally, the development and integration of a similar set of board and assembly-level reliability tools.

## INTRODUCTION

The present study, Phase II of the "Effects of Long-term Storage on Electronic Devices" project sponsored by the U.S. Army ARDEC, deals with the effects of long-term storage on smart munition electronics. This section discusses the motivation for this project, provides an overview of prior work in storage reliability, and outlines the project scope.

### Motivation

Dependable smart weapon systems are critical to the U.S. Military. Weapons systems rely increasingly on electronics for sensing, signal processing, and control and will often be stored for long periods of time in uncontrolled environments. Indeed, the reliability of these often complex electrical systems will, to a large extent, determine the ultimate success of the weaponry.

The life-cycle environment of smart munition electronics is unique from all other major electronics applications. In a study of industrial, automotive and consumer products, Harris [1980] found that the usage rate of most equipment was generally less than 25%. Even the equipment with the lowest usage, built-in test for military equipment, was used an estimated 1% of the time. With the long storage durations (up to 20 years) and comparatively short operating life (minutes), the usage rate of munitions would be in the parts per million range.

Although the non-operational storage condition might seem benign, since there are no thermal gradients from internal device self heating, the environmental stresses on the equipment can actually be harsh. Weapons systems can experience the extreme climates of the world: from polar wastelands to tropical deserts. Storage environments are usually thermally uncontrolled and can be unsheltered. Thermomechanical loads arise from the diurnal temperature cycle and solar radiation. Corrosive stresses are induced from high ambient humidity. During storage, electrostatic and radiation sources can also have an adverse impact on electronic life.

How well electronics survive the environment stresses depends on a number of design and processing attributes, such as: material properties, material interfaces, design geometries, and device defects. The study of the electronics failure has been pursued vigorously in the last several decades by many scientists and organizations. Through empirical test and sophisticated analysis, detailed models have been developed which quantitatively estimate time-to-failure under different environmental conditions. These models form the growing basis for understanding the effect of environmental stresses on electronics failure modes and mechanisms. The application of this knowledge is important throughout the electronics life cycle. Known as the Physics-of-Failure (PoF) approach, this method of optimizing reliability early in the design process is gaining increased acceptance by the military and electronics industry.

Through initial funding from the U.S. Army, the University of Maryland's CALCE Electronic Packaging Research Center developed a software tool which helps automate the PoF process for electronic devices. The software is called Computer Aided Design of Microelectronic Packages, CADMP-II. CADMP-II organizes the many available reliability models to allow effective design trade-offs, accelerated test tailoring, shelf life determination and root cause failure analysis. It also provides a comprehensive database structure of material properties, environments, and accelerated tests/screens to support the reliability assessment.

Tremendous recurring and non-recurring cost savings can be realized by addressing reliability early in the design process. Because of the variety of design options, environmental requirements, and high performance of smart munitions systems, computer simulation is the best way to cost effectively optimize designs. One study [Dataquest Inc. 1990] showed that the concept definition and design account for only 5 to 8 percent of the nonrecurring cost of product development. During this stage, however, 60 to 80% of product cost is committed. Accurate software simulations can provide timely information early in the design process.

Large savings have also been realized by extending the shelf-life of munitions systems beyond what was originally specified. The rated shelf life is similar to a product's expiration date. When the shelf life date passes, the weapon can no longer be used and must be destroyed. The Patriot Missile realized some \$2.4 billion in cost avoidance by extending

Large savings have also been realized by extending the shelf-life of munitions systems beyond what was originally specified. The rated shelf life is similar to a product's expiration date. When the shelf life date passes, the weapon can no longer be used and must be destroyed. The Patriot Missile realized some \$2.4 billion in cost avoidance by extending shelf life from five years to ten years [Howard 1994]. In order to justify shelf-life extension, reliability assessments had to be performed for the storage environment.

## **Prior Work**

Through the last several decades, a number of DoD-sponsored projects have studied electronics storage reliability. Generally these have taken a data collection approach from supplier's accelerated life tests and some field storage experience. Any reliability predictions which are performed typically employ probabilistic models based on steady state temperatures and assume a constant failure rate. Although there is a fair amount of data for general electronics, most investigators indicated difficulty in obtaining substantial data for more specialized devices that have limited field history.

Coit and Priore [1985] gathered storage data for existing equipment and developed probabilistic models for storage reliability on a component level. The result was published as RADCw-TR-85-91 which predicts storage reliability similar to the way MIL-HDBK-217 predicts operational reliability. The device models were classified by technology and type. Part level data from many sources was used. Although device failures were separated from system maintenance actions, the root cause of individual failures was not generally available. Probabilistic models are typically based on the Arrhenius equation with multipliers or  $\pi$  factors which generalize attributes such as an environment factor, non-operating quality. The only direct environment input to the models is steady state temperature; the important attributes of temperature cycling and humidity are not included. Unlike the physics-of-failure approach, specific design attributes like die size, material properties of the die, package, and interconnects are not directly included in the probabilistic models.

The RADC models used an exponential failure distribution to predict mean-time-to-failure. The assumption that all storage failures are exponentially distributed is not valid for many failure mechanisms such as thermomechanical fatigue or device leakage. A thermomechanical wearout mechanism such as interconnect fatigue has been shown to follow a Weibull distribution; the failure rate increases with time.

The "K" factor approach assumes that the failure rate in the storage environment is directly proportional to that of the operating environment. The ratio of operating failure rate to non-operational failure rate, K, has been as low as 10 to 1 and as high as 80 to 1. [Harris 1980] Because of the large differences between operational and non-operational stresses, these are not, in fact, proportional. The K factor technique is only a crude approximation that has little physical basis.

Two studies [Ailles 1989; Melmed 1990] focused more specifically on infrared and millimeter wave electronics. These provide a good overview of the variety of electronic devices in smart munitions. Some failure mechanisms are included that qualitatively describe the types of electronics deterioration in storage. Electrical parametric test data was provided for a few devices and some assemblies. Both studies expressed difficulty in obtaining information on more specialized electronics such as infrared sensors and millimeter wave devices. Ailles [1989] performed some reliability prediction based on probabilistic methods and steady state temperature.

The need for understanding the interaction between electronics design and environment is widely recognized. Ailles [1989] highlighted the importance of a “thorough understanding of failure modes and mechanisms. Only by thoroughly understanding their strengths and weaknesses can a designer properly weigh alternatives for a given application.”

The physics-based approach considers each root cause of failure separately and uses models to quantitatively determine time-to-failure. Physics-of-failure is a methodology to assess the reliability of an electronic package based on failure mechanisms, failure sites, design geometry, material properties, and the application environment [Cushing 1993,1994]. Figure 1 shows that the reliability assessment is based on operational loads, environmental loads, and the product materials, geometry and architecture. Reliability analysis is performed on thermal and stress gradients of the product and determines a time-to-failure for each failure mechanism. Detailed sensitivity analysis can be performed which provides a function of product life to various design and environmental parameters.

### **Scope of the Present Study**

The purpose of this project is to provide a methodology, associated software tool and documentation to aid in assessing long term (storage) reliability, in terms of potential failure mechanisms in packages with a focus on infrared sensors and millimeter wave devices, and associated smart munition electronic packages.

The Statement of Work defines the project's three main tasks as follows:

1. Define physics-of-failure based models.
2. Develop software for storage reliability modeling and assessment.
3. Deliver software and final report.

### **Define Physics-of-Failure Based Models**

A literature search was conducted to define failure mechanisms associated with the critical electronics located in Infrared (IR) and Millimeter Wave (MMW) sensors, and associated smart munition electronics. Some findings of the Phase I effort were updated.

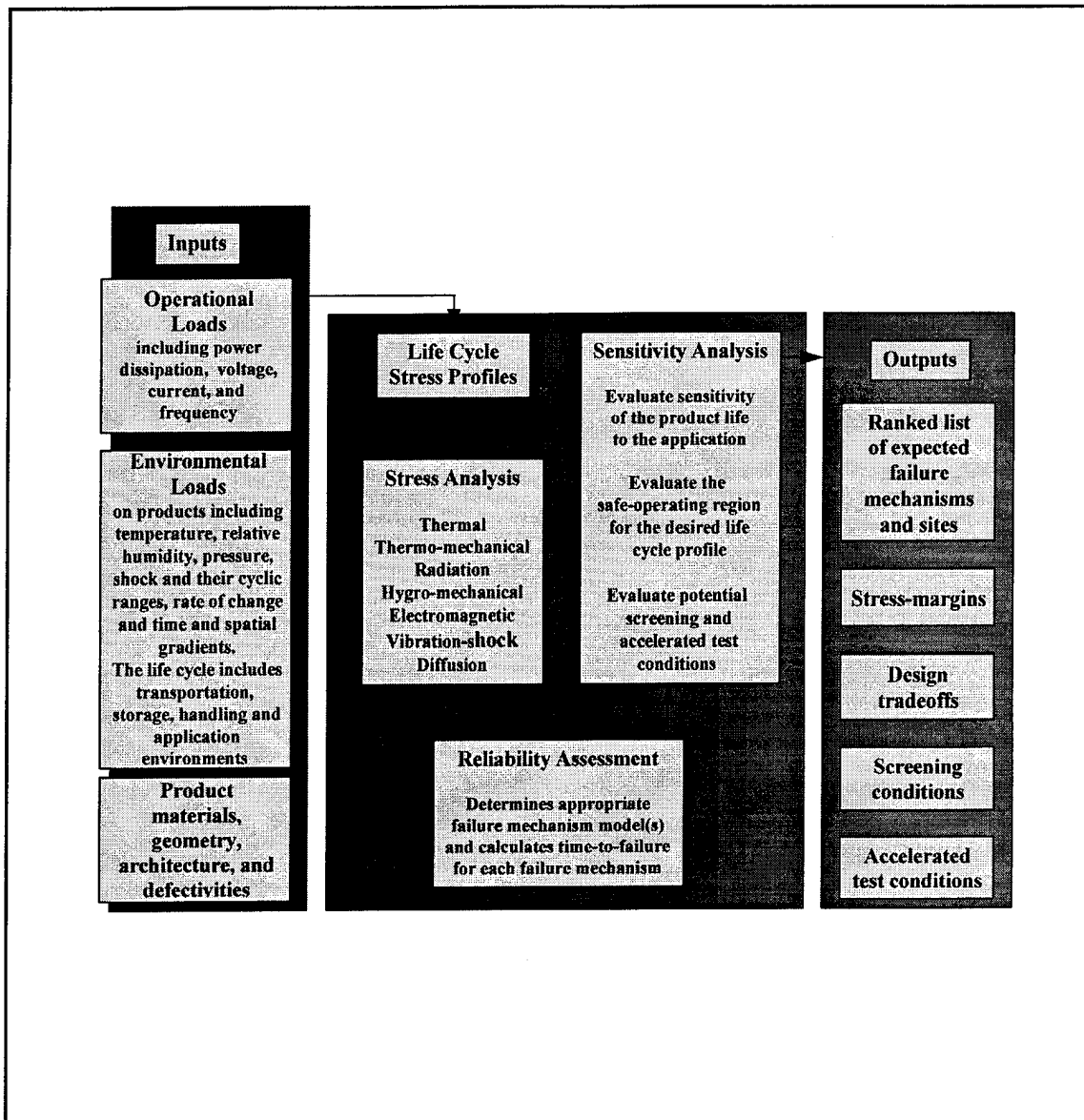


Figure 1 The physics-of-failure process.

### Develop Software for Storage Reliability Modeling and Assessment

Pecht Associates enhanced the Army funded CADMP-II software to include long term storage reliability models and assessment software. The enhanced CADMP-II (called CADMP-IIe) software can be used to aid in assessing storage reliability and to point out potential failure mechanisms associated with packaging methods, mounting methods, new technologies, materials and designs with a focus on IR, MMW and associated smart munition electronics. Input(s) to the software include geometric, material and mounting characteristics of the devices. The following sites in the package can be assessed; circuitry on die, die, die

attach, circuitry on substrate, substrate, substrate attach, interconnections, case lid, lid seal, lead, and lead seal. The software is developed to run on IBM compatible personal computers. The user is not required to manipulate the equations.

In this report and in the software, Pecht Associates provides information on:

- Unique material data known to Pecht Associates.
- Failure mechanism models under various storage conditions (for components, packaging methods, mounting methods and design layouts).
- Associated stress conditions.

The software provides:

- Failure mechanisms to address storage reliability, including description, validation methods, assumptions, and all references.
- The capability to evaluate reliability in terms of average time-to-failure.
- Prediction of the time a first failure would occur.
- Analysis and ranking for each potential failure mechanism.
- Highlighting of dominant failure mechanisms.

### **Deliver Software and Final Report**

The deliverables of the project include this final report, the book on storage reliability, findings for IR, MMW and associated smart munition electronics, software, and software documentation. A complete listing of the source code developed by Pecht Associates is provided with the software and documentation.

## **DEFINING PHYSICS OF FAILURE MODELS**

A variety of techniques were used to define physics-of-failure based reliability models and storage reliability data for IR and MMW devices, these included: literature search, questionnaire to experts, and telephone conversations with device suppliers and contractors. During the course of this research, a reference text was developed called, "Long-term Non-operating Reliability of Electronic Devices."

### **Questionnaire**

Besides a literature search, it was desired to tap the body of unpublished knowledge addressing the issue of non-operational reliability in general, and IR and MMW electronics in particular. Hence, a questionnaire was formulated and sent to experts in the field in order to obtain their opinion and "first hand" knowledge on this topic. The main aim of the

questionnaire was to obtain information about failure mechanisms in non-operational electronics and specific failure mechanism models.

The questionnaire was prepared in consultation with the U.S. Army ARDEC at Picatinny Arsenal, NJ. A cover letter signed by the Chief, Electronics and Producibility Branch at ARDEC accompanied the questionnaire. It was sent to some 83 IR and MMW experts from a variety of organizations: device suppliers, systems houses, major contractors, universities, and government agencies. The questionnaire requested failure mechanisms, accelerated test and field reliability information for IR and MMW devices.

In the questionnaire, a list of IR, MMW and signal processing electronics was provided, and the respondents were asked to check those components that they were familiar with or that their organizations manufacture, test, or utilize.

Other questions were:

- Have you conducted reliability assessment (operational or storage) on any of these components? If yes, please circle the relevant components and provide details and results of the assessment and any data obtained.
- In your opinion what are the predominant failure mechanisms in these components under long-term storage conditions? Also, please mention any failure mechanism models that you might be aware of.

Most of the questionnaire's responses suggested that operational or storage reliability assessment is not routinely done on the device level. No new parametric models were obtained as a result of the questionnaire. Some failures mechanisms which were thought to be prominent in storage were moisture leakage in hermetic packages and IR detectors, solid state diffusion, loss of memory in EPROM devices, and various assembly related defects. While there is no known model describing the loss of memory in EPROM devices, models for metallization corrosion due to hermetic package leakage, stress-driven diffusive voiding, excessive intermetallics, and element fracturing based on initial defects are included in CADMP-IIe. The questionnaire and summarized results are included as Appendix A.

### **Storage Reliability Reference Book**

As a result of the research of this project, Pecht Associates developed a reference text titled, "Long-term Non-operating Reliability of Electronic Devices." [Pecht 1995] The book reviews non-operating electronics reliability issues, storage conditions and environmental stresses, and the failure mechanisms that cause device failure.

The text discusses the storage environment and the impact that geography and climate can have on electronics. The two main approaches to reliability assessment, probabilistic and physics-based, are detailed.

Four types of storage failure mechanisms: electrical, corrosion, radiation and mechanical are discussed in the book. Electrical failure mechanisms which occur under storage conditions are electrostatic discharge and contamination induced parameter degradation. The cause and effects of different corrosion mechanisms are explained. Radiation stresses degrade electronics both mechanically and electrically. Mechanical stresses in non-operating environments are generally thermally induced by temperature cycling or high steady state temperatures. Examples are fatigue failure, intermetallic formation, and cracking of packages. Several examples of failures in specific components are discussed which include general packaging and MMW and IR components. The kind of testing which can be used to help assure reliability in storage is discussed, and a framework for implementing a physics-based approach to storage reliability is outlined.

## **CADMP-IIe: PHYSICS-BASED RELIABILITY SOFTWARE**

The enhanced version of Computer-aided Design of Microelectronic Packages (CADMP-IIe) software implements a physics-of-failure reliability assessment methodology for microelectronic devices. CADMP-IIe organizes the many failure mechanisms currently available from literature and handbooks. It provides the design or system engineer with the ability to quickly and systematically assess microelectronic device, package and interconnection reliability. The software has the capability to analyze not only single-chip packages but also hybrids and multichip modules.

The CADMP-IIe tool includes not only the more common package architectures (e.g. DIPs, PGAs, PQFPs) but also more specialized packages used for IR sensors and MMW devices (e.g. Dewars, Focal Plane Arrays and Gunn Diodes). Many failure mechanisms, materials and material properties have been added to support the IR and MMW package architectures.

### **Introduction**

This section provides a general overview of the software tool, its modules and functionality. While not intended to replace the CADMP-IIe Reference Manual, this section provides the reader with a basic software understanding needed for later sections of this report.



CADMP-IIe fills a unique and important role in the design of microelectronic packages. Figure 2 outlines the relationship to other activities in the design process. CADMP-IIe fills a niche not addressed by commercially available microelectronic design tools. Because the geometric data required to create and layout a package in CADMP-IIe is simple for the user to input, complicated interfacing to the package layout tools is not usually necessary.

The inputs to the stress analysis and reliability assessment tool include the environment, test/screen, failure model and materials libraries and package modeler. The

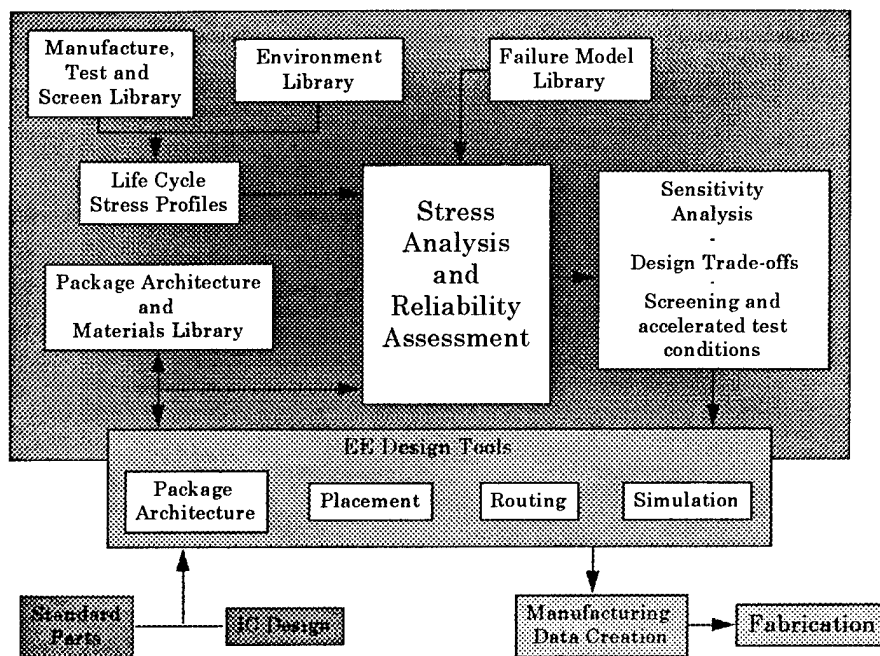


**Figure 2** CADMP-IIe in the design process.

stress analysis includes a thermal analysis to simulate thermal stresses on an operating device. Reliability assessment performs calculations of the selected failure mechanisms and ranks those mechanisms in terms of time-to-failure. The analysis of sensitivity of models with individual design attributes or material properties can be calculated for each failure mechanism. An important function of the tool is to determine effective screening and accelerated test conditions which target particular defects or key failure mechanisms.

The hardware requirements for CADMP-IIe are:

- 386™ or 486™ personal computer running DOS 3.3 or later
- Minimum 20 MB hard drive space on single partition
- VGA Graphics
- Math Co-processor
- Mouse (highly recommended)
- Minimum 580 KB free RAM

The software provides detailed text reports which highlight the dominant failure mechanisms and rank the failure mechanisms according to time-to-failure. Presentation quality graphics reports can be obtained via a screen capture program.

The CADMP tool is analogous to a finite element package such as Patran or ANSYS. To efficiently automate the code for similar problems, input files and macros are often written in its high level, parametric design language. Material properties are also researched and added to a common library. Once the finite element packages are tailored to specific problems, similar problems can be more easily solved by others.

The software development hierarchy is illustrated in Figure 3. CADMP-IIe has been tailored by Pecht Associates, Inc. to allow it to address the unique problems of IR and MMW electronics and storage reliability in general. This includes the storage environments, failure mechanisms and package architectures appropriate to IR and millimeter wave technology. CADMP-IIe provides the packaging engineer a way to easily define the design and analysis parameters, and conduct the desired reliability analyses. The software is documented with the CADMP-IIe Reference Manual. The CADMP-IIe software tutorial includes a step-by-step example of how the software can be used to model an Infrared Dewar Package.

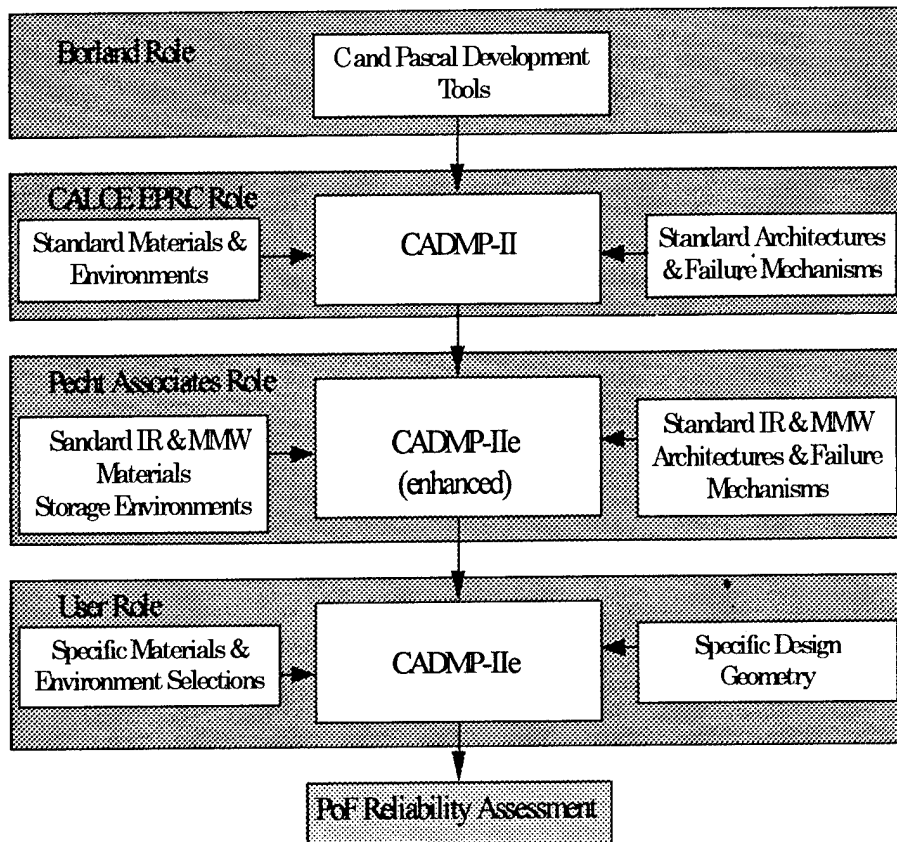


**Figure 3** Hierarchy and ownership of CADMP-II software.

### **CADMP-IIe Functionality**

This section provides a general overview of the key software modules. More detailed information can be found in the CADMP-IIe Reference Manual. CADMP-IIe accesses commands and pull-down menus via hot-keys or the mouse. The user is not required to use a programming language or manipulate equations. The system executive screen is the gateway to CADMP-IIe's six major menu options:

- Parts: Activates and manages the projects.
- Model: Defines package design and interconnects and mission profiles.
- Analyze: Selects analysis and defines model parameters.
- Libraries: Allows editing the materials, environment, and failure mechanism libraries.
- Display: Allows creation of reports and viewing thermal results.

- Options: Manages directories, menu modifications, and report printing.

Most of the software's technical functionality is found in the Libraries, Model, and Analyze options. The important functions of these options are described below.

### **Libraries Option**

As shown in Figure 2, the libraries are a fundamental input for the stress analysis and reliability assessment. The library option allows the user to view and edit data in CADMP-IIe's Materials, Environments, Test/Screen, Power Spectral Density (PSD) Curve, and Failure Mechanism libraries, as well as to access the library Report Manager. Within each library is a text field which provides the reference source of the information.

The Materials Library contains material properties from a variety of sources. Table 1 shows the variety of material classifications which are available. Within each classification are many specific material and properties. Pecht Associates has added new properties and many new materials associated with infrared and millimeter wave devices and packaging. The basic properties supplied with CADMP-IIe cannot be edited, although new materials can be added by the user. Viewing and adding the material properties utilizes a familiar spreadsheet format. Because many material properties are functions of environment parameters, the library has the capability to store these dependencies. Temperature, frequency, moisture, and strain-rate are some of the available dependency options.

**Table 1 CADMP-IIe material types**

Attach Materials	Package Materials
Bond Pad Material	PWB Materials
Conformal Coating Materials	Rad. Contam. Mat.
Flip Chip materials	Resistor Materials
Fluid Materials	Semiconductor Materials
Lead Materials	Solder Materials
Lead Seal materials	Substrate Materials
Lid Materials	TAB Materials
Lid Seal Materials	Window Materials
Metallization Materials	Wire Materials

The CADMP-IIe environment library contains Indoor Storage, Outdoor Storage, Transportation and Usage classifications. Under the Phase II contract, Pecht Associates has added many environments to the Indoor and Outdoor Storage. The details of the specific environments are described in Section 4.3.

The Test/Stress Library is a compilation of common test/stress conditions. Failure mechanisms can be evaluated with these just as with the environments to determine the

expected life in a accelerated test or screening condition. A wide variety of test types are included: temperature, pressure, vibration, humidity, and electrostatic discharge. Within each test condition key parameters can be viewed and edited.

The Failure Mechanisms Library contains the model and required constants, factors, and submodels for each failure mechanism. With the library, the models can be viewed, created, and edited. A pop-up screen containing the descriptions of each models' parameters can be viewed. The source, assumptions, limitations, and validation histories for each model are also available in the Failure Mechanism Library. Table 2 lists the many failure mechanisms available in CADMP-IIe.

**Table 2** CADMP-IIe failure mechanisms

Cracking of Windows	Modular Case Fatigue
Dewar Heat Leakage	Modular Case Fracture
Dewar Outgassing	Stress Driven Diffusive Voiding (SDDV)
Die Attach Fatigue	Slow Trapping
Die Fracture	Substrate Attach Fatigue
Electromigration	Substrate Fracture
Electrostatic Discharge	Time Dependent Dielectric Breakdown
Excessive Intermetallics	(TDDB)
Flip Chip Solder Fatigue	TAB Corrosion
Lead Seal Fracture	TAB Fatigue
Lead Solder Joint Fatigue	Window Shatter
Lid Seal Fracture	Wire Bond Fatigue
Metallization Corrosion	Wire Fatigue

### Model Option

The Model Option menu contains two entries, Profile and Package. The Profile module allows the definition of a mission profile. Specific environments are selected from the environmental or test/screen libraries. The duration of each environment is defined as they are sequenced together to completely describe the stress loads of a device. For smart munitions, the long term storage environment represents a significant part of the total profile.

Through the Package Designer, the user defines the design constraints and attributes of the microelectronic device. The Package designer has an active graphics display, showing the user geometric and placement changes as the design progresses. The attributes are defined for each item of the package: the element, element attach, substrate, substrate attach, leads, lid, case, and interconnects.

## **Analyze Option**

With the Analyze option, the user can launch the thermal, reliability, derating or testing analytical tools. The thermal analysis employs a finite difference analysis technique to model the operating device. The user defines boundary conditions through a simple graphic interface and receives temperature contour plots which can be saved or screen captured. The results of the thermal analysis are passed to the reliability assessment module. (Note: the thermal module is not required for a storage reliability assessment.)

The Reliability analysis identifies the dominant failure mechanisms of the microelectronic circuit. From this information, the designer can make adjustments to the package or environments to optimize the design. The user selects reliability models from a pick-list; those models which have been sufficiently defined and relevant (i.e. which have all required attributes for the calculation) are highlighted and may be selected. Reliability is quantified in terms of a mean-time-to-failure for each selected failure mechanism.

The Derating analysis enables the evaluation of the stress margin in terms of any design or environment attribute. The stress margin is usually the ratio of the actual stress load against the rated strength. The derating tool allows the designer to optimize the margin-of-safety of critical design parameters. Any package, material, or environment attribute can be plotted with respect to the stress margin or any other attribute.

The purpose of the Testing option is to evaluate the effectiveness of accelerated tests. The tool enables the user to simulate an accelerated test by choosing the test duration and having the software find the test conditions. The failure mechanism models are linked to specific environmental stresses. Failure modes or stresses can also be selected by the designer, and a sensitivity analysis can be performed on design, material, or environment attributes. Combining multiple mechanisms in this analysis will show the user which are the most critical and will cause the device to fail first.

## **Storage Environments**

Storage climatic conditions are broadly classified as desert, tropical, polar and temperate. Various environmental storage conditions have been input into the CADMP-IIe software to facilitate storage reliability assessment of electronics. Information from these storage conditions is used to create an electronics mission profile which is accessed by the software's failure mechanism models. An effort has been made to include probable storage profiles in various parts of the world. Following each profile is a brief description of the geographical locations where these profiles are most likely to be seen.

## **Desert Climates**

Deserts typically have very high temperatures (up to 50°C) and moderate relative humidities (less than 30%). Because the air has such low moisture, corrosion is not a dominant failure mechanism. Solar radiation is intense. One study [Australian Ordnance Council 1983] showed that solar radiation could increase the environmental temperature by as much as 30°C. Thus, within an electronic package the temperature could reach 70°C. Due to solar radiation, complex temperature gradients could be present within the device. This, combined with up to 20°C daily temperature changes, could cause thermomechanical fatigue, rupturing of seals, and warping of assemblies.

Materials degradation can be caused by a number of effects. Sealant viscosities are lowered, and wind-blown sand can cause surface erosion and pitting. Elastomers and plastics can warp due to very low air moisture or disintegrate from intense ultraviolet rays [Jowett 1973].

## **Tropical Climates**

Humidity and moisture has been reported as being the single most important factor in an electronics storage environment [Ailles 1989]. The heat and humidity of the tropical regions is certainly a dominant factor in long-term storage reliability. Rychtera [1963] observes that some 26 percent of the earth's land area is considered tropical; of this, 16 percent has humid and 10 percent has semi-humid conditions. Relative humidity in these areas range from 75% to 100%. The temperatures can be as high as 31°C to 41°C; although, the most extreme temperature conditions are accompanied by lower relative humidities. The daily temperature cycle can often be 20°C due to intense solar radiation and cold night-time temperatures. The cool nights cause moisture condensation inside and outside the equipment which together with ionic contamination can cause corrosive cells. Insulating materials can absorb moisture which reduces surface and volume resistivity, eventually leading to dielectric breakdown. Moisture can also cause mechanical defects through material swelling and delaminating.

Because tropical regions have frequent rain, growing conditions are ideal for fungi, insects and microorganisms. Bacterial growth and fungi can be very detrimental to electronic packaging; these feed on many kinds of organic materials. The fungus can provide a path for current leakage [Jowett 1973].

## **Polar Climates**

Polar regions are characterized by below-zero temperatures; at night, these can be as low as  $-45^{\circ}\text{C}$ . Because these regions are usually at the most extreme latitudes, the daily magnitude and duration of solar radiation is small. Such extreme low temperatures can significantly alter the properties of common electronic packaging materials. Daily temperature cycles of  $20^{\circ}\text{C}$  are frequent in the fall and spring. Not only can materials used in electronics packaging and assemblies can have significant coefficient of thermal expansion mismatch, but they can have significant residual stresses due to processing and curing at much higher temperatures. The low temperature swings can be very damaging from overstress and fatigue mechanisms.

Moisture condensation combined with freezing can be hazardous to electronics. Water in some polar regions can be acidic and corrosive. At near-zero temperatures, tin-plated finishes can form whisker growth called 'tin pest' which can lead to short circuits.

## **Temperate Climates**

Europe and North America comprises the temperate zone. These regions can have mild summers and somewhat harsh winters. The mean winter temperature of temperate regions ranges from  $-5$  to  $15^{\circ}\text{C}$ . In the summer, the mean temperatures are  $15$  to  $25^{\circ}\text{C}$  [Rychtera, 1963]. The environmental stress associated with long term electronics storage in temperate conditions is much less than in the desert, tropical, and polar regions.

## **CADMP-IIe Environment Definition**

The following definitions are used by CADMP-IIe for the parameter entry fields.

**Min. Temperature:** The minimum temperature ( $^{\circ}\text{C}$ ) that occurs in the environment. The range for this field is  $-55$  to  $125^{\circ}\text{C}$ .

**Max. Temperature:** The maximum temperature ( $^{\circ}\text{C}$ ) that occurs in the environment. The range for this field is  $-55$  to  $125^{\circ}\text{C}$ .

**Avg. Temperature:** The environment's average temperature. It is used as the ambient temperature by the CADMP-IIe programs that perform calculations concerning temperature cycling loads. The range for this field is  $-55$  to  $125^{\circ}\text{C}$ .

**Temperature Cycle:** The environment's average temperature variation. The CADMP-IIe fatigue analysis programs that determine time-to-failure use this field. The range for this field is  $0$  to  $180^{\circ}\text{C}$ .



**Temp. Cycles per Year:** The number of temperature cycles that the environment undergoes in a year. The range for this field is 0 to 10,000 cycles.

**Dwell Time:** The number of minutes the temperature will remain at the minimum and maximum temperature of the temperature cycle.

**Min. Relative Humidity:** The minimum relative humidity that occurs in the environment. The range for this field is 0 to 100%.

**Max. Relative Humidity:** The maximum relative humidity that occurs in the environment. The range for this field is 0 to 100%.

**Avg. Relative Humidity:** The average relative humidity (RH) that occurs in the environment. The range for this field is 0 to 100%.

**RH cycle:** The average variation of relative humidity in the environment.

**RH Cycles/Year:** The number of RH cycles the environment undergoes during a year. The range for this field is 0 to 10,000 cycles.

**Vibration Mode:** The vibration mode the component assembly is exposed to (Random, Harmonic or Shock). For storage environments this field is set to NONE.

**Acceleration PSD (APSD):** The maximum power spectral density applied to the package.

**Maximum G:** The maximum acceleration applied to the package. Used to define both the harmonic and shock loadings. The range for this field is 1-10,000 and it is expressed in dimensions of Gs.

**Excitation frequency:** Frequency of excitation for sinusoidal vibrations. The range for this field is 1 to 10,000 Hz.

**Wave Form:** The shape of the shock wave used to excite the package for shock loading. The wave form shapes can be half-sine, unit impulse, ramp step, decreasing exponential, terminal sawtooth, step ramp, increasing exponential or cosine step.

**The time of the pulse:** The duration in seconds of the shock load. The range of this field is 1e-4 to 1 second.

**Maximum Acceleration:** The maximum acceleration applied in dimensionless Gs to the package. The range for this field is 1 to 10,000Gs.

**Wind:** a qualitative assessment of the wind intensity in a region. Allowable entries are HIGH, MEDIUM, LOW, and N/A.

**Rain/Snow:** a qualitative assessment of the precipitation in a region. Allowable entries are HIGH, MEDIUM, LOW, and N/A.

**Sand/Dust:** a qualitative assessment of the air-borne sand and dust in a region. Allowable entries are HIGH, MEDIUM, LOW, and N/A.

**Salt Spray:** a qualitative assessment of the air-borne salt spray in a region. Allowable entries are HIGH, MEDIUM, LOW, and N/A.

**Solar Radiation:** a qualitative assessment of the solar radiation intensity in a region. Allowable entries are HIGH, MEDIUM, LOW, and N/A.

### CADMP-IIe Storage Environments

Figure 4 shows a listing of the storage environments available in the environment library. The parameters of the CADMP-IIe software are in Figure 5. Each storage environment is described and documented as illustrated in Figure 6. The parametric information from the storage environments are based on a variety of sources: including: MIL-STD 210C, 1987; Resnick, 1965; AR 70-38 1979; and Pompei, 1985.

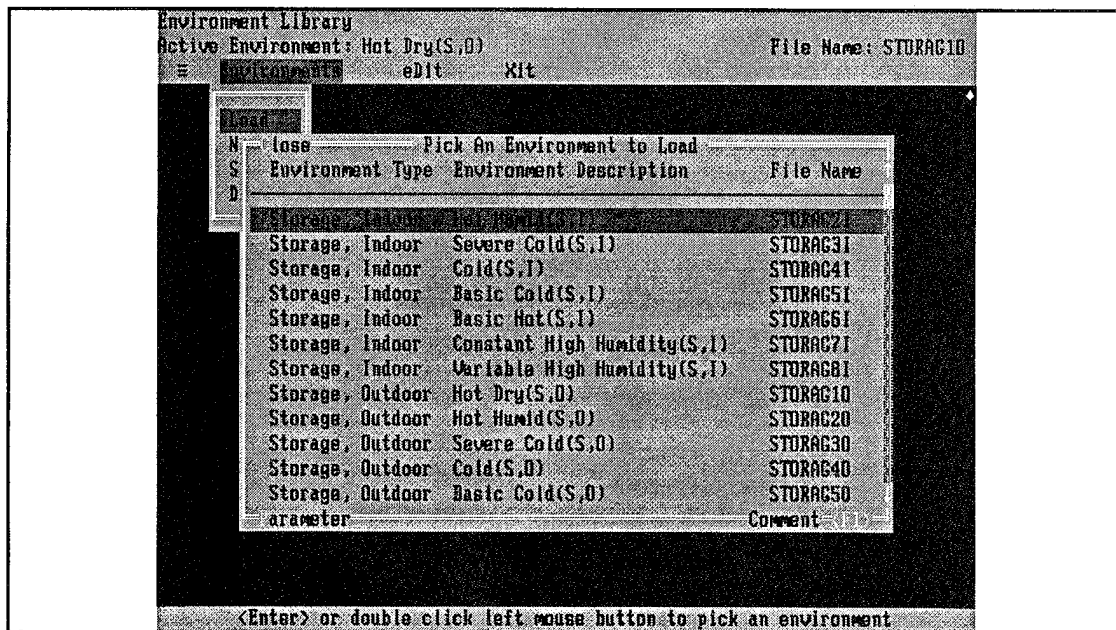


**Figure 4** Storage environments in CADMP-IIe

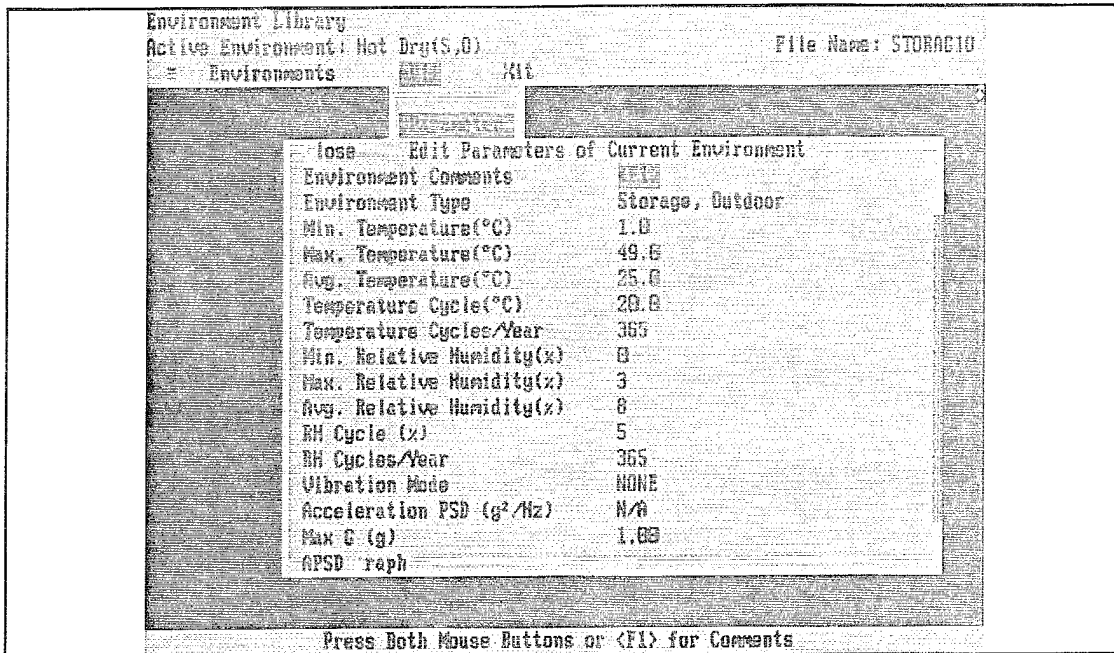


Figure 5 Example parameters of the storage environment

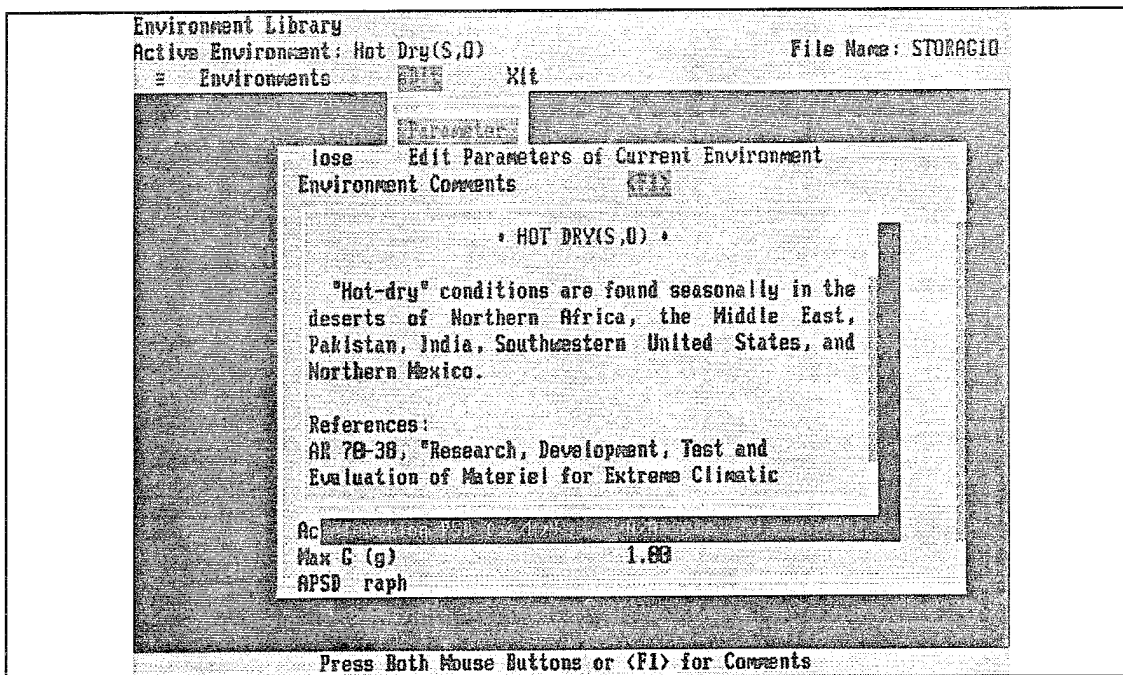


Figure 6 Example descriptive text and reference source for storage environment

**Desert, Outdoor.** This environment is typical of deserts such as Yuma in Arizona. Peak solar radiation occurs during May and June while maximum ambient and ground temperatures occur during July, August and September. (Table 3)

**Table 3** Desert, Outdoor environmental parameters. [Resnick 1965]

	Storage, Outdoor
Minimum Temperature °C	4
Maximum Temperature °C	53
Average Temperature °C	23
Temperature Cycle °C	26
Temperature Cycles/year	365
Min. Relative Humidity %	17
Max. Relative Humidity %	52
Average Relative Humidity %	35
Relative Humidity Cycle %	35
Relative Humidity Cycles/year	365
Vibration Mode	NONE
Power Spectral Density (g <sup>2</sup> /Hz)	N/A
Maximum G (g)	1
Wave Form	N/A
Time of Pulse (secs)	.001
Maximum Acceleration (g)	1
Wind	HIGH
Rain / Snow	N/A
Sand/Dust	HIGH
Salt Spray	N/A
Solar Radiation	HIGH

Arctic, Outdoor. This environment is found in the Arctic regions such as Alaska where the minimum temperature goes down to as low as -54°C, with temperature cycles of 21°C. (Table 4)

Table 4 Arctic, Outdoor environmental parameters. [Resnick 1965]

	Storage, Outdoor
Minimum Temperature °C	-54
Maximum Temperature °C	32
Average Temperature °C	10
Temperature Cycle °C	21
Temperature Cycles/year	365
Min. Relative Humidity %	70
Max. Relative Humidity %	80
Average Relative Humidity %	75
Relative Humidity Cycle %	100.0
Relative Humidity Cycles/year	0.0
Vibration Mode	NONE
Power Spectral Density (g <sup>2</sup> /Hz)	N/A
Maximum G (g)	1
Wave Form	N/A
Time of Pulse (secs)	.001
Maximum Acceleration (g)	1
Wind	N/A
Rain / Snow	HIGH
Sand/Dust	N/A
Salt Spray	N/A
Solar Radiation	N/A

**Tropical Rainforest, Outdoor.** This environment is typical of tropical rainforest regions which are constantly hot and wet. The hottest time of the year just south of the equator is January to March when rainfall is least and most direct rainfall reaches the ground. Coolest days and nights are in July and August when the sun is lowest. (Table 5)

**Table 5** Tropical Rainforest, Outdoor environmental parameters. [Resnick 1965]

	Storage, Outdoor
Minimum Temperature °C	16
Maximum Temperature °C	34
Average Temperature °C	26
Temperature Cycle °C	10
Temperature Cycles/year	365
Min. Relative Humidity %	75
Max. Relative Humidity %	100
Average Relative Humidity %	88
Relative Humidity Cycle %	15
Relative Humidity Cycles/year	365
Vibration Mode	NONE
Power Spectral Density (g <sup>2</sup> /Hz)	N/A
Maximum G (g)	1
Wave Form	N/A
Time of Pulse (secs)	.001
Maximum Acceleration (g)	1
Wind	N/A
Rain / Snow	N/A
Sand/Dust	N/A
Salt Spray	N/A
Solar Radiation	N/A

Tropical Marine, Outdoor. The tropical marine weather is typical of isolated Pacific islands as far north as 20 N. All tropical Marine regions have extremely variable rainfall, from 18 to 90 or more inches. (Table 6)

Table 6 Tropical Marine, Outdoor environmental parameters. [Resnick 1965]

	Storage, Outdoor
Minimum Temperature °C	19
Maximum Temperature °C	27
Average Temperature °C	24
Temperature Cycle °C	6
Temperature Cycles/year	365
Min. Relative Humidity %	75
Max. Relative Humidity %	100
Average Relative Humidity %	88
Relative Humidity Cycle %	15
Relative Humidity Cycles/year	365
Vibration Mode	NONE
Power Spectral Density (g <sup>2</sup> /Hz)	N/A
Maximum G (g)	1
Wave Form	N/A
Time of Pulse (secs)	.001
Maximum Acceleration (g)	1
Wind	N/A
Rain / Snow	N/A
Sand/Dust	N/A
Salt Spray	HIGH
Solar Radiation	N/A

**Tropical Monsoon, Outdoor.** The region of tropical monsoon includes India and Southeast Asia. This region is thoroughly seasonal with great extremes. June and July are generally the hottest. From June until late September, the south-west monsoons bring in continual rain, drizzle and cloudiness. (Table 7)

**Table 7** Tropical Monsoon, Outdoor environmental parameters. [Resnick 1965]

	Storage, Outdoor
Minimum Temperature °C	9
Maximum Temperature °C	43
Average Temperature °C	25
Temperature Cycle °C	10
Temperature Cycles/year	365
Min. Relative Humidity %	80
Max. Relative Humidity %	100
Average Relative Humidity %	90
Relative Humidity Cycle %	20
Relative Humidity Cycles/year	365
Vibration Mode	NONE
Power Spectral Density (g <sup>2</sup> /Hz)	N/A
Maximum G (g)	1
Wave Form	N/A
Time of Pulse (secs)	.001
Maximum Acceleration (g)	1
Wind	N/A
Rain / Snow	HIGH
Sand/Dust	N/A
Salt Spray	N/A
Solar Radiation	N/A



Tropical Desert, Outdoor. North Africa and the Middle-East are in the tropical desert region. Precipitation in this region is very low and there are constant cloudless skies producing bright sunlight and hot noondays. Wind abrasion can be dominant in this region. (Table 8)

Table 8 Tropical Monsoon, Outdoor environmental parameters. [Resnick 1965]

	Storage, Outdoor
Minimum Temperature °C	9
Maximum Temperature °C	52.0
Average Temperature °C	31.2
Temperature Cycle °C	10
Temperature Cycles/year	365
Min. Relative Humidity %	17.0
Max. Relative Humidity %	52.0
Average Relative Humidity %	35.0
Relative Humidity Cycle %	35.0
Relative Humidity Cycles/year	365
Vibration Mode	NONE
Power Spectral Density (g <sup>2</sup> /Hz)	N/A
Maximum G (g)	1
Wave Form	N/A
Time of Pulse (secs)	.001
Maximum Acceleration (g)	1
Wind	N/A
Rain / Snow	N/A
Sand/Dust	HIGH
Salt Spray	N/A
Solar Radiation	N/A

**Hot-Humid, Indoor.** Hot-humid conditions occur in very narrow coastal regions bordering bodies of water with high surface temperatures such as the Persian Gulf and the Red Sea. (Table 9)

**Table 9** Hot-humid, Indoor environment parameters [AR70-38 1979]

	Storage, Indoor
Minimum Temperature °C	33
Maximum Temperature °C	71
Average Temperature °C	48
Temperature Cycle °C	20
Temperature Cycles/year	365
Min. Relative Humidity %	14
Max. Relative Humidity %	80
Average Relative Humidity %	46
Relative Humidity Cycle %	66
Relative Humidity Cycles/year	365
Vibration Mode	NONE
Power Spectral Density (g <sup>2</sup> /Hz)	N/A
Maximum G (g)	1
Wave Form	N/A
Time of Pulse (secs)	.001
Maximum Acceleration (g)	1
Wind	N/A
Rain / Snow	N/A
Sand/Dust	MEDIUM
Salt Spray	N/A
Solar Radiation	N/A

Hot-Humid, Outdoor. Hot-humid conditions occur in very narrow coastal regions bordering bodies of water with high surface temperatures such as the Persian Gulf and the Red Sea. (Table 10)

Table 10 Hot-humid, Outdoor environment parameters [AR70-38 1979]

	Storage, Outdoor
Minimum Temperature °C	31
Maximum Temperature °C	41
Average Temperature °C	35
Temperature Cycle °C	10
Temperature Cycles/year	365
Min. Relative Humidity %	59
Max. Relative Humidity %	88
Average Relative Humidity %	75
Relative Humidity Cycle %	29
Relative Humidity Cycles/year	365
Vibration Mode	NONE
Power Spectral Density (g <sup>2</sup> /Hz)	N/A
Maximum G (g)	1
Wave Form	N/A
Time of Pulse (secs)	.001
Maximum Acceleration (g)	1
Wind	HIGH
Rain / Snow	MEDIUM
Sand/Dust	HIGH
Salt Spray	LOW
Solar Radiation	MEDIUM

**Severe Cold, Indoor.** "Severe cold" conditions are found in the interior of Alaska extending into the Yukon in Canada, on the Greenland icecap, Northern Asia, and the interior of the Northern islands of the Canadian Archipelago. (Table 11)

**Table 11** Severe Cold, Indoor environment parameters [AR70-38 1979]

	Storage, Indoor
Minimum Temperature °C	-51
Maximum Temperature °C	-40
Average Temperature °C	-50
Temperature Cycle °C	10
Temperature Cycles/year	365
Min. Relative Humidity %	70
Max. Relative Humidity %	100
Average Relative Humidity %	80
Relative Humidity Cycle %	10
Relative Humidity Cycles/year	365
Vibration Mode	NONE
Power Spectral Density (g <sup>2</sup> /Hz)	N/A
Maximum G (g)	1
Wave Form	N/A
Time of Pulse (secs)	.001
Maximum Acceleration (g)	1
Wind	MEDIUM
Rain / Snow	MEDIUM
Sand/Dust	N/A
Salt Spray	N/A
Solar Radiation	N/A

Severe Cold, Outdoor. "Severe cold" conditions are found in the interior of Alaska extending into the Yukon in Canada, on the Greenland icecap, Northern Asia, and the interior of the Northern islands of the Canadian Archipelago. (Table 12)

Table 12 Severe Cold, Outdoor environment parameters [AR70-38 1979]

	Storage, Outdoor
Minimum Temperature °C	-51
Maximum Temperature °C	-40
Average Temperature °C	-50
Temperature Cycle °C	10
Temperature Cycles/year	365
Min. Relative Humidity %	70
Max. Relative Humidity %	100
Average Relative Humidity %	80
Relative Humidity Cycle %	10
Relative Humidity Cycles/year	365
Vibration Mode	NONE
Power Spectral Density (g <sup>2</sup> /Hz)	N/A
Maximum G (g)	1
Wave Form	N/A
Time of Pulse (secs)	.001
Maximum Acceleration (g)	1
Wind	HIGH
Rain / Snow	HIGH
Sand/Dust	LOW
Salt Spray	LOW
Solar Radiation	LOW

**Cold, Indoor.** "Cold" conditions are found in Canada, Alaska, Greenland, northern Scandinavia, northern Asia, and Tibet. Also they are found at higher elevations (e.g., Alps, Himalayas, and the Andes). (Table 13)

**Table 13** Cold, Indoor environmental conditions. [AR70-38 1979]

	Storage, Indoor
Minimum Temperature °C	-46
Maximum Temperature °C	-37
Average Temperature °C	-42
Temperature Cycle °C	8
Temperature Cycles/year	365
Min. Relative Humidity %	70
Max. Relative Humidity %	100
Average Relative Humidity %	80
Relative Humidity Cycle %	10
Relative Humidity Cycles/year	365
Vibration Mode	NONE
Power Spectral Density ( $g^2/Hz$ )	N/A
Maximum G (g)	1
Wave Form	N/A
Time of Pulse (secs)	.001
Maximum Acceleration (g)	1
Wind	N/A
Rain / Snow	MEDIUM
Sand/Dust	N/A
Salt Spray	N/A
Solar Radiation	N/A

Cold, Outdoor. "Cold" conditions are found in Canada, Alaska, Greenland, northern Scandinavia, northern Asia, and Tibet. Also they are found at higher elevations (e.g., Alps, Himalayas, and the Andes). (Table 14)

Table 14 Cold, outdoor environmental conditions. [AR70-38 1979]

	Storage, Outdoor
Minimum Temperature °C	-46
Maximum Temperature °C	-37
Average Temperature °C	-42
Temperature Cycle °C	8
Temperature Cycles/year	365
Min. Relative Humidity %	70
Max. Relative Humidity %	100
Average Relative Humidity %	80
Relative Humidity Cycle %	30
Relative Humidity Cycles/year	365
Vibration Mode	NONE
Power Spectral Density (g <sup>2</sup> /Hz)	N/A
Maximum G (g)	1
Wave Form	N/A
Time of Pulse (secs)	.001
Maximum Acceleration (g)	1
Wind	HIGH
Rain / Snow	HIGH
Sand/Dust	LOW
Salt Spray	LOW
Solar Radiation	LOW

**Basic Cold, Indoor.** "Basic cold" conditions are found in the Northern Hemisphere south of the coldest areas and on high latitude coasts (e.g. southern coast of Alaska) where maritime effects prevent occurrence of very low temperatures. (Table 15)

**Table 15** Basic Cold, Indoor environmental parameters [AR70-38 1979]

	Storage, Indoor
Minimum Temperature °C	-33
Maximum Temperature °C	-25
Average Temperature °C	-31
Temperature Cycle °C	5
Temperature Cycles/year	365
Min. Relative Humidity %	70
Max. Relative Humidity %	100
Average Relative Humidity %	80
Relative Humidity Cycle %	10
Relative Humidity Cycles/year	365
Vibration Mode	NONE
Power Spectral Density (g <sup>2</sup> /Hz)	N/A
Maximum G (g)	1
Wave Form	N/A
Time of Pulse (secs)	.001
Maximum Acceleration (g)	1
Wind	N/A
Rain / Snow	MEDIUM
Sand/Dust	N/A
Salt Spray	N/A
Solar Radiation	N/A



Basic Cold, Outdoor. "Basic cold" conditions are found in the Northern Hemisphere south of the coldest areas and on high latitude coasts (e.g. southern coast of Alaska) where maritime effects prevent occurrence of very low temperatures. (Table 16)

Table 16 Basic Cold, Outdoor environmental parameters [AR70-38 1979]

	Storage, Outdoor
Minimum Temperature °C	-32
Maximum Temperature °C	-21
Average Temperature °C	-27
Temperature Cycle °C	11
Temperature Cycles/year	365
Min. Relative Humidity %	70
Max. Relative Humidity %	100
Average Relative Humidity %	80
Relative Humidity Cycle %	30
Relative Humidity Cycles/year	365
Vibration Mode	NONE
Power Spectral Density (g <sup>2</sup> /Hz)	N/A
Maximum G (g)	1
Wave Form	N/A
Time of Pulse (secs)	.001
Maximum Acceleration (g)	1
Wind	MEDIUM
Rain / Snow	HIGH
Sand/Dust	LOW
Salt Spray	LOW
Solar Radiation	LOW

**Basic Hot, Indoor.** "Basic hot" conditions occur in areas bordering those with hot-dry conditions. They also occur in southern Africa, South America, southern Spain, and southwest Asia. (Table 17)

**Table 17** Basic Hot, Indoor environmental conditions. [AR70-38 1979]

	Storage, Indoor
Minimum Temperature °C	30
Maximum Temperature °C	63
Average Temperature °C	44
Temperature Cycle °C	5
Temperature Cycles/year	365
Min. Relative Humidity %	5
Max. Relative Humidity %	44
Average Relative Humidity %	22
Relative Humidity Cycle %	39
Relative Humidity Cycles/year	365
Vibration Mode	NONE
Power Spectral Density (g <sup>2</sup> /Hz)	N/A
Maximum G (g)	1
Wave Form	N/A
Time of Pulse (secs)	.001
Maximum Acceleration (g)	1
Wind	N/A
Rain / Snow	LOW
Sand/Dust	N/A
Salt Spray	N/A
Solar Radiation	N/A

Basic Hot, Outdoor. "Basic hot" conditions occur in areas bordering those with hot-dry conditions. They also occur in southern Africa, South America, southern Spain, and southwest Asia. (Table 18)

Table 18 Basic Hot, Outdoor environmental conditions. [AR70-38 1979]

	Storage, Outdoor
Minimum Temperature °C	30
Maximum Temperature °C	43
Average Temperature °C	37
Temperature Cycle °C	13
Temperature Cycles/year	365
Min. Relative Humidity %	14
Max. Relative Humidity %	44
Average Relative Humidity %	27
Relative Humidity Cycle %	30
Relative Humidity Cycles/year	365
Vibration Mode	NONE
Power Spectral Density (g <sup>2</sup> /Hz)	N/A
Maximum G (g)	1
Wave Form	N/A
Time of Pulse (secs)	.001
Maximum Acceleration (g)	1
Wind	MEDIUM
Rain / Snow	MEDIUM
Sand/Dust	MEDIUM
Salt Spray	MEDIUM
Solar Radiation	MEDIUM

**Constant High Humidity, Indoor.** "Constant high humidity" represents the heavily forested areas in the tropics where nearly constant conditions may prevail during raining and wet seasons. Therefore, the material is likely to be constantly wet or damp for many days at a time. (Table 19)

**Table 19** Constant High Humidity, Indoor environmental conditions. [AR70-38 1979]

	Storage, Indoor
Minimum Temperature °C	27
Maximum Temperature °C	27
Average Temperature °C	27
Temperature Cycle °C	0
Temperature Cycles/year	0
Min. Relative Humidity %	95
Max. Relative Humidity %	100
Average Relative Humidity %	97
Relative Humidity Cycle %	0
Relative Humidity Cycles/year	0
Vibration Mode	NONE
Power Spectral Density (g <sup>2</sup> /Hz)	N/A
Maximum G (g)	1
Wave Form	N/A
Time of Pulse (secs)	.001
Maximum Acceleration (g)	1
Wind	MEDIUM
Rain / Snow	N/A
Sand/Dust	N/A
Salt Spray	N/A
Solar Radiation	N/A

Constant High Humidity, Outdoor. "Constant high humidity" represents the heavily forested areas in the tropics where nearly constant conditions may prevail during raining and wet seasons. Therefore, the material is likely to be constantly wet or damp for many days at a time. (Table 20)

Table 20 Constant High Humidity, Outdoor environmental conditions. [AR70-38 1979]

	Storage, Outdoor
Minimum Temperature °C	24
Maximum Temperature °C	24
Average Temperature °C	24
Temperature Cycle °C	0.0
Temperature Cycles/year	0.0
Min. Relative Humidity %	95
Max. Relative Humidity %	100
Average Relative Humidity %	97
Relative Humidity Cycle %	0
Relative Humidity Cycles/year	0
Vibration Mode	NONE
Power Spectral Density (g <sup>2</sup> /Hz)	N/A
Maximum G (g)	1
Wave Form	N/A
Time of Pulse (secs)	.001
Maximum Acceleration (g)	1
Wind	LOW
Rain / Snow	HIGH
Sand/Dust	MEDIUM
Salt Spray	MEDIUM
Solar Radiation	LOW

**Variable High Humidity, Indoor.** "Variable high humidity" conditions are found in open tropical areas. Exposed items are subject to alternate wetting and drying. (Table 21)

**Table 21** Variable High Humidity, Indoor environmental conditions. [AR70-38 1979]

	Storage, Indoor
Minimum Temperature °C	30
Maximum Temperature °C	63
Average Temperature °C	44
Temperature Cycle °C	33
Temperature Cycles/year	365
Min. Relative Humidity %	19
Max. Relative Humidity %	75
Average Relative Humidity %	46
Relative Humidity Cycle %	54
Relative Humidity Cycles/year	365
Vibration Mode	NONE
Power Spectral Density (g <sup>2</sup> /Hz)	N/A
Maximum G (g)	1
Wave Form	N/A
Time of Pulse (secs)	.001
Maximum Acceleration (g)	1
Wind	N/A
Rain / Snow	MEDIUM
Sand/Dust	N/A
Salt Spray	N/A
Solar Radiation	N/A

Variable High Humidity, Outdoor. "Variable high humidity" conditions are found in open tropical areas. Exposed items are subject to alternate wetting and drying. (Table 22)

Table 22 Variable High Humidity, Outdoor environmental conditions. [AR70-38 1979]

	Storage, Outdoor
Minimum Temperature °C	26
Maximum Temperature °C	35
Average Temperature °C	30
Temperature Cycle °C	9
Temperature Cycles/year	365
Min. Relative Humidity %	74
Max. Relative Humidity %	100
Average Relative Humidity %	86
Relative Humidity Cycle %	26
Relative Humidity Cycles/year	365
Vibration Mode	NONE
Power Spectral Density (g <sup>2</sup> /Hz)	N/A
Maximum G (g)	1
Wave Form	N/A
Time of Pulse (secs)	.001
Maximum Acceleration (g)	1
Wind	MEDIUM
Rain / Snow	HIGH
Sand/Dust	HIGH
Salt Spray	HIGH
Solar Radiation	MEDIUM

## IR and MMW Devices

Infrared and millimeter wave weapons systems contain a variety of devices and package architectures which are used in sensing and signal processing. This section provides a description of many unique IR and MMW components found in smart munitions. Examples of CADMP-IIe architecture representations are also provided.

"Smart Sensors" are defined as those sensors which contain both sensing and signal processing capabilities, with objectives ranging from simple viewing to sophisticated remote sensing, surveillance, search/track, weapon guidance, robotics, perceptronics, and intelligence applications [Corsi 1991]. The "smart sensor" concept is an emulation of the human eye allowing pattern recognition and objects discrimination with rejection of unwanted signals.

### Components of Infrared Sensors and Failure Mechanisms

Infrared sensors, used in smart munition applications, detect the presence of targets which radiate energy in the infrared portion of the spectrum. The atmosphere attenuates the radiation from the targets and the remaining radiation is then collected by the optical system. The radiation is then passed through various filters and coatings to reject undesired radiation from the background. The optical system helps in focusing the rays onto the detector. The detector senses the target-emitted energy and transforms it into electrical signals. Detector sensitivity is improved by using coolers. The electrical signals are fed into preamps and then to signal processors where they are acted upon by software algorithms.

**Detectors.** Detectors are devices that actually detect the infrared radiation from the targets. Photon induced changes, in the conductivity of the detector, modulate the current flowing through the detector and the load resistor connected to it. Some of the commonly used intrinsic detector materials include silicon (Si), germanium (Ge), lead sulfide (PbS), lead selenide (PbSe), indium arsenide (InAs), indium antimonide (InSb), and mercury cadmium telluride (HgCdTe).

There are two main classes of infrared detectors - the thermal and the photon. Thermal detectors sense temperature change resulting from absorption of infrared radiation by a suitable element which has some temperature sensitive electrical property such as resistivity, thus enabling temperature change to be sensed electrically. In the Golay detector, the absorbed radiation causes a change in temperature of a gas which is sensed by the resulting pressure change.

In the photon type of detector, a photon of infrared radiation is absorbed by a semiconductor electron which raises its energy level into a conduction band. Photons with less energy than the band gap produce no signal. Photon detectors generally require cooling



to prevent excessive conduction by ambient temperature excitation of electrons into the conduction band [Astheimer 1983]. The detection mechanism is either photovoltaic, photoconductive, photoemissive, Schottky barrier, quantum well, or superconducting detectors.

In the photovoltaic detectors, the incident photons generate a potential across a p-n junction, and as in solar cells, the current carriers created by the ionizing radiation are separated by the built-in potential. In the photoconductive detectors, the incident photons cause a resistance change. The current carriers created by the ionizing radiation increase conductivity and lower device resistance. In the photoemissive detectors, the incident photons knock electrons free and into a vacuum. The photocathode material and the surface treatment determine the sensitivity and wavelength response. Figure 7 is a schematic representation of these three processes. In the Schottky barrier detectors, the incident photons are detected in a two step process: in the first step the photons are absorbed in the metal of the semiconductor-metal junction, causing internal photoemission; and in the second step, the positive charge created in the metal tunnels into the semiconductor and is absorbed. In the quantum well detectors, a sandwich of epitaxial layers creates potential wells in the conduction band; and the superconducting detectors use the principle of the Josephson junction. Superconducting detectors are used only in research and very specialized applications at present.

Lead-sulfide detectors are mainly used to detect radiation in the 1 to 3 $\mu$ m range. They are fabricated by chemical deposition of PbS films on a substrate. The substrate is either fused quartz, crystal quartz, single-crystal sapphire, glass, various ceramics, single crystal strontium titanate, IRTRAN II (ZnS), silicon, or germanium. Fused quartz is often used as the substrate material, but its very low linear coefficient of thermal expansion, relative to PbS films, results in poor detector performance. This thermally induced strain in the polycrystalline PbS film is believed to cause increased detector current noise [Johnson 1983].

The PbS film is deposited on a substrate. The outer electrode is a bimetallic film such as titanium-gold (TiAu). Film thicknesses are range from 200 $\text{\AA}$  to 2000 $\text{\AA}$ . The inner electrodes are gold films, deposited by vacuum deposition or by electroplating. They provide electrical connection from the active PbS element to the outer TiAu electrodes. A passivation overcoating is provided using materials such as arsenic trisulfide ( $\text{As}_2\text{S}_3$ ). The passivation layer provides optimization of the effective transmission of photon energy into the PbS film, and surface passivation of the PbS film. The detector cover/window is used to minimize "aging effects."

The cover of the PbS detector is generally fabricated of the same material as the detector substrate, and has the same crystal orientation. The top surfaces of these covers are coated with an anti-reflection coating with a material such as magnesium fluoride ( $\text{MgF}_2$ ).

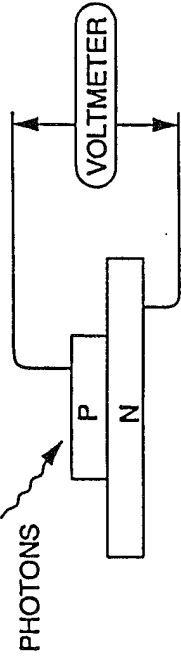
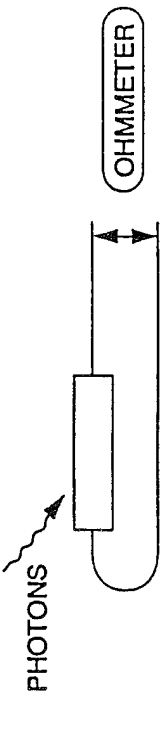
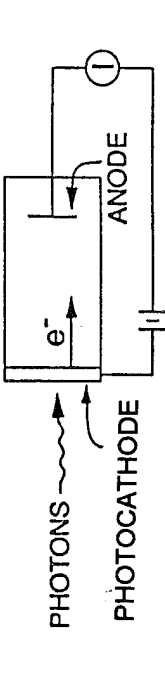
DETECTOR	MECHANISM
PHOTOVOLTAIC (DIODE)	<p data-bbox="305 394 370 1050">INCIDENT PHOTONS GENERATE A POTENTIAL ACROSS A P-N JUNCTION:</p> 
PHOTOCONDUCTIVE	<p data-bbox="639 352 678 1087">INCIDENT PHOTONS CAUSE RESISTANCE CHANGE:</p> 
PHOTOEMISSIVE	<p data-bbox="932 386 997 1058">INCIDENT PHOTONS KNOCK ELECTRONS FREE INTO A VACUUM:</p> 

Figure 7 Detector mechanisms [Georgia Tech 1994]

The cover cements most commonly used are various epoxy resins or organic silicone polymers. The thicknesses of these cements are kept below 0.02 mm to minimize any optical absorption or mechanical stresses to the PbS film structure during temperature cycling. The linear coefficient of thermal expansion of the organic resins is typically on the order of 30 ppm/°C. The vacuum outgassing characteristics of the cured resin are also important. Small diameter gold wires (0.025 mm) are welded to the outer electrode traces using ultrasonic, split gap electrode or thermal compression bonding methods.

A typical single-element detector Dewar package is shown in Figures 8 and 9. One face of the detector is exposed to the infrared radiation, while the other face rests against the Dewar surface which is cooled with a cryogen. The package has windows made of IR transmitting material and a filter which allows transmitting of a particular wavelength of radiation.

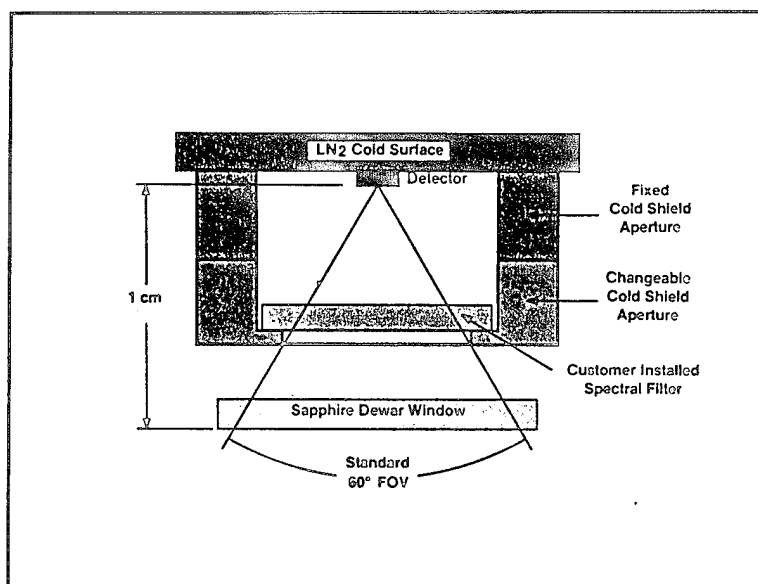
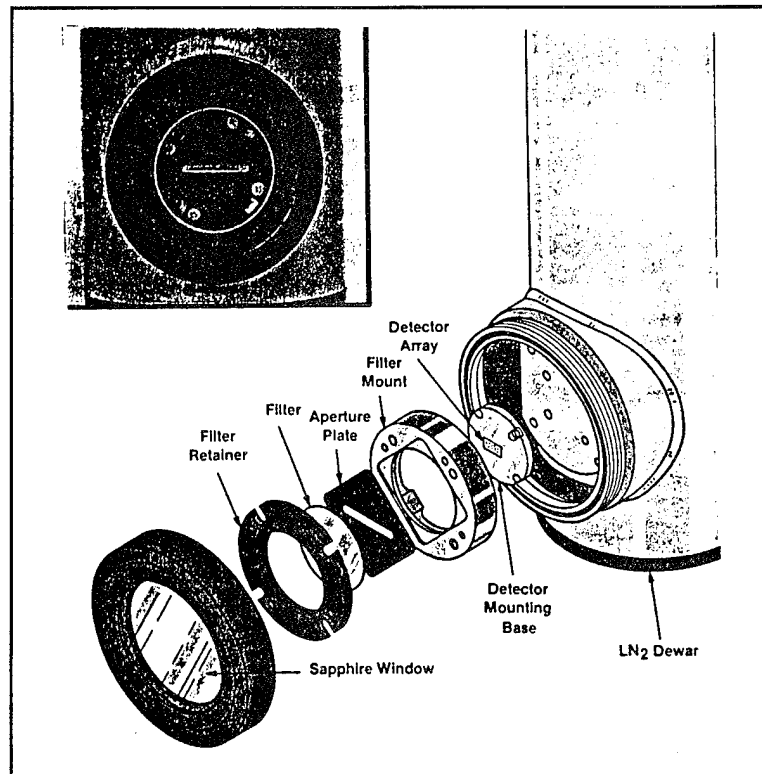


Figure 8 Schematic of a typical detector package  
[Cincinnati]

**Focal Plane Arrays.** Conventional Focal Plane Arrays (FPAs) are a group of discrete detectors where each detector has its own leads, preamplifiers and postprocessors. There is a practical limit to how many of such "channels" can be physically integrated into a system. This is dependent on whether it is a line array or a square array. A practical limit is about 200 detectors in an array.

These arrays can be either monolithic or hybrid in construction. The monolithic arrays use the same material, HgCdTe for example, for photon detection and for readout or signal processing. A major problem with this architecture is that a good photon detecting material

might not be a good signal processing material and vice-versa. A monolithic FPA is shown in Figure 10.



**Figure 10** Detector, cold shield and filter mounting configuration for multiple-element array [Cincinnati]

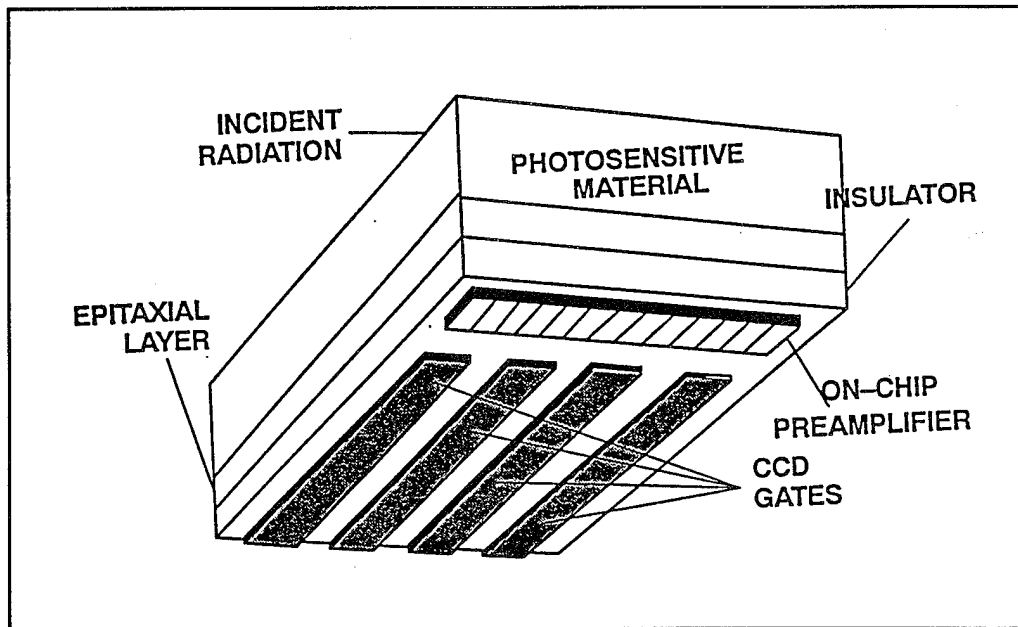


**Figure 9** Monolithic array [Georgia Tech 1994]

The "hybrid" architecture calls for making the readout structure from a material that is different from the detecting material. The goal is to make a sandwich device that consists of material layers where each layer is made of a material that is ideally suited for the function that it performs. The way the different layers of material are physically and electrically connected is through the use of solder bumps, usually indium as shown in Figure 11. The term "hybrid array" means the physical and electrical mating of a two-dimensional mosaic array of detectors to a multiplexer, with individual interconnects between each detector and the corresponding input to the multiplexer, to form a Focal Plane Array [Rode 1983].

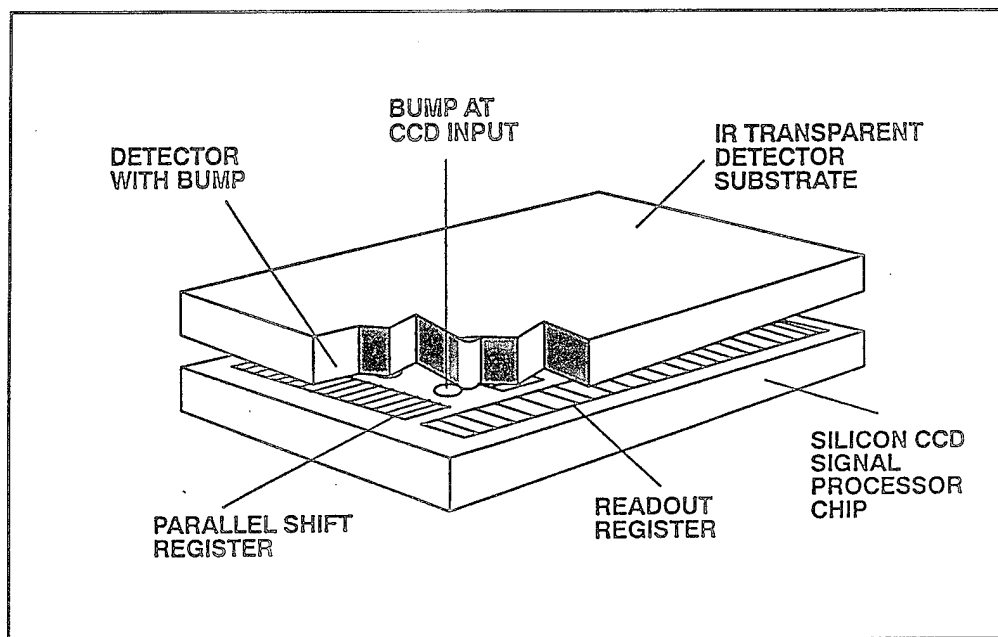
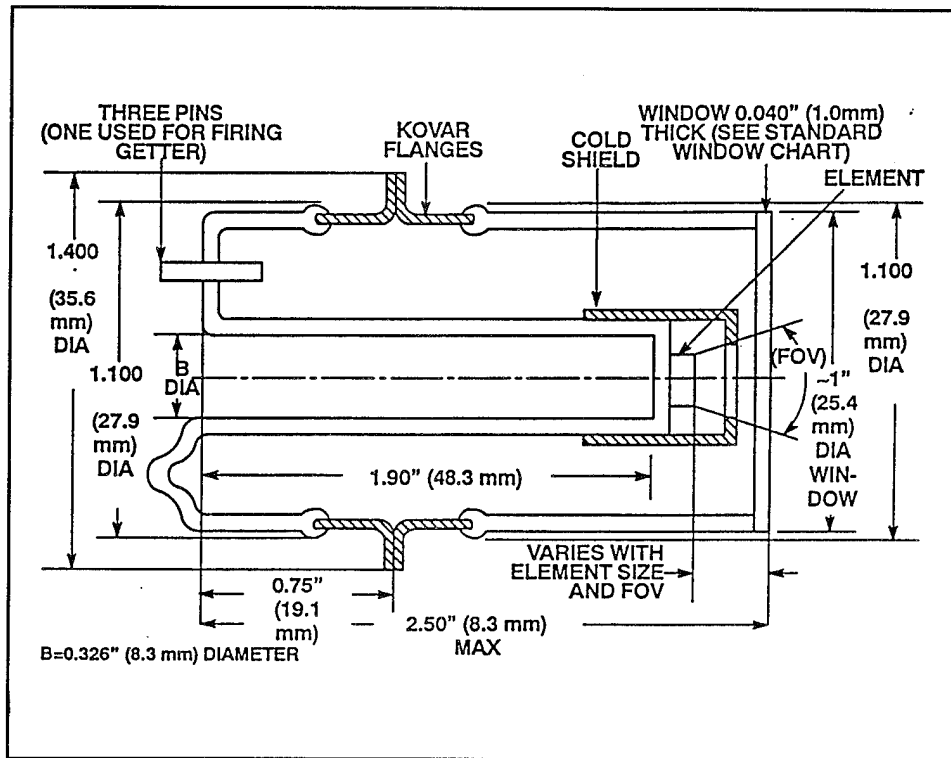


Figure 11 Hybrid array [Georgia Tech 1994]

**Coolers.** Cooling of detectors is essential to reduce the width of the forbidden gap in the detectors. Most detectors are cooled, either because they will not operate at room temperature or because they operate much better when cooled. Installing a cooling system on a IR detector is a complex process because the detector must be mounted such that it will be cold, but at the same time not be covered by condensation and still be accessible to the infrared. Either a cryogen (a very cold liquid) or a refrigerator of some kind is used for this purpose. Thermoelectric coolers are also being used for this purpose.

*Cryogenic Coolers:* Cryogenic coolers are generally open-cycle, expendable systems which use: stored cryogenics in either the subcritical or supercritical liquid state; solid cryogenics; or stored, high-pressure gas with a Joule-Thomson (J-T) expansion. Cryogenic fluids stored as liquids in equilibrium with their vapors (subcritical storage) can provide a

convenient, constant-temperature control system. Liquids are available which provide temperature ranges from 4.2 to 240 K. Fluids can be stored at pressures above their critical pressures (supercritical storage) as homogenous fluids, thus eliminating the phase-separation problems encountered during weightless conditions in space. Stored solid cryogenics provide a reliable refrigeration system for low power heat sources for one to three years or longer, depending on weight and volume limitations [Wolfe, 1989]. Figure 12 shows the construction schematic of a typical Dewar.



**Figure 12** Schematic of a detector Dewar [Georgia Tech]

The Joule-Thomson coolers use a cryostat which is a miniature gas liquefier that is placed directly in the coolant chamber of the detector package.

*Thermoelectric coolers.* These coolers use the Peltier effect; that is, when current flows in a circuit consisting of two dissimilar metals, heat is absorbed at one junction and released at the other. Bismuth Telluride is the most commonly used material in thermoelectric coolers. These coolers are generally constructed from a series of p and n doped bismuth telluride elements, soldered to copper bus-bars within a sandwich of ceramic plates. A schematic cross section of one such cooler is shown in Figure 13. These coolers are fragile devices and are vulnerable to mechanical stresses arising from mounting them within the package, and also due to the thermal mismatch existing between the cooler and the other package materials [Sim 1993]. Loss of cooling efficiency is also seen as a result of diffusion of metal into the elements from the solder or metallization. Metallurgical reactions in solders

can also lead to weakened joints and cracked elements [Sim 1986]. Sim [1993] has shown the effect of degradation of the performance of a Peltier Cooler during a life test at 70°C; this is shown in Figure 14. The maximum cooling that could be achieved by the cooler was reduced to around 20°C, compared to an initial value of greater than 40°C.

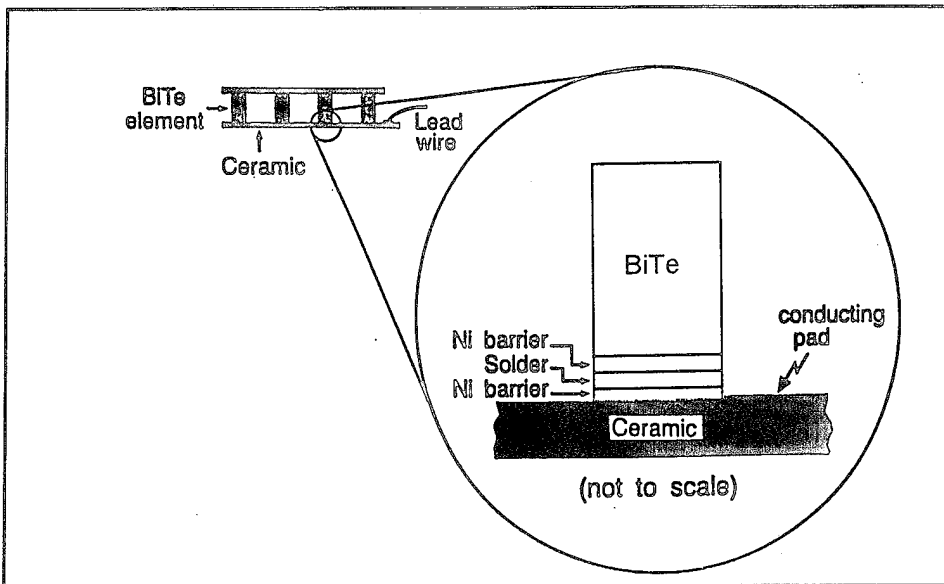


Figure 13 Schematic cross-section of a Peltier Cooler [Sim 1993]

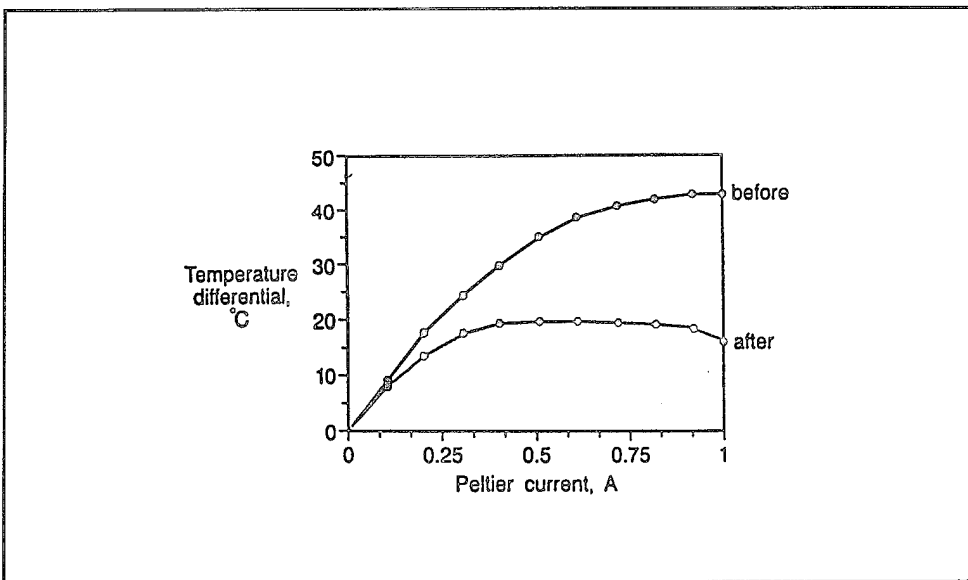


Figure 14 Effects of degradation on characteristics of a Peltier cooler [Sim 1993]

Optics. Both refractive (lenses) and reflective (mirrors) optics are used to gather and condense incoming IR radiation. A field lens is used to focus radiation to the sensitive

surface of the detector. Antireflection coatings are used to prevent reflective losses that occur when IR radiation is incident upon an air-material interface. Magnesium fluoride, silicon monoxide, and zinc sulfide are the commonly used coatings. High reflection coatings are deposited by metal evaporation techniques. Silver is the most commonly used material for this type of coating.

An ideal mirror blank is very smooth and stable, highly rigid, and has a very low coefficient of thermal expansion. Once an optical surface has been fabricated, the mirror blank must not change shape. A common source of instability is due to the release of internal stresses left by production and forming processes. This release can occur during a long-term storage condition. Deformation in the mirror depends on the material, its dimensions, method of support, and orientation in a gravitational field. One can assume that a flat, rectangular plate rests concentrically on a flat, annular ring. The combination is horizontal. The deformation is given by [Wolfe 1989]:

$$\delta = K \left( 1 - \nu^2, \frac{b}{r} \right) \left[ \left( \frac{r^2}{t} \right)^2 \frac{\rho}{E} \right] \quad (1)$$

where,

$\delta$  = deformation at the edge

$r$  = radius of the plate

$t$  = thickness of the plate

$\rho$  = density of the plate

$E$  = Young's modulus

$\nu$  = Poisson's ratio of the plate

$b$  = inside radius of the support ring

$K$  = a function of  $\nu$  and  $b/r$

Table 23 gives the density and Young's modulus of some commonly used mirror blank materials.

**Optical Filters.** Optical filters are used to pass IR radiation of a particular wavelength band through the optical system to the sensitive surface of the detector. This process is known as spectral filtering. Absorption, reflection, and interference filters are used for this purpose. The failure mechanisms in filters under non-operational conditions are the same as those seen in windows.

**Focal Plane Header Assembly.** A focal plane header assembly is an assembly which contains various IR detector components, cooling mechanisms, amplifiers, impedance matching networks, and IR filters. This assembly may or may not contain the cooling system and the pre-amp.



Table 23 Density and Young's modulus data for selected mirror blank materials [Wolfe 1989]

	Density, $\rho$ (g cm <sup>-3</sup> )	Modulus, $E$ (g cm <sup>-1</sup> sec <sup>-2</sup> 10 <sup>-12</sup> )	$\rho/E$ (sec <sup>2</sup> cm <sup>-2</sup> 10 <sup>-12</sup> )
Beryllius	1.82	2.8	0.65
Beryllia	3.03	-	-
Alumina	3.85	3.5	1.1
Cer-Vit*	2.50	0.92	2.7
Fused silica (7940)	2.20	0.73	3.0
ULE fused silica (7971)	2.21	0.68	3.2
Pyrex**	2.35	0.68	3.5
Aluminum	2.70	0.69	3.9
Magnesium	1.74	0.45	3.9

\* Cer-Vit is a registered trademark of Owens-Illinois.

\*\* Pyrex is a registered trademark of Corning Glass Works.

#### Components of Millimeter Wave Systems

A radar is an electromagnetic system used for the detection and location of objects. A radar transmits a particular type of wave form (e.g., a pulse-modulated sine wave), and detects the nature of the signal echoed from the target object. A radar is different from human vision in that it can operate in conditions like darkness, fog, rain, snow, and haze where the eye fails. Another important advantage is that, apart from detecting an object, it can also measure the distance and velocity of the object.

A basic radar consists of an oscillator that generates electro-magnetic radiation, and which is transmitted by a transmitting antenna. The receiving antenna receives the echoed energy that is reflected from the target object in all directions. This received radiation is sent to a receiver where it is processed, and the location, distance, and velocity of the target are detected. The distance is measured by calculating the time taken by the radar signal to travel to the target and back. The angle of arrival of the reflected wave gives the angular position of the target. A shift in the carrier frequency of the reflected wave (doppler effect) is a measure of the relative velocity of the target.

Radars can operate in a wide range of the electromagnetic spectrum. The millimeter wave (MMW) region of the spectrum includes the frequency range from 30 GHz to 300 GHz or wavelengths from 1 cm to 1mm. The *near millimeter waves* range from approximately 100 GHz to 1000 GHz and the *submillimeter waves* range from about 150 GHz to 300 GHz. MMW systems are considered superior to optical and infrared systems owing to their penetration capability of smoke, fog, haze, dust, clouds, and other adverse environments

[Currie 1987]. Some of the typical applications of these radars are in surveillance and target acquisition; instrumentation and measurement; and fire control and tracking.

The basic components of a MMW radar are briefly explained below. The transducer used for SADARM (Sense and Destroy Armor), a smart munition being developed by the Army, is a millimeter-wave radar using discrete GaAs diodes, duroid substrates containing DMAT microstrip transmission lines, and alumina based components.

**The Gunn Diode.** The Gunn Diode is the source of the MMW transmitter and is a solid-state device. Solid-state devices are preferred over tube sources like the magnetron tube due to their low cost, reliability, and simplicity of operation. Gunn and IMPATT (impact ionization avalanche transit time) diodes, and field-effect transistors (FETs) are some of the commonly used sources in MMW devices. The upper frequency limit of a GaAs Gunn Oscillator is about 110 GHz. The Gunn oscillators are much quieter than the IMPATTs, as they depend on bulk semiconductor effects rather than junction semiconductor effects [McMillan 1987].

Under long-term storage, the failure mechanisms in the Gunn diode include die fatigue and cracking, lid-seal fatigue, corrosion, and intermetallic formation. These failure mechanisms are outlined in the section on signal processing electronics and in the Phase I report [Pecht Associates 1991].

**The Varactor Diode.** Varactor diodes are variable capacitance semiconductor elements that can be used as a switch in the diode phase shifter. Frequency modulation of solid-state sources can be implemented using varactor modulators. Varactor-tuned oscillators are available at frequencies up to 100 GHz with 3GHz tuning bandwidth. The technology used to produce Gunn Diodes is also used to produce Varactor diodes [Ailles 1989]. Hence the same failure mechanisms seen in Gunn diodes are also found in varactors under non-operational conditions.

**Mixer Diode.** The mixer diode is a part of the radar receiver and helps in the conversion of the received signal, collected by the antenna (which has a frequency corresponding to the approximate transmitted frequency), to a lower or intermediate frequency (IF) where it can be easily filtered.

Some other devices found in MMW radars include IMPATT diodes, injection locked amplifiers, magnetrons, klystrons, gyrotrons, travelling-wave tubes (TWT), crossed filed amplifiers (CFA), extended interaction amplifiers (EIA), power grid tubes, circulators, low noise amplifiers (LNA), duplexer, RF switches, pin diodes, feedthroughs and microstrip antennas. Some of the common failure mechanisms found in these devices under long-term storage are discussed in the section on signal processing electronics and in the Phase I report [Pecht Associates 1991].

## CADMP-IIe IR and MMW Architectures

This section documents some new package architectures that have been incorporated in the CADMP-IIe software to facilitate storage reliability assessment of electronics for infrared sensors and millimeter-wave radars. This section also provides some useful tips on creating particular architectures and suggests some possible failure mechanisms in those packages.

The package architectures covered in this report include the infrared Dewar with the related optical window and filter architecture; the hybrid focal plane array architecture including the interconnecting bumps connecting the detector chip with the signal processing chip; three leaded-devices such as those used for varactors; metallic cans such as those used in crystal oscillators; and, Gunn diodes. A beam lead die interconnect selection which is common in varactors, PIN diodes, and microwave monolithic integrated circuits (MMICs) is also now part of the Package Designer module.

Screen dumps from the CADMP-IIe software have been used to illustrate the new package architectures. Top views and cross-sectional side views of each package architecture are shown. In addition, input parameter fields required to create the particular architecture are provided.

**Infrared Dewar Architecture.** The representation of the infrared Dewar package is shown in Figures 15 through 17. Package type "DEWAR" has to be chosen in the "constraints" option of the package designer. Figure 18 shows the window materials and parameters that are accessed under the "lid" option of the package designer. Figure 19 illustrates the Dewar parameters and choice of cryogenic materials which are accessed under the "case" option of the package designer.

Some relevant failure mechanisms for the Dewar package are:

- ⊙ Stress-corrosion cracking of windows,
- ⊙ Shattering of windows,
- ⊙ Dewar heat leakage, and
- ⊙ Dewar outgassing.

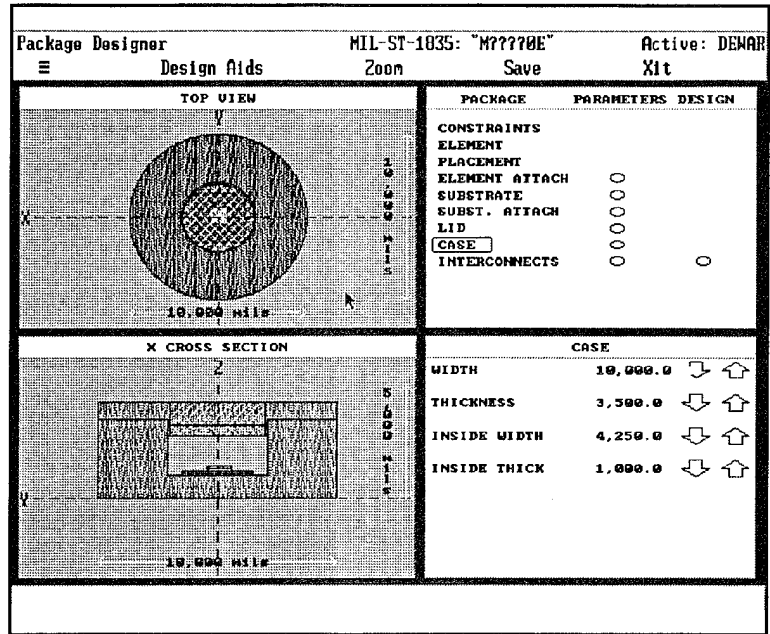


Figure 15 Dewar design options

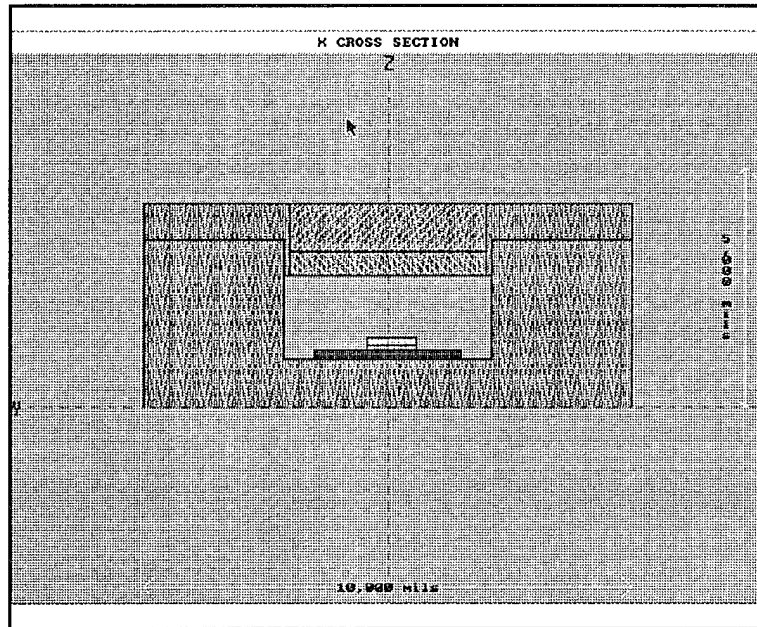


Figure 16 Cross sectional view of Dewar

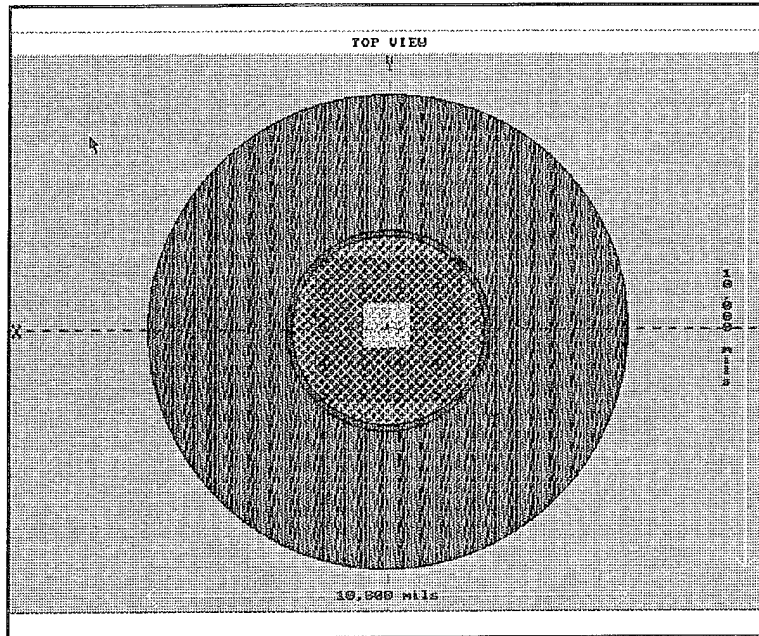


Figure 17 Top view of Dewar

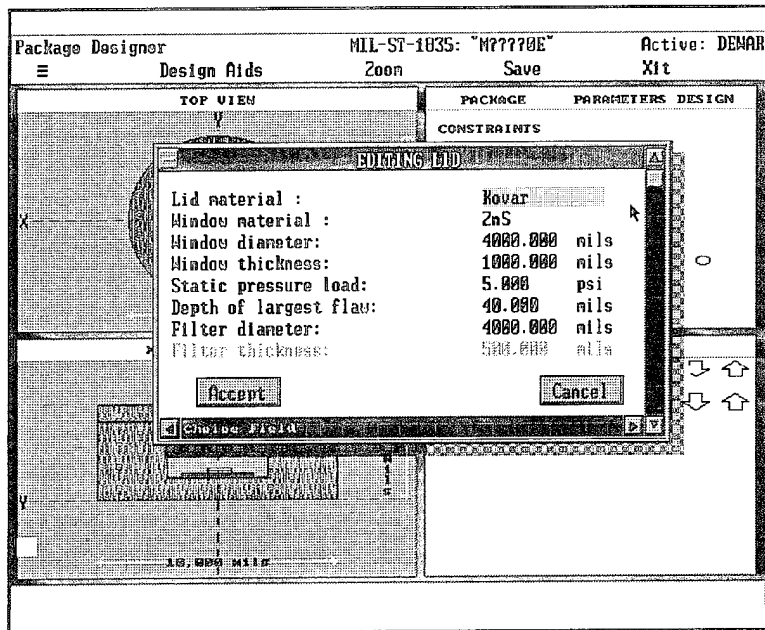


Figure 18 Window (Lid) parameters

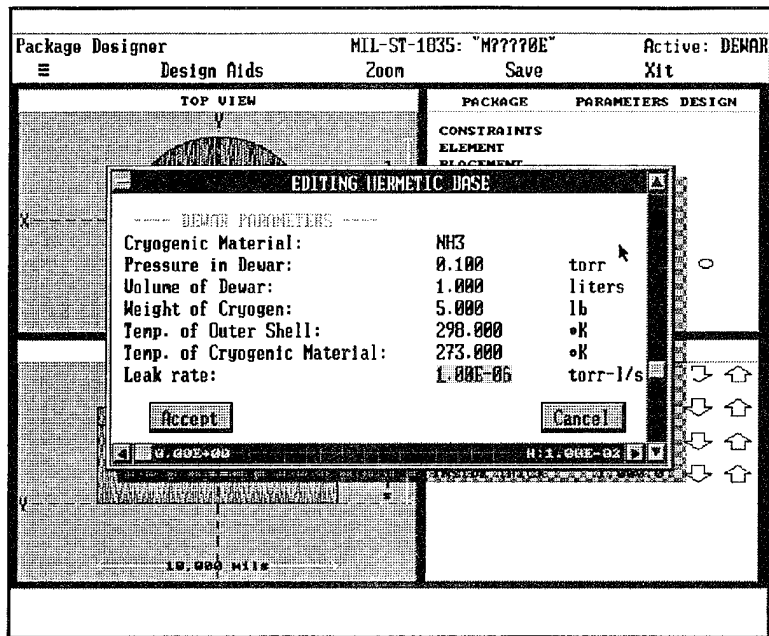


Figure 19 Dewar (case) parameters

**Hybrid Focal Plane Array.** The hybrid Focal Plane Array architecture is used in conjunction with the Dewar package. This is a hybrid architecture, detector over signal processing chip connected by means of solder bumps. Both the signal processing chip and the detector are first specified under the "elements" option of the package designer (See Figure 20). The user then goes into the element definition screen of the detector. In the **Stacked on top of die** attribute the user enters the identification of the processor die as shown in Figure 21. Figure 22 shows the resulting stacked Focal Plane Array elements. To address flip chip solder fatigue, a new model, "Hybrid Flip-Chip Model" has been created.

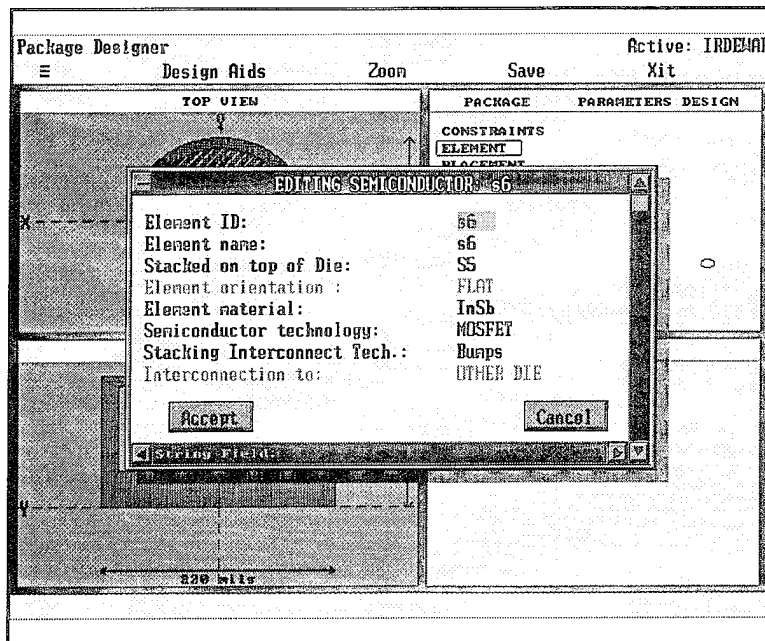


Figure 20 Defining Stacked on Top of Die attribute

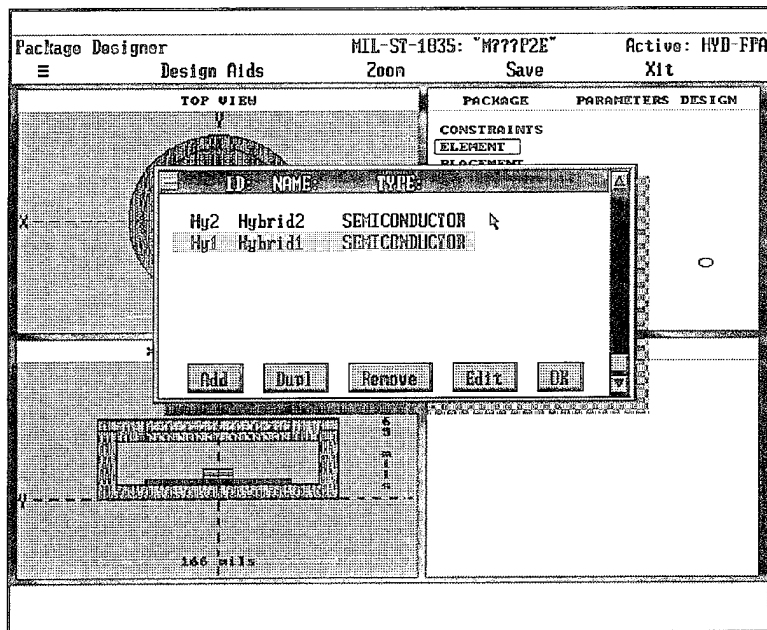
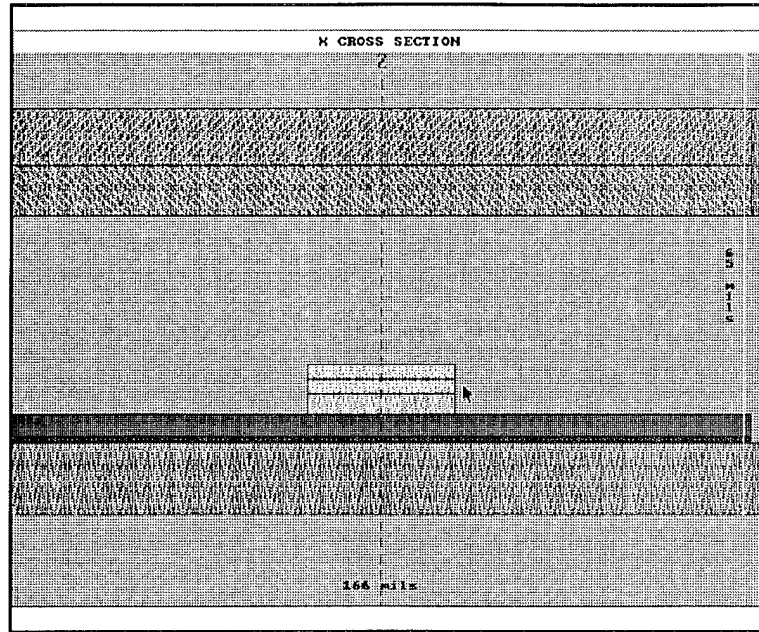


Figure 21 Two elements, detector and processor die.



**Figure 22** Zoomed-in view showing hybrid FPA stack

**Three-leaded Devices.** Varactors, transistors, and some MMICs have three lead architectures. An odd-number of leads can now be designed by deactivating leads from a package having an even number of leads. In the package designer, the "lead" option is chosen (by clicking on the word "lead"), and a screen such as shown in Figure 23 appears. Using the space bar and the mouse, leads not needed can be deactivated to obtain the required number of leads. The resulting three-leaded device is shown in Figure 24.



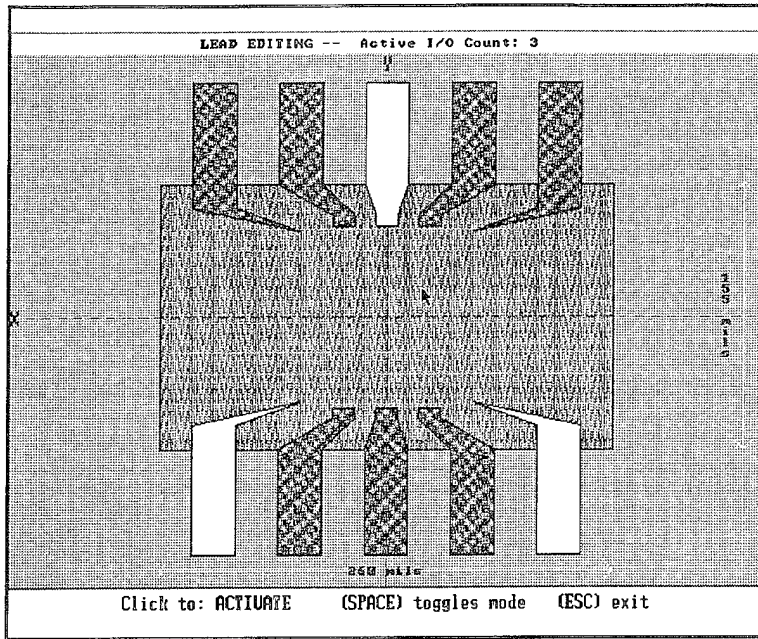


Figure 23 Activating and deactivating leads

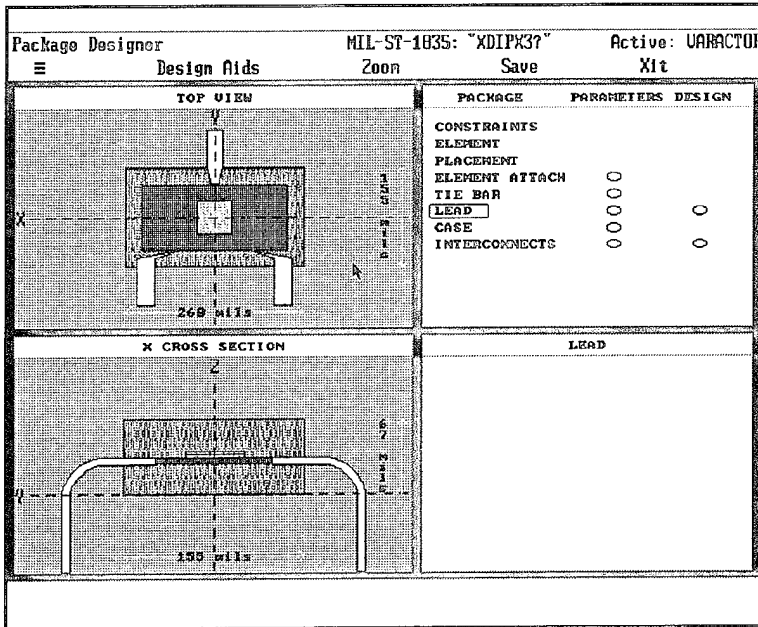


Figure 24 Three leaded device in the package designer

**Metallic Can.** The package type "METALLIC CAN" is chosen in the "constraints" option of CADMP-IIe's package designer. (Figures 25 through 27) Metal cans are used in crystal oscillators and transistors used in millimeter-wave radars.

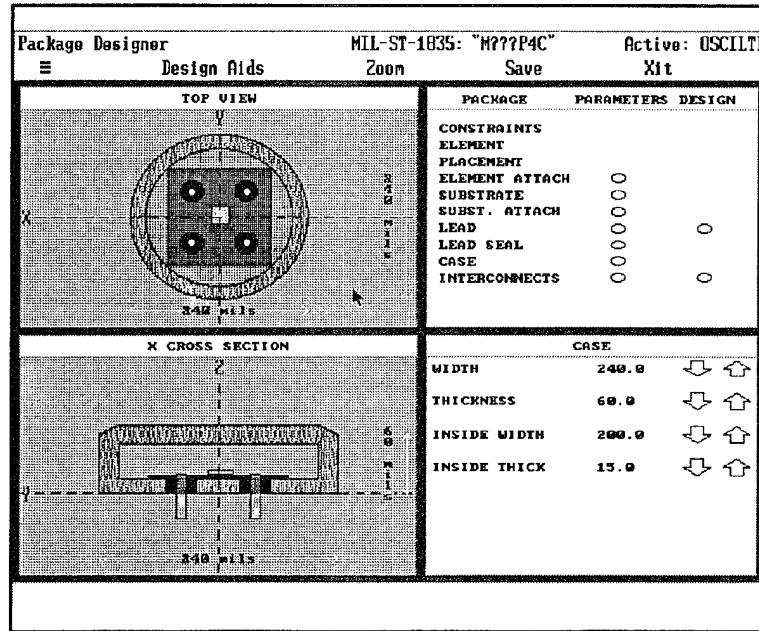


Figure 25 Metallic can package

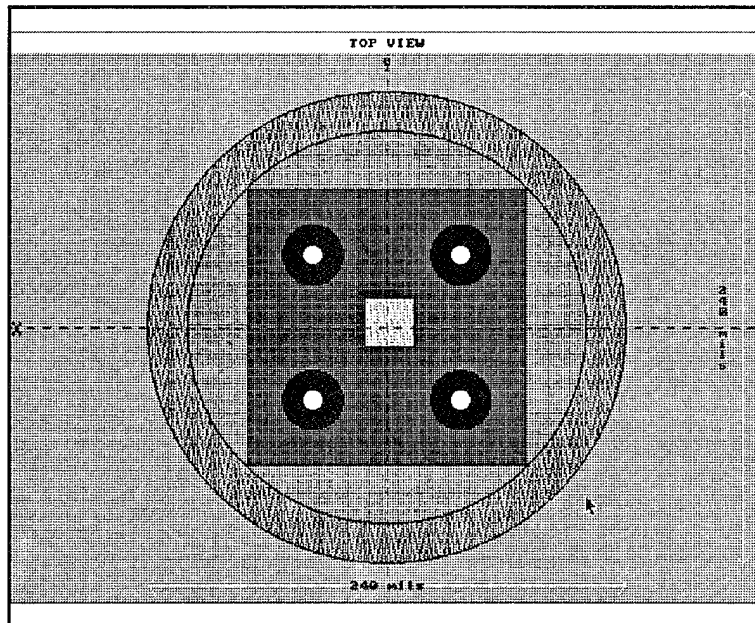


Figure 26 Top view of metallic can package

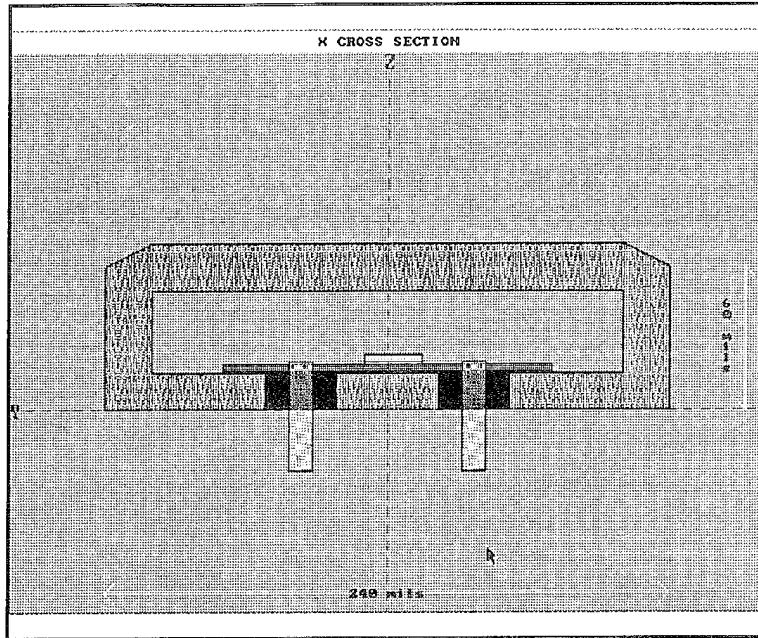


Figure 27 Cross-sectional view of metallic can package

Gunn Diode Architecture. The Gunn Diode is selected under the “constraints” option in the Package Designer. Because the Gunn diode has such high power dissipation, the active device is usually mounted to a threaded heatsink. Because the case and die are very small in comparison, most of the heatsink is omitted in the CADMP-IIe representation. Break lines indicate the heatsink as shown in Figure 28. Figures 29 and 30 show the top and side views.

Package Designer		Active: GUNN	
Design Aids	Zoom	Save	Exit
<p><b>TOP VIEW</b></p> <p>29 mils</p>	<p><b>PACKAGE</b></p> <p>CONSTRAINTS</p> <p>ELEMENT</p> <p>PLACEMENT</p> <p>ELEMENT ATTACH</p> <p>SUBSTRATE</p> <p>LID</p> <p>LID SEAL</p> <p>CASE</p> <p>INTERCONNECTS</p>	<p><b>PARAMETERS</b></p> <p><input type="radio"/></p> <p><input type="radio"/></p> <p><input type="radio"/></p> <p><input type="radio"/></p> <p><input type="radio"/></p>	<p><b>DESIGN</b></p> <p><input type="radio"/></p>
<p><b>X CROSS SECTION</b></p> <p>29 mils</p>	<p><b>CASE</b></p> <p>MIDTH 29.5</p> <p>THICKNESS 35.0</p> <p>INSIDE WIDTH 20.0</p> <p>INSIDE THICK 25.0</p>	<p>⇩ ⇧</p> <p>⇩ ⇧</p> <p>⇩ ⇧</p> <p>⇩ ⇧</p>	

Figure 28 The Gunn diode package

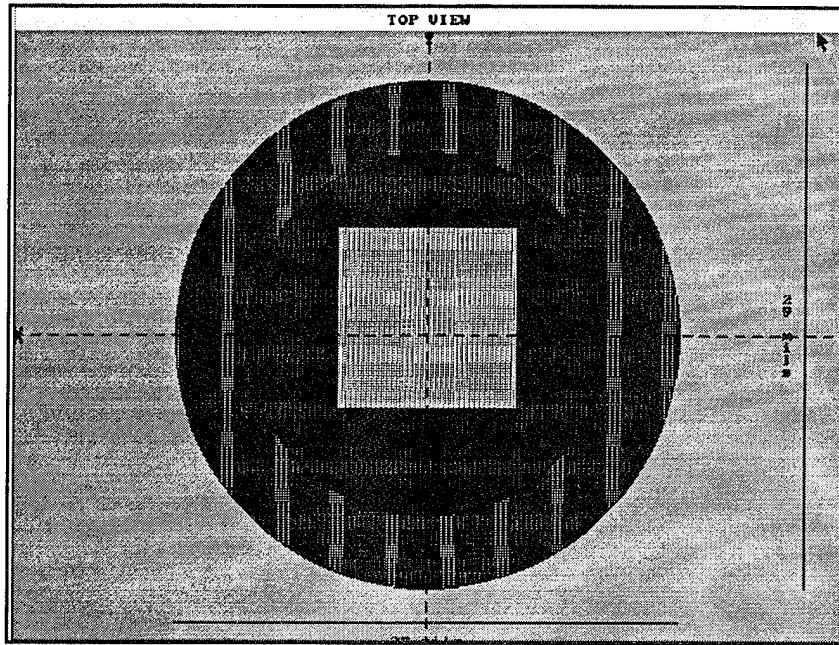


Figure 29 Top view of Gunn diode

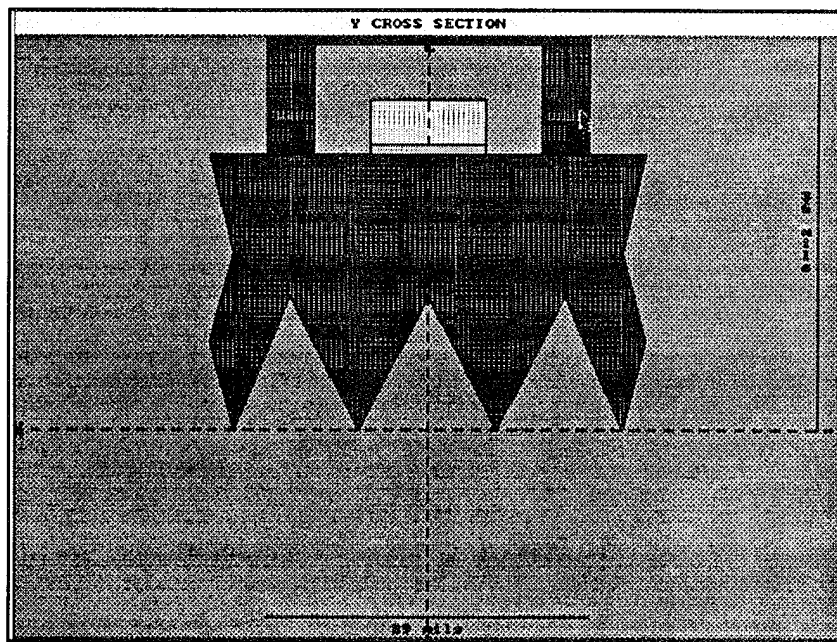


Figure 30 Cross-sectional view of Gunn diode package

## Failure Mechanisms in CADMP-IIe

This section documents some failure mechanisms that occur in infrared and millimeter-wave radar electronics under long-term storage conditions that have been input into the CADMP-IIe software. The failure mechanism models are provided and the criteria for failure are outlined.

The failure mechanisms include the stress corrosion cracking of the infrared windows due to static pressure loading and residual stresses from manufacturing processes; shattering of the infrared windows due to environmental temperature cycling; heat leakage from the Dewar; Dewar outgassing; and fatigue in the flip-chip bumps of the hybrid detectors due to temperature cycling stresses.

The input parameters to every failure mechanism model are listed and the parameters to be input by the user are specified. The corresponding CADMP-IIe software windows where these parameters are input by the user are shown in the form of actual screen-dumps from the software.

CADMP-IIe has a description field and comments at the end of every failure mechanism discussed. This field provides the reference in literature from where the user can obtain more information about the model.

### Stress Corrosion Cracking of Windows

Stress-corrosion induced cracking of infrared windows is a possible failure mechanism under storage conditions, especially when these windows are stored for long periods of time, at high altitudes, when there is a static pressure load acting on them. This problem is also present with windows used in airborne applications. Stress corrosion cracking can occur even without external loads, because residual stresses from conventional manufacturing practices are sufficient to initiate the attack. When materials are under a load or stress, even a mild corrosive attack can cause failure.

Stress corrosion cracking is an interaction between the two mechanisms of fracture and corrosion that occur due to simultaneous mechanical stress and corrosion. This cracking results from a stress concentration, applied or residual, at corrosion-generated surface flaws (as quantified by the stress intensity factor,  $K$ ). When a critical value of stress concentration ( $K_{crit}$ ) is reached, mechanical fracture occurs [Davis 1987]. Although stress concentrations do occur at such flaws, these do not exceed the critical value required to cause mechanical fracture of the material in an inert environment. Thus, stress corrosion essentially reduces the fracture strength of the material so that failure occurs before  $K_{crit}$  for the material is reached. The process is synergistic; that is, the combined simultaneous interaction of mechanical and chemical forces results in crack propagation, whereas neither factor acting

independently or alternately would produce the same result [Davis 1987]. Stress corrosion differs from other types of corrosion in that tensile stress is required.

Zinc sulfide (ZnS) and zinc selenide (ZnSe), two of the more commonly used infrared window materials, are characteristically brittle materials. The grinding and polishing processes result in surface flaws, which can lead to structural failure. In a water-free environment, these flaws are static and do not grow or propagate at sub-critical stress levels. But in humid environments, sub-critical stresses will result in crack growth [Pruszynski 1991]. The window will fracture when a critical flaw depth is reached and the material-dependent critical fracture stress level is reached. The time-to-failure of these windows is dependent upon the initial crack size and the mechanical stress level.

The crack velocity in the material, in the presence of water, varies as a function of the stress intensity factor,  $K_I$ . For a long, shallow crack of depth  $L$ ,  $K_I$  is defined by:

$$K_I = \sigma \sqrt{\pi L} \quad (2)$$

where  $\sigma$  is the macroscopic stress level in the region of the crack induced by pressure loading on the window. At the point of catastrophic failure, the value of stress intensity factor is known as  $K_{IC}$ . From Equation (2), it is seen that the stress intensity factor is a function of both the macroscopic window stress level and the size of the flaws or cracks in the window. This implies that the window will fail at the largest flaw when:

$$\sigma \sqrt{\pi L_{\max}} > K_{IC} \quad (3)$$

where  $L_{\max}$  is the depth of the largest flaw in the window. Since  $L_{\max}$  is not easily determinable, the values of  $K_{IC}$  are determined according to available charts.

There is a highly non-linear relationship between the crack growth rate and the stress intensity factor. For ZnS and ZnSe, the relationship takes the form [Cramer]:

$$V = AK_I^n \quad (4)$$

where  $V$  is the crack velocity and  $a$  and  $n$  are material dependent constants. These values too are available from open literature [Cramer; Evans 1974] and for ZnS and ZnSe are as outlined in Table 24.

Table 24 Crack growth exponent and coefficient for ZnSe and ZnS

Parameter	Zinc Selenide	Zinc Sulfide
Crack growth exponent (n)	40	76
Calculated crack growth coefficient (a)	$4.3 \times 10^{-108}$	$9.63 \times 10^{-218}$

Manipulating equations 2-4 above, the window time-to-failure may be determined :

$$t_{fail} = \int_{K_{I0}}^{K_{Ic}} \frac{2K_I}{\sigma^2 \pi V} dK_I \quad (5)$$

where  $K_I$  is the window stress intensity factor when the window is placed in storage. This is given by equation 1 by substituting  $L$  by  $L_{ini}$  which is the initial crack length. The stress level  $\sigma$  for a circular window with ring support (where the maximum window tensile stress occurs at the center of the window on the outside of the surface) is given by:

$$\sigma_r = \sigma_\theta = \frac{3(3 + \nu)P a^2}{8 t^2} \quad (6)$$

where  $\sigma_r$ ,  $\sigma_\theta$  are the radial and tangential stresses,  $\nu$  is the Poisson's ratio,  $P$  is the static pressure load on the window,  $a$  is the window radius, and  $t$  is the window thickness.

**CADMP-IIe Implementation.** The implementation of Stress Corrosion Cracking into CADMP-IIe is outlined below. Figure 31 shows the CADMP-IIe formation of the model. Definitions of each attribute are shown in Appendix B. Attribute definition can also be obtained in the Failure Mechanism library by positioning the mouse cursor over the attribute and hitting the <F1> key. Figure 32 shows the comments screen that is available for this and all other failure mechanisms. This includes the description of the model and the source of information.

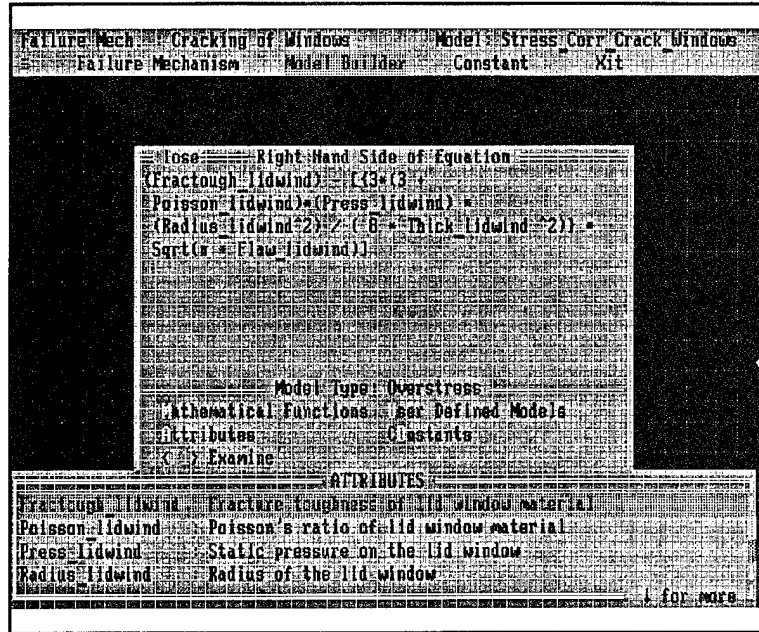


Figure 31 Cracking of Windows failure mechanism

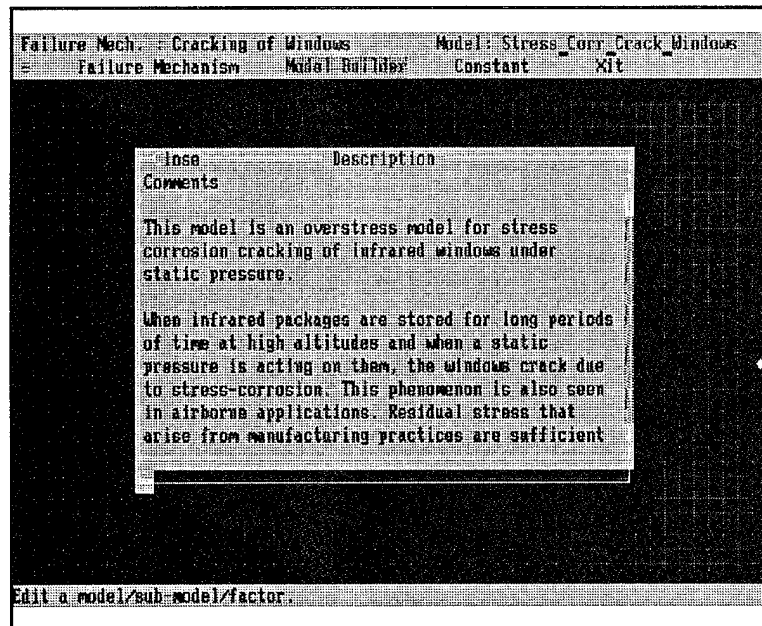


Figure 32 Comments on Cracking of Windows

Failure Mechanism : Stress Corrosion Cracking of Windows  
 Stress : Static Pressure Load and Residual Stresses from Manufacturing  
 Mechanism Type : Overstress  
 Criterion for failure : Stress intensity exceeding a critical value



Model : The window fails if

$$\sigma \sqrt{\pi L_{\max}} > K_{IC} \quad (7)$$

where  $\sigma$  is the macroscopic stress level in the region of the crack induced by pressure loading on the window,  $L_{\max}$  is the depth of the largest flaw in the window,  $K_{IC}$  is the stress intensity factor.  $\sigma$  is given by

$$\sigma = \frac{3(3 + \nu)P a^2}{8 t^2} \quad (8)$$

where,  $\nu$  is the Poisson's ratio,  $P$  is the static pressure load on the window,  $a$  is the window radius, and  $t$  is the window thickness.

Input to the Model :  $\nu$  (from material database for particular window material)

$K_{IC}$  (from material database for particular window material)

$P$  (user input - see Figure 33)

$a$  (user input - see Figure 33)

$t$  (user input - see Figure 33)

$L_{\max}$  (user input - see Figure 33)

Output

: Pass or Fail

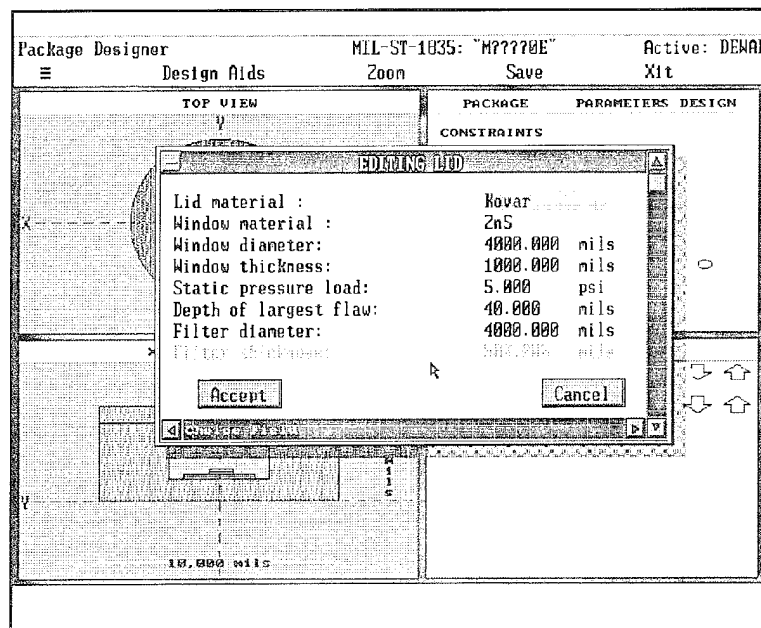


Figure 33 : User input of window parameters

**CADMP-IIe Description.** This model is an overstress model for stress corrosion cracking of infrared windows under static pressure. When infrared packages are stored for long periods of time at high altitudes and when a static pressure is acting on them, the windows crack due to stress-corrosion. This phenomenon is also seen in airborne applications. Residual stress that arise from manufacturing practices are sufficient to initiate the attack. The equations used in this model are taken from a paper by Pruszynski [1991].

### Shattering of Windows

Under storage conditions, infrared windows might crack if exposed to a thermal shock stress. For optical systems that use substantially thick optical substrates, the phenomenon of thermal shock imposes a damage on the system. Experiments of Kuster and Ebert [1980] have shown that the optical surface may be badly disrupted as a function of the material and coatings that are mismatched with the substrate. For germanium and silicon, for example, the thermal shock temperature required to shatter the window is given by [Palmer 1987]:

$$\Delta T_{shock} = \frac{\epsilon E_c (1 - \nu)}{E_c \alpha_s} \quad (9)$$

where,

$\epsilon E_c$  = modulus of rupture N/cm<sup>2</sup>

$E_c$  = Young's modulus N/cm<sup>2</sup>

$\alpha_s$  = Linear coefficient of expansion for the substrate material, /°C

$\nu$  = Poisson's ratio (for dielectrics ~0.20)

If the window is coated with an optical thin film coat to maximize reflectance at the wavelength of interest, then the mismatch in the coefficient of thermal expansion between the coating and the substrate will lead to disruption of the optical surface under thermal shock. The thermal shock temperature required to shatter the window under these circumstances is given by :

$$\Delta T_{shock} = \frac{\epsilon E_c (1 - \nu)}{E_c (\alpha_s - \alpha_c)} \quad (10)$$

where,

$\epsilon E_c$  = modulus of rupture N/cm<sup>2</sup>

$E_c$  = Young's modulus N/cm<sup>2</sup>

$\alpha_s$  = Linear coefficient of expansion for the substrate material, /°C

$\alpha_c$  = Linear coefficient of expansion for the coating material, /°C

$\nu$  = Poisson's ratio (for dielectrics ~0.20)

CADMP-IIe Implementation. The implementation of the window shattering model into CADMP-IIe is outlined below. Figure 34 shows the CADMP-IIe formation of the model. Definitions of each attribute are shown in Appendix B. Attribute definition can also be obtained in the Failure Mechanism library by positioning the mouse cursor over the attribute and hitting the <F1> key. Figure 35 shows the comments screen that is available for this and all other failure mechanisms. This includes the description of the model and the source of information.

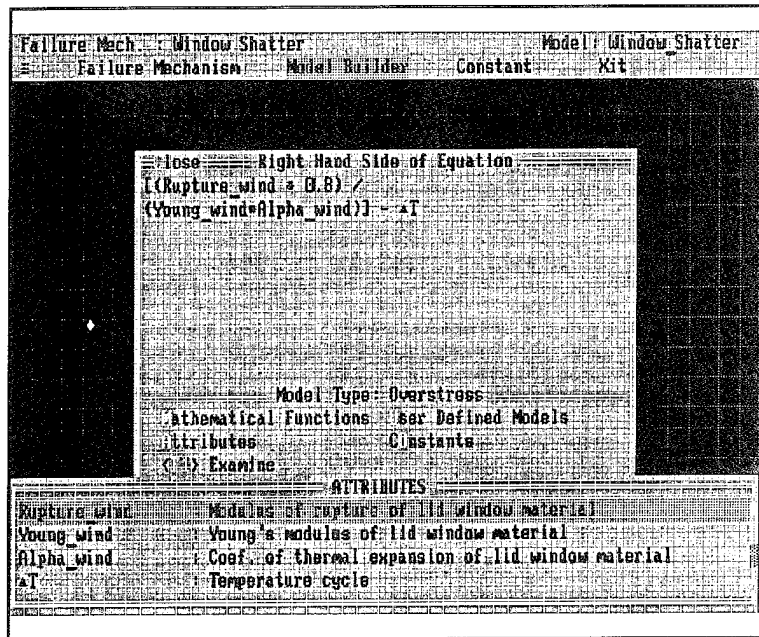


Figure 34 Window Shatter failure mechanism

Failure Mechanism : Shattering of Windows  
 Stress : Thermal Shock  
 Mechanism Type : Overstress  
 Criterion for failure : Environmental temperature cycle exceeding thermal shock temperature

$$\Delta T_{environ} > \Delta T_{Shock} \tag{11}$$

Model : The window shatters if

$$\Delta T_{shock} = \frac{\epsilon E_c (1 - \nu)}{E_c \alpha_s} \tag{12}$$

where,  $\epsilon E_c$  is the modulus of rupture  $N/cm^2$ ,  $E_c$  is the Young's modulus  $N/cm^2$ ,  $\alpha_s$  is the linear coefficient of expansion for the substrate material,  $^{\circ}C$ ,  $\nu$  is the Poisson's ratio (for dielectrics  $\sim 0.20$ )

Input to the Model :  $\epsilon E_c$  (from material database for particular window material)  
 $E_c$  (from material database for particular window material)  
 $\alpha_s$  (from material database for particular window material)  
 $\Delta_{\text{environ}}$  (from environmental database for chosen environment)

Output : Pass or Fail

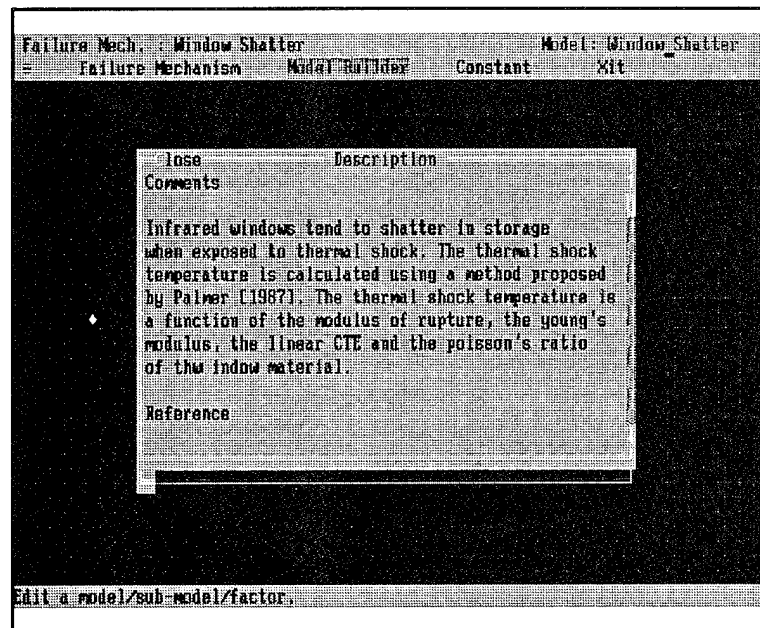


Figure 35 Comments on Window Shatter

**CADMP-IIe Description.** Infrared windows tend to shatter in storage when exposed to thermal shock. The thermal shock temperature is calculated using a method proposed by Palmer [1987]. The thermal shock temperature is a function of the modulus of rupture, the young's modulus, the linear CTE and the Poisson's ratio of the window material.

## Dewar Heat Leakage

An expression can be derived [Breckenridge, 1973] for the required, ideal weight of the cryogen (liquid or solid) as a function of cryogen properties, mission time, and environmental conditions. The following idealized conditions are assumed:

- 1) a spherical cryogen-Dewar for which the surface area for heat transfer is assumed to be  $\pi D^2$  and the volume available for the cryogen,  $\pi D^3/6$ , where D is the diameter.
- 2) The Dewar is insulated with a MLI system which is characterized by an effective emissivity of  $\epsilon_{\text{eff}}$ .
- 3) The only heat-leak into the cryogen is through the MLI.
- 4) The heat absorbed by the cryogen is the product of heat-leak and total elapsed time.

**CADMP-IIe Implementation.** The implementation of the window shattering model into CADMP-IIe is outlined below. Figure 36 shows the CADMP-IIe formation of the model. Definitions of each attribute are shown in Appendix B. Figure 37 shows the comments screen that is available for this and all other failure mechanisms. This includes the description of the model and the source of information.

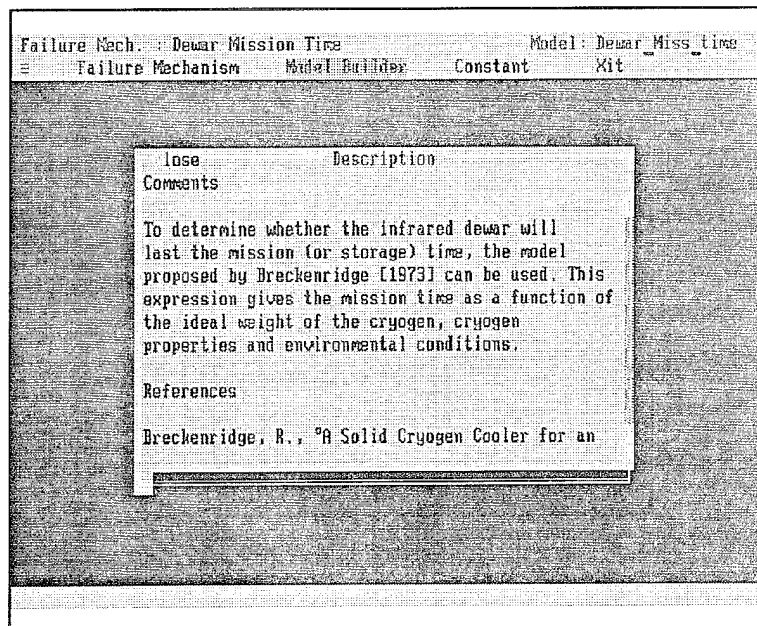
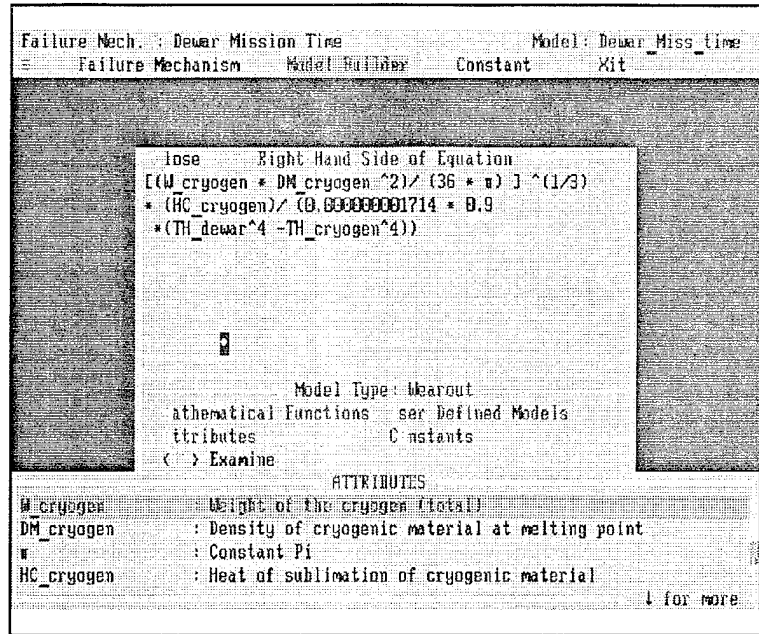


Figure 36 : Comments on Dewar Mission Time



**Figure 37** Dewar Mission Time failure mechanism

Failure Mechanism : Heat Leakage from Dewars  
 Stress : Temperature  
 Mechanism Type : Wearout  
 Criterion for failure : Storage time exceeds rated mission time of Dewar

Model : Mission time of Dewar is given by

$$t = \left[ \frac{W_c \rho^2}{36 \pi} \right]^{1/3} \frac{h_c}{\sigma \epsilon_{eff} (T_s^4 - T_c^4)} \quad (13)$$

where,  $W_c$  is the weight of cryogen required, lb;  $\rho$  is the density of cryogen, lb-f<sup>3</sup>;  $\sigma$  is the Stefan-Boltzmann constant,  $\epsilon_{eff}$  is the effective emissivity, dimensionless;  $T_s$  is the absolute temperature of the outer shell of vessel, K;  $T_c$  is the absolute temperature of the cryogen and inner shell of the MLI, K;  $t$  is the total elapsed time in hours;  $h_c$  is the latent heat of cryogen (heat of vaporization for a liquid or heat sublimation for a solid) Btu lb<sup>-1</sup>.

Input:  $W_c$  (user input, see Figure 38)  
 $\rho, h_c$  (from material database for particular cryogen chosen)  
 $T_c, T_s$  (user inputs, see Figure 38)

Output : Mission time in hours

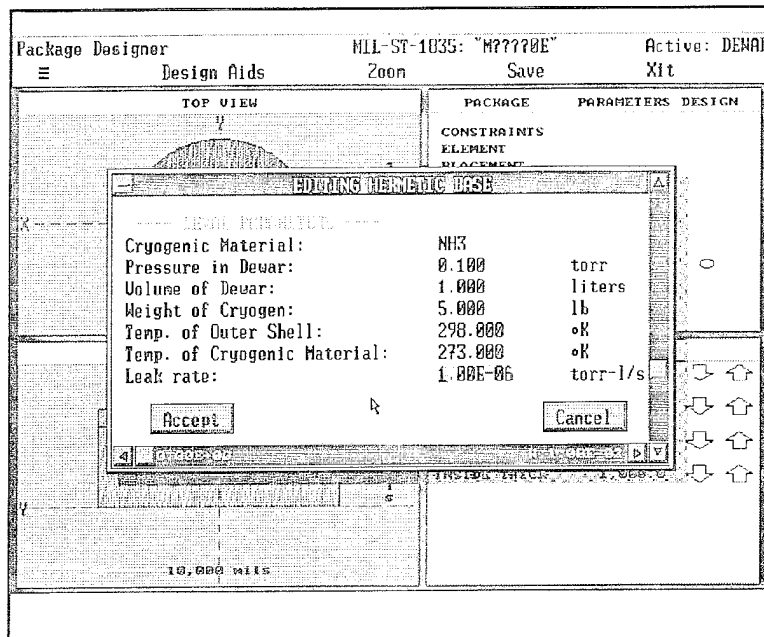


Figure 38 : User input of Dewar parameters

**CADMP-IIe Description.** To determine whether the infrared Dewar will last the mission (or storage) time, the model proposed by Breckenridge [1973] can be used. This expression gives the mission time as a function of the ideal weight of the cryogen, cryogen properties and environmental conditions.

### Dewar Outgassing

Cryogenes need to be isolated from room temperatures to keep them liquid and ready for use. This is normally done by keeping them in Dewars designed for the purpose. Storage Dewars normally have a large capacity and small-neck diameters. They are often provided by the cryogen supplier.

In these types of Dewars, leakage of the coolant and outgassing are often observed under long-term storage. Manufacturers and users of Dewars acknowledge that it is almost impossible to obtain a leak-free cryogenic cooler. The storage life of a Dewar can be calculated from the outgassing time as follows:

$$\frac{\left(\frac{P}{V}\right)}{L} = t_l \quad (14)$$

where  $P$  is the pressure in torr the Dewar is required to maintain,  $V$  is the volume of the Dewar in liters,  $L$  is the leak rate in (torr)L/sec, and  $t_l$  is the leak time or outgassing time.

**CADMP-IIe Implementation.** The implementation of the Dewar Outgassing model in CADMP-IIe is outlined below. Figure 39 shows the CADMP-IIe formation of the model. Definitions of each attribute are shown in Appendix B. Figure 40 shows the comments screen that is available for this and all other failure mechanisms. This includes the description of the model and the source of information.

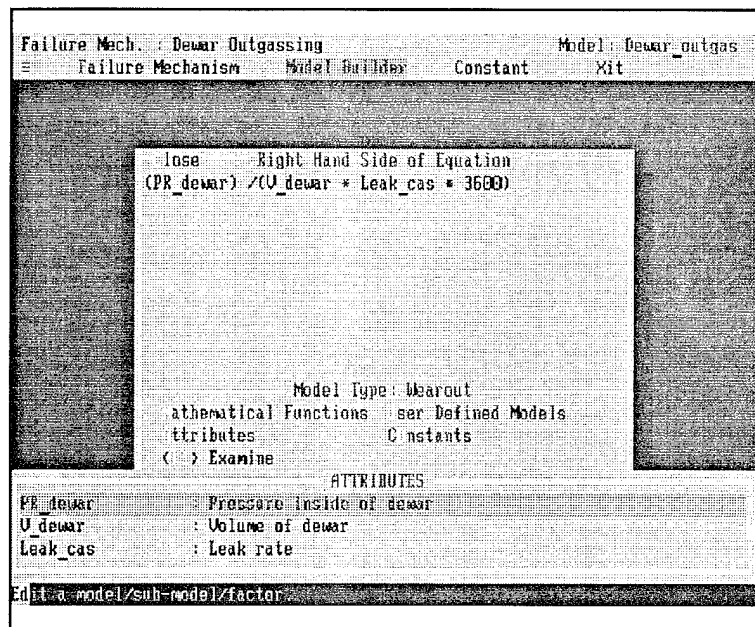


**Figure 39** Dewar Outgassing failure mechanism

Failure Mechanism : Dewar Outgassing  
 Stress : Leakage  
 Mechanism Type : Wearout  
 Criterion for failure : Storage time exceeds rated outgassing time of Dewar

Model : Outgassing time of Dewar is given by



$$\frac{\left(\frac{P}{V}\right)}{L} = t_l \quad (15)$$

where  $P$  is the pressure in torr the Dewar is required to maintain;  $V$  is the volume of the Dewar in liters;  $L$  is the leak rate in (torr)L/sec; and  $t_l$  is the leak time or outgassing time.

Input to the Model :  $P$  (user input, see Figure 41)  
 $V$  (user input, see Figure 41)  
 $L$  (user input, see Figure 41)

Output : Outgassing time in hours

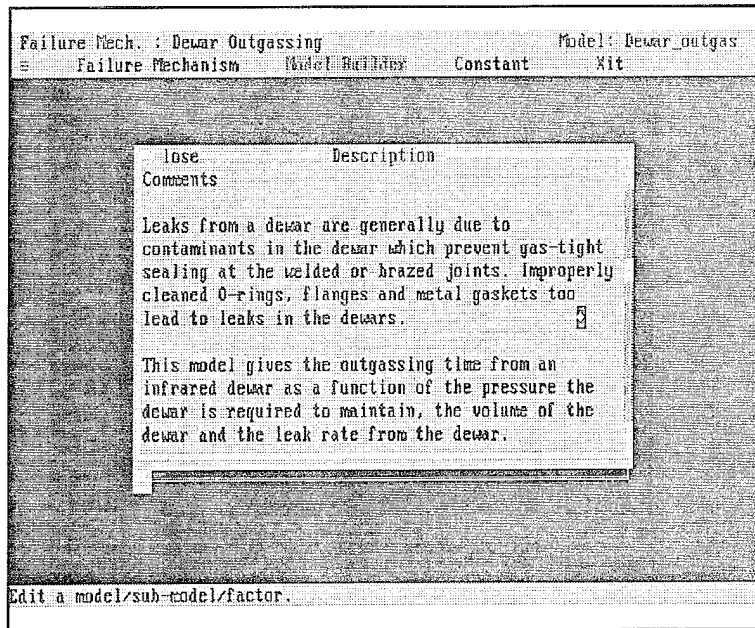


Figure 40 Comments on Dewar Outgassing

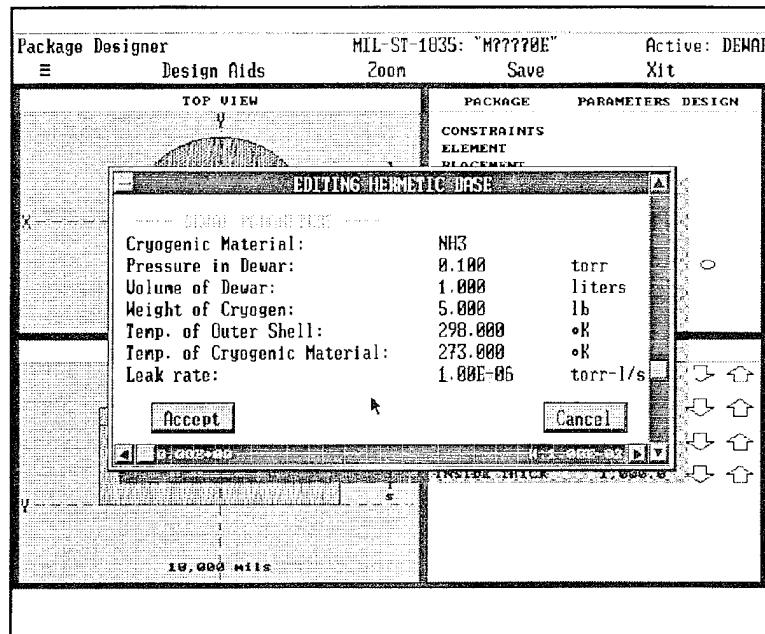


Figure 41 : User input of Dewar parameters

**CADMP-IIe Description.** Leaks from a Dewar are generally due to contaminants in the Dewar which prevent gas-tight sealing at the welded or brazed joints. Improperly cleaned O-rings, flanges and metal gaskets can lead to leaks in the Dewars. This model gives the outgassing time from an infrared Dewar as a function of the pressure the Dewar is required to maintain, the volume of the Dewar and the leak rate from the Dewar.

### Fatigue in Flip-chip Bumps of Hybrid Detectors

In hybrid Focal Plane Arrays there is a solder bump connection between the detector and the signal processing chip. The fatigue failure of these bumps during temperature cycling is one of the main failure modes in this package.

The mismatch in the coefficient of thermal expansion (CTE) between the chip and the detector material causes a shear displacement to be applied on each bump, which can lead to low-cycle fatigue failure due to thermal cycling. The flip-chip solder fatigue life is determined by modifying the Engelmaier model [1989] for leadless surface-mounted components. This equation incorporates elastic and inelastic strains, applicable for temperature changes of 10°C or above. For temperature cycles below 10°C, only elastic strain is involved and the Engelmaier equation no longer applies. Since low-cycle fatigue lives generally follow the Coffin-Manson low-cycle relationship, the mean cyclic fatigue life,  $N_f$ , is

$$N_f = \frac{1}{2} \left( \frac{\Delta\gamma}{2\epsilon_f} \right)^{\frac{1}{c}} \quad (16)$$

Where  $c$  is the fatigue ductility exponent, given by,

$$c = \alpha + \beta T_A + \gamma \ln \left( 1 + \frac{360}{t_D} \right) \quad (17)$$

and  $\epsilon_f$  is the fatigue ductility coefficient of the solder material,  $\Delta\gamma$  is the total cyclic strain range,  $T_A$  is the average temperature of the environment, and  $t_D$  is the half-cycle dwell time in minutes. Engelmaier computed  $\alpha$ ,  $\beta$ , and  $\gamma$  to be -0.442, -0.0006, and 0.0174 for 60/40 solder. The fatigue ductility coefficient plays an important role in enhancing the thermal fatigue life of the solder. A high fatigue ductility coefficient is required to accommodate strains induced due to the thermal coefficient of expansion mismatch between the chip and the detector and to avoid premature thermal fatigue failure. The maximum cyclic strain range,  $\Delta\gamma$ , is estimated by:

$$\Delta\gamma = \frac{d (\alpha_c - \alpha_d) \Delta T}{h} \quad (18)$$

where  $d$  is the distance of the bump from neutral axis,  $h$  is the height of the bump,  $\alpha_c$  and  $\alpha_d$  are the coefficients of thermal expansion of the chip and the detector, respectively, and  $\Delta T$  is the environmental temperature cycle.

Instead of determining the maximum cyclic strain range, a complicated procedure because of the time and temperature dependence of the percentage of strain due to creep and the percentage due to plasticity, Engelmaier uses Coffin's [1973] approach and determines the maximum cyclic strain range in terms of maximum available displacement and the time- and temperature-dependent fatigue ductility exponent to account for any remaining residual stresses. The maximum cyclic strain range is determined with the following assumptions:

- the bonding strength of the two interfaces (chip-to-bump and bump-to-detector) is strong enough to transmit the stress into the bump without any failure, thereby enabling all the strain in the joint to be absorbed by the bump;
- the joint is a homogeneous body and the distribution of strain depends only on the geometrical shape of the bump; and
- the joint has the shape of a truncated sphere.

**CADMP-IIe Implementation.** The flip-chip bump fatigue model has been implemented to CADMP-IIe as shown in Figure 42. Definitions of each attribute are shown in Appendix B. Figure 43 shows the comments screen that is available for this failure mechanism. This includes the description of the model and the source of information.

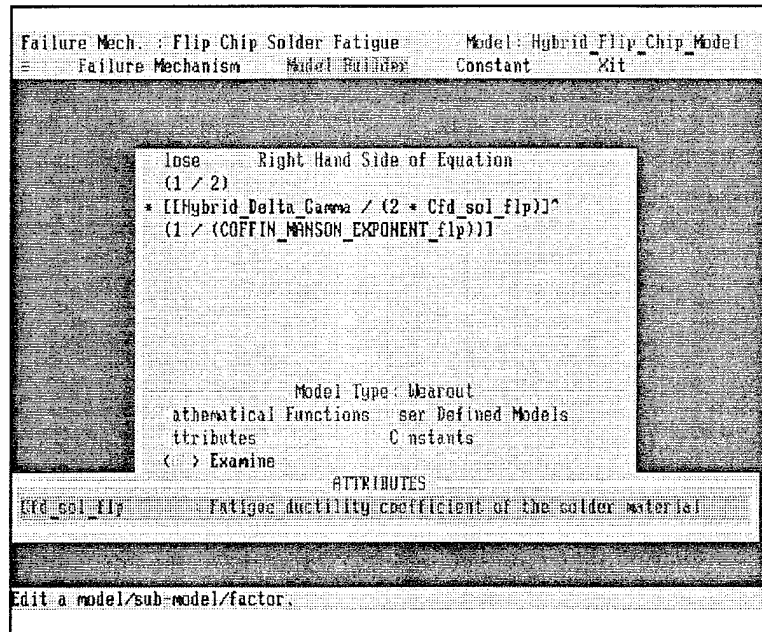


Figure 42 Flip Chip Solder Fatigue failure model

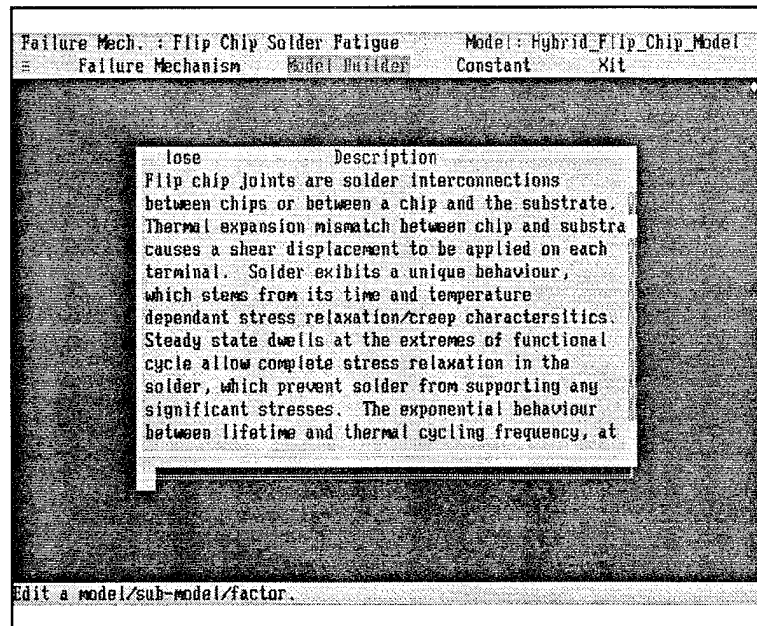


Figure 43 : Comments on Flip Chip Solder Fatigue

Failure Mechanism : Fatigue failure of bumps  
 Stress : Temperature Cycling  
 Mechanism Type : Wearout  
 Criterion for failure : Reaching end of low-cycle fatigue life

Model : Low cycle fatigue life of the bumps is given by

$$N_f = \frac{1}{2} \left( \frac{\Delta\gamma}{2\epsilon_f} \right)^{\frac{1}{c}} \quad (19)$$

where  $c$  is the fatigue ductility exponent, given by,

$$c = \alpha + \beta T_A + \gamma \ln \left( 1 + \frac{360}{t_D} \right) \quad (20)$$

and  $t_f$  is the fatigue ductility coefficient of the solder material,  $\Delta\gamma$  is the total cyclic strain range,  $T_A$  is the average temperature of the environment, and  $t_D$  is the half-cycle dwell time in minutes. the maximum cyclic strain range is given by:

$$\Delta\gamma = \frac{d (\alpha_c - \alpha_d) \Delta T}{h} \quad (21)$$

where  $d$  is the distance of the bump from neutral axis,  $h$  is the height of the bump,  $\alpha_c$  and  $\alpha_d$  are the coefficients of thermal expansion of the chip and the detector, respectively, and  $\Delta T$  is the environmental temperature cycle.

Input to the Model :  $N_f$  (from material database depending on flip-chip material chosen)  
 $c$  ( $\alpha$  and  $\beta$  from literature,  $T_A$  from environmental database)  
 $\alpha_c$ ,  $\alpha_d$  (from material database)  
 $d$  and  $h$  (depending on flip-chip type chosen, Figure 44)  
 $\Delta T$  (from environmental database)

Output : Low-cycle fatigue life of the bumps (number of cycles to failure)

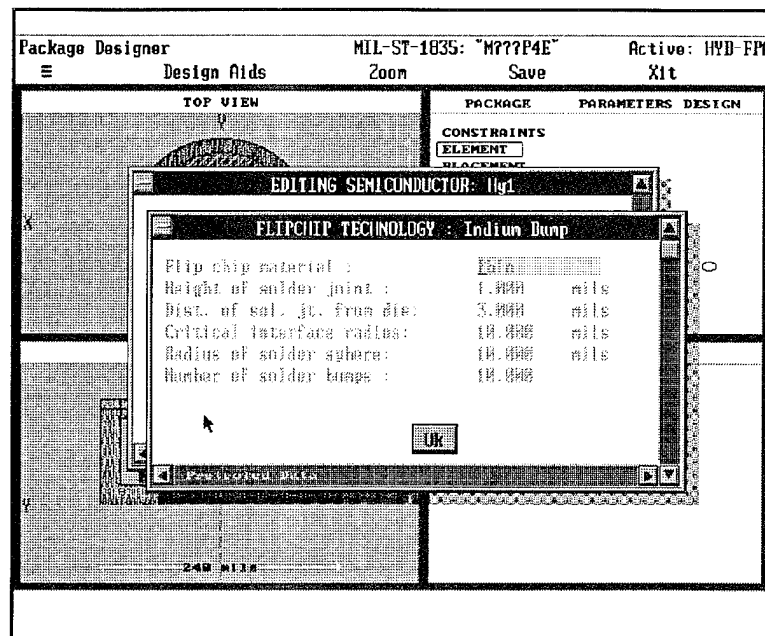


**Figure 44** : User input of flip-chip parameters

**CADMP-IIe Description.** Flip chip joints are solder interconnections between chips or between a chip and the substrate. Thermal expansion mismatch between the two chips causes a shear displacement to be applied on each terminal. Solder exhibits a unique behavior, which stems from its time and temperature dependant stress relaxation/creep characteristics. Steady state dwells at the extremes of the functional cycle allow complete stress relaxation in the solder, which prevent solder from supporting any significant stresses. The exponential behavior between lifetime and thermal cycling frequency, at constant strain amplitude, is widely documented for PbSn solders.

### Material Properties

To facilitate storage reliability assessment of electronics associated with infrared and millimeter-wave devices, the existing materials library had to be enhanced by adding new materials, property fields (in the software), and material property data. This report outlines the materials, fields, and properties which have been added to the library either under existing categories and new categories.

## Infrared Window Materials

Material	Strength (psi)	Fracture Toughness ( $K_{IC}$ ) (psi $\sqrt{in}$ )	Poisson's Ratio	Young's Modulus (psi)	Modulus of Rupture (psi)	Coefficient of Thermal Expansion ( $^{\circ}C$ )
ZnS	$1.5 \times 10^4$	730	0.29	$1.08 \times 10^7$	$1.08 \times 10^4$	$6.5 \times 10^{-6}$
ZnSe	$8.0 \times 10^3$	455	0.28	$9.75 \times 10^6$	$9.75 \times 10^3$	$7.57 \times 10^{-6}$
Si	$1.7 \times 10^4$	818	0.22	$2.17 \times 10^7$	$2.17 \times 10^4$	$2.5 \times 10^{-6}$
Ge	$1.8 \times 10^4$	818	0.28	$1.74 \times 10^7$	$1.74 \times 10^4$	$5.9 \times 10^{-6}$

Source : Pruszynski, C.J., "Overpressure Proof Testing of Large Infrared Windows for Aircraft Applications," in Tactical Infrared Systems, Proc. of SPIE, 1498, 1991, pp 165.

Pecht, M., "Handbook of Electronic Package Design," Marcel Dekker, 1991.

Optics Catalog and Optical Material Properties Sheet, II-VI, Inc., Saxonburg, PA 16056

### Solid Cryogen Properties

Symbol	Cryogen	Heat of Sublimation (Btu/lb)	Density of Solid at Melting Point (lb/ft <sup>3</sup> )	Operating Temperature Range (K) at 0.10 mm Hg
NH <sub>3</sub>	Ammonia	739.0	51.3	150.0
CO <sub>2</sub>	Carbondioxide	246.6	97.5	125.0
CH <sub>4</sub>	Methane	244.5	31.1	59.8
O <sub>2</sub>	Oxygen	97.5	81.3	48.1
A	Argon	79.8	107.0	47.8
CO	Carbon monoxide	126.0	58.0	45.5
N <sub>2</sub>	Nitrogen	96.6	63.8	43.4
Ne	Neon	45.5	89.8	13.5
H <sub>2</sub>	Hydrogen	218.5	5.02	8.3

Source : Donabedian, M., "Cooling Systems," Chapter in The Infrared Handbook, Environmental Research Institute, 1989, pp 15-23.



Ceramics for 3-5 Micron IR Transmission

Property	Magnesium Fluoride (MgF <sub>2</sub> )	Spinel (MgAl <sub>2</sub> O <sub>4</sub> )
Density (g/cm <sup>3</sup> )	3.18	3.58
Melting Point (°C)	1263	2130
Flexural Strength (MPa)	150	200
Young's Modulus (GPa)	114	270
Knoop Hardness	600	1400
Thermal Expansion Coefficient (10 <sup>-6</sup> K <sup>-1</sup> )		
25 - 200°C	10.4	6.7
25 - 500°C	11.7	7.7
Thermal Conductivity (W/mK)	15.9	16.9
Dielectric Constant (10 GHz)	5.05	8.10
Refractive Index (4μm)	1.353	1.685

Source : Shibata, K., Nakamura, H., Fujii, A., " Ceramics for 3-5 micron IR Transmission," Infrared Technology XV, Proc. of SPIE, 11517, pp 296, 1989.

## IR Optical Materials

Property	Ge	GaAs	GaP	Diamond IIa
Melting Point (°C)	937	1,238	1,467	3,770
Hardness (Kg/mm <sup>2</sup> )	850	700	845	9,000
Flexural Strength (psi)	13,500	8-14,000	15,000	120-150,000
Poisson's Ratio	0.28	0.31	0.31	0.16
Young's Modulus (GPa)	103.3	85.5	102.6	1,050
Thermal Expansion (10 <sup>-6</sup> /K)				
23°C	6.0	5.7	5.3	1.2
200°C	-	6.4	5.8	2.0
Thermal Conductivity (W/cm K)	0.6	0.53	0.97	0.52
Fracture Toughness (MPa m <sup>1/2</sup> )	0.66	0.43, 0.8	0.80	7.0

Source : Klocek, P, et al., "Optical Properties of GaAs, GaP, and CVD Diamond," Tactical Infrared Systems, Proc. SPIE, 1498, pp 148.

## Materials Database Enhancements in CADMP-IIe

Figures 45 through 47 are screens from the CADMP-IIe materials databases.

VIEW/EDIT DATA						ACTIVE : Window Materials	
Close	Material	Material	Edit	End	Menu		
Code #	Material ID	Material Name	Strength (psi)	Fracture Toughness (psi <sup>1/2</sup> in)	Poisson Ratio (Dimensionless)		
Dependence >							
402	ZnS	Zinc Sulfide	1.500E+04	7.3E+02	0.2900		
403	ZnSe	Zinc Selenide	8.000E+03	4.6E+02	0.2800		
404	Si	Silicon	1.700E+04	8.2E+02	0.2200		
405	Ge	Germanium	1.800E+04	8.2E+02	0.2800		

Figure 45 : Infrared Window Materials

VIEW/EDIT DATA						ACTIVE : Cryogenic Materials	
Close	Material	Material	Edit	End	Menu		
Code #	Material ID	Material Name	Heat of Sublimation (btu/lb)	Density at Melting Point (lb/ft <sup>3</sup> )	Op. Temp. Range (°K)		
Dependence >							
406	NH3	Nitrogen	739.00	51.30	150.		
407	CO2	Carbon dioxide	246.60	97.50	125.		
408	CH4	Methane	246.60	31.10	59.		
409	O2	Oxygen	244.50	81.30	48.		
410	Ar	Argon	97.50	107.00	47.		
411	CO	Carbon monoxide	79.00	50.00	45.		
412	N2	Nitrogen	126.00	63.00	43.		
413	Ne	Neon	96.60	89.00	13.		
414	H2	Hydrogen	218.50	5.02	8.		

Figure 46 : Cryogenic Materials

VIEW/EDIT DATA		ACTIVE : Lid Materials			
Code	Material ID	Material Name	Tensile Strength (Pa)	Poisson's Ratio (dimensionless)	Flexural Strength (Pa)
1	BeO	Beryllia-(99.5%)	1.520E+08	0.26	2.300E+07
2	SiC	Silicon-Carbide	1.190E+08	0.15	3.100E+07
3	AlN	Aluminum-Nitride	2.270E+08	0.25	2.700E+07
4	Al2O3	Alumina (white)	1.930E+08	0.22	3.500E+07
5	Mullite	Mullite	1.930E+08	0.22	1.400E+07
7	CuW	Copper-Tungsten	3.370E+09	0.30	1.100E+07
8	Kovar	Kovar	5.520E+08	0.30	7.400E+06
9	SiC-Al	SiC-Al MMC	1.380E+09	0.27	4.800E+06
10	Alloy42	Alloy 42	5.650E+08	0.30	7.400E+06
201	Al	Aluminum	8.190E+07	0.35	-
402	MgF2 (IR)	Magnesium Fl	-	0.30	1.500E+07
403	MgAl2O4 (IR)	Spinel	-	0.30	2.000E+07
404	ZnS (IR)	Zinc Sulfide	-	0.29	9.653E+06
405	GaP (IR)	Gallium Phosphide	-	0.31	1.034E+07
406	Diamond (IR)	Diamond IIa	-	0.16	1.034E+07

Figure 47 : IR Optical Materials (numbered 400 and above)

## CADMP-IIe Reliability Analysis

This section provides an overview of the kinds of storage analyses available from CADMP-IIe: reliability assessment, derating or sensitivity analysis, and acceleration testing analysis. For details on how to use these software features, consult the CADMP-IIe Tutorial or Reference Manual.

### Reliability Assessment

After the package is defined and the mission profile is set, the user can perform a reliability assessment. Reliability assessment actually performs calculations on each of the user-selected failure models and outputs the results to the screen or printer. The format of the output will depend on the type of failure mechanisms, wearout or overstress. If wearout, the output is in terms of time-to-failure; if overstress, the output is either pass or fail. The results are ranked in order of increasing time to failure followed by the overstress results as shown in Figure 48.

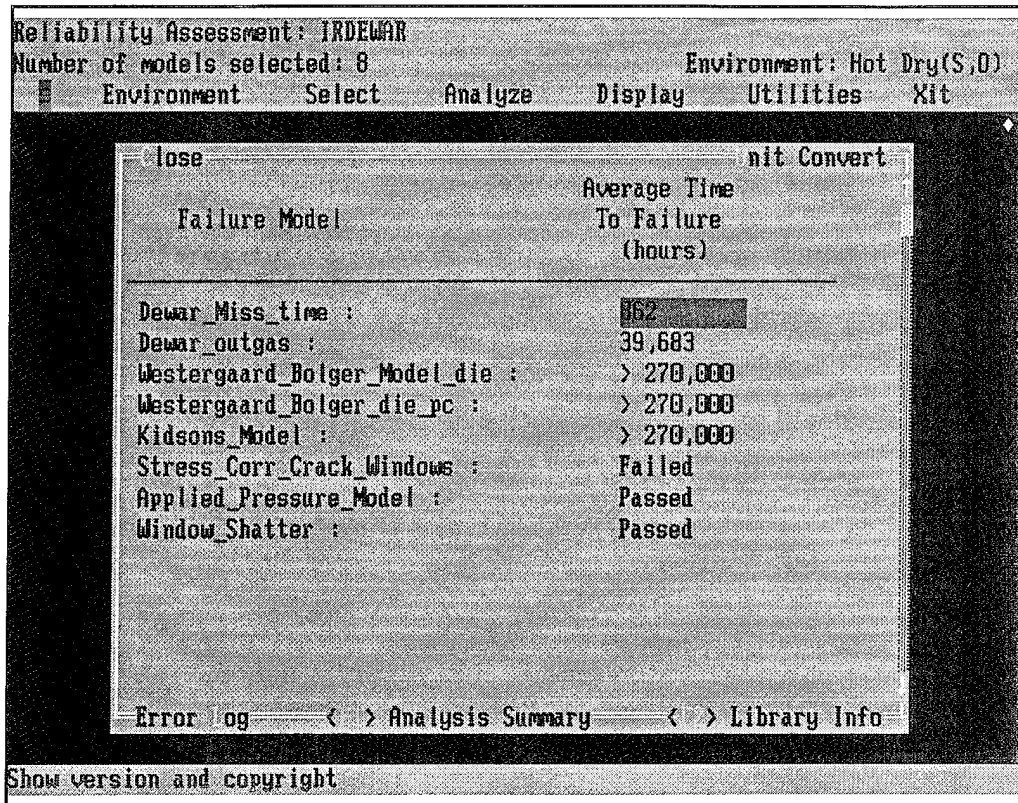


Figure 48 Ranked results of the reliability assessment

### Derating Option

The Derating option allows the user to optimize the operational loads versus rated strength relationship. There are two ways to do this: either the loads can be reduced versus rated strength or the strength can be increased for a given load. For wearout mechanisms, the stress margin is a nondimensional measure of the strength to load ratio. In overstress mechanisms, the stress margin is defined as the rated strength minus the applied load. In the Derating option, the function of the stress margin is plotted against either a design or environment attribute. This gives the user a graphical representation with which design trade-offs can be made.

Figure 49 illustrates a derating graph of the stress corrosion cracking mechanism which is found in Dewar packages. In this particular example, the thickness of the lid window is plotted against the stress margin. Since window stress corrosion cracking is an overstress mechanism, the stress margin is defined as the difference between the rated strength (stress intensity factor) and the load stress. In this case, if the stress margin is negative, the Dewar window will fracture. The dotted indicator in the chart highlights the point at which the stress margin is zero; i.e., that point at which the stress load is just equal to the stress

intensity factor. Figure 49 shows that to keep the window from cracking, its thickness must be greater than 3.3 mils.

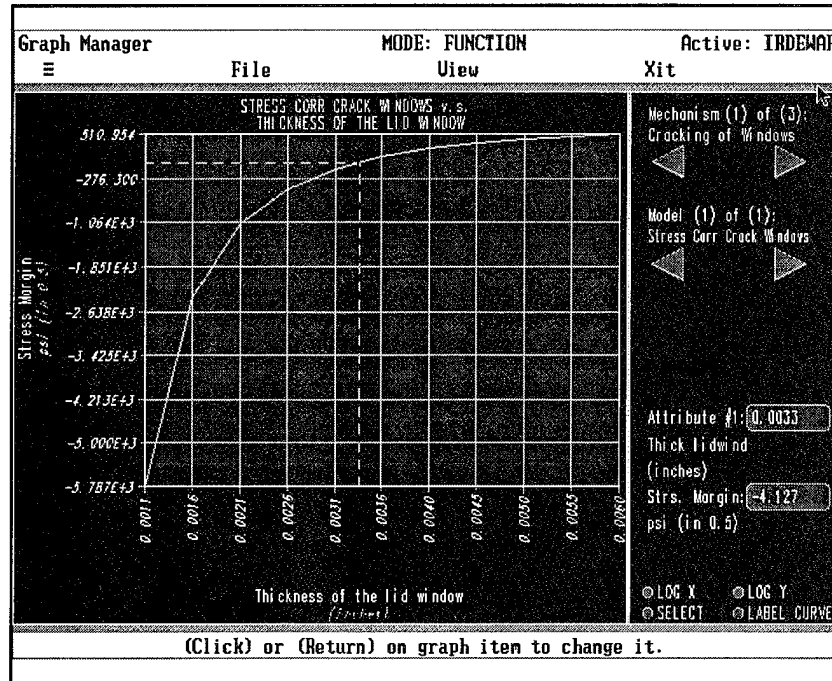


Figure 49 Example of the CADMP-IIe derating function

### Accelerated Testing Analysis

In accelerated tests, components are exposed to more severe loading than would be experienced in storage or operation. The purpose of the tests are to assess, demonstrate, and improve reliability in the design process. The Testing analysis tool can solve two types of problems: the sensitivity of the device life can be determined with respect to environment, design and material attributes, or the sensitivity of one variable can be plotted against another while keeping the life constant. The first problem is similar to the type of problem described in Derating analysis; the accelerated test environment is selected instead of the operational or storage environment. The second problem is particularly useful for determining what the accelerated test environment should be in order to have a test of a certain time duration. In the Testing screen, the user identifies the stresses, failure modes of interest, and fixed time limit. Figure 50 shows an example of a pressure test of a Dewar package which was limited to 150 hours. In this case Dewar pressure and leak rate are the variables of consideration.

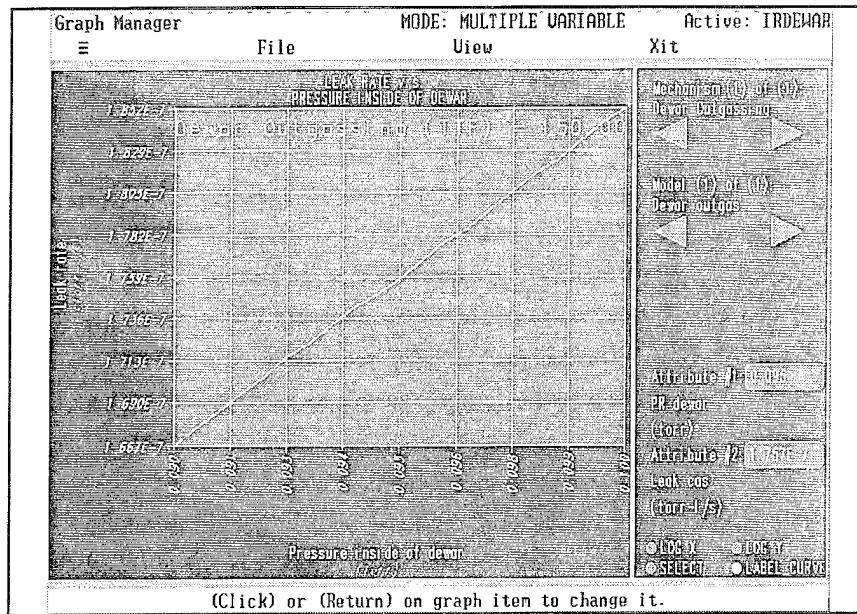


Figure 50 The Accelerated Test Results window

## CONCLUSIONS

The effort to identify failure mechanisms and PoF models consisted of a questionnaire and literature search. A questionnaire requesting information for IR and MMW failure mechanisms, was developed and sent to experts from a variety of organizations: device suppliers, systems houses, major contractors, universities, and government agencies. The responses, conversations with respondents, and literature search provided background for the engineering reference book titled, "Long-term Non-operating Reliability of Electronic Products," to be published by CRC Press. This book provides a documented investigation into the area of electronic storage reliability, and outlines failure models for key electrical, corrosion, radiation and mechanical failure mechanisms.

A software tool which facilitates the physics-of-failure reliability analysis for microcircuits subject to long-term storage was developed. This was called CADMP-IIe. Inputs to the software include geometric, material, and mounting characteristics of the device. Many storage environments from typical munitions storage climates are part of the software's environment database. Besides the general electronics packages (DIP, LCC, PGA, QFP, etc.), CADMP-IIe includes millimeter wave and infrared package architectures. Several failure mechanisms were added to address the unique aspects of these IR and MMW devices.

The software tool provides a useful design aid to assess storage reliability and to point out potential failure mechanisms associated with packaging methods, new technologies, materials and designs. Reliability evaluations can be performed at the major failure sites of a microelectronic package, including: the die, circuitry on the die, die attach, the substrate, circuitry on the substrate, substrate attach, interconnections, case, lid, lid seal, lead, and lead seal.

The CADMP-IIe software runs on IBM compatible personal computers. It is menu driven, and the user is not required to manipulate equations. The description, assumptions, validation methods and reference source for the models, materials, and storage environments are accessible within the software. The software allows the user to evaluate reliability in terms of average-time-to-failure and rank the dominance of each potential failure mechanism. Sensitivity analysis and derating provides optimization of the design and accelerated tests.

## RECOMMENDATIONS

Although in present form, CADMP-IIe is a useful design tool, certain upgrades and features should be added to allow better integration into the electronics design process. Three future projects are recommended:

- Develop a UNIX version of CADMP-IIe,
- Enhance capability to assess plastic encapsulated microcircuits,
- Develop and integrate CADMP-IIe with board- and assembly-level reliability tools.

### UNIX-based CADMP-IIe

A UNIX implementation of CADMP-IIe would have several advantages over the DOS version. UNIX on engineering workstations has more processing power and allows for multitasking. Multitasking would give flexibility to the user by allowing parallel running of different design cases on a single machine. Thus, a UNIX version of CADMP-IIe would bring greater acceptance, enhanced functionality, and increased flexibility and speed. In addition, it would be more compatible with the platform most often used in electronics design. Throughout industry, simulation, layout, and assembly software tools are generally UNIX-based. In discussions with electronics design engineers, several have requested a UNIX version of CADMP-IIe, leading us to believe that UNIX would probably enjoy greater user acceptance than the DOS version.

A second advantage of UNIX is that it would enable more sophisticated analysis by interfacing to finite element analysis (FEA) software. CADMP-IIe would be a convenient



front-end for the finite element program. The design, materials, and geometry could be defined in CADMP-IIe, and then sent to the FEA program for meshing and analysis. The results could be returned to CADMP-IIe to be combined with the rest of the reliability assessment.

#### Enhance Plastic Encapsulated Microcircuit Capability

With plastic encapsulated microcircuits now being designed into many military systems, maintaining high reliability (during storage and operation) is very important. PEM design methods, screens, and acceleration tests should be introduced into the CADMP-IIe software.

To withstand high acceleration loads, smart weapon electronics assemblies are often potted with polymeric compounds. After curing, some potting materials can impose high residual stresses on the devices and leads. These initial stresses may have an impact on interconnect and device reliability. Potting materials also absorb moisture and can contain ionic impurities which contribute to corrosion or conductive filament growth. Models to address these issues should be investigated and included in CADMP-IIe.

#### Develop Assembly Reliability Tools and Integrate with CADMP-IIe

Integrating board- and assembly-level stresses with the device level would be extremely valuable. For example, circuit board vibration is not considered in CADMP-IIe, although the capability to define the vibration environment does exist. By including vibration dependent failure mechanisms such as high cycle lead fatigue, the reliability effects of transportation environments could be more accurately assessed. The magnitude of these vibrational loads at the component level depend on the several variables, including: component placement, component size, board fixturing, board materials and design geometry. Software needs to be developed which addresses these variables in solder joint and printed wiring board failure mechanisms.

This software tool should be compatible with and supplement existing electrical CAE design frameworks, thus facilitating its acceptance by the electronics design community. An important interface would link the PWB design/layout tools and the CADMP-IIe software input, making it possible to easily pass component and placement information between them. Reliability assessments can thus be performed almost simultaneously with board design. This linkage would truly bring the key reliability considerations into the design process.

## REFERENCES

AR70-38, "Research, Development, Test and Evaluation of Materiel for Extreme Climatic Conditions," September 1979.

Ailles, C.R. and Neira, G., "Dormant Storage Effects on Electronic Devices," U.S. Army ARDEC Report no. ARFSD-CR-89014, August 1989.

Asthemier, R.W., "Thermistor Infrared Detectors," Infrared Detectors, Proceedings of SPIE 443, pp. 95-109, 1983.

Australian Ordnance Council, "Effects of Solar Radiation on Ammunition," Proceeding 14/83 (1983).

Breckenridge, R., "A Solid Cryogen Cooler for an X-ray Spectrometer," presented at the NASA Cryogenic Workshop, Marshall Space Flight Center, Huntsville, AL, March 29-30, 1973.

Coit, D.W. and Priore, M.G., "Impact of Nonoperating Periods on Equipment Reliability," (RADC-TR-85-91), Rome Air Development Center, Air Force System Command, Griffiss Air Force Base, NY, (May 1985).

Coffin, L.F., "Fatigue at High Temperatures," ASTM, STP 520 PA, 1973.

Corsi, C., "Smart Sensors," Infrared and Optoelectronic Materials and Devices, Proceedings of SPIE 1512, pp 52-59, 1991.

Cramer, D.C., et.al., "Moisture and Water Induced Crack Growth in Optical Materials," Ceramics Division, National Institute of Science and Technology.

CVD, Inc., "Infrared Materials Product Brochure."

Currie, N.C. and Brown, C.E., "Principles and Applications of Millimeter-Wave Radar," Artech House, Inc., Norwood, MA, 1987.

Cushing, M., et.al., "Comparison of Electronics Reliability Assessment Approaches," *IEEE Transactions on Reliability*, 42 (December 1993), 600-607.

Cushing, M., et.al., "Design Reliability Evaluation of Competing Causes of Failure in Support of Test-Time Compression," *Proceedings of the Institute of Environmental Sciences*, (1994).

Dataquest Inc., "Computer Aided Manufacturing International," 1990.

Davis, J.R., et.al., *Metals Handbook Corrosion*, 9th edition, 13, ASM International, Metals Park, Menlo, OH, 1987.

Donabedian, M., "Cooling Systems," Chapter in *The Infrared Handbook*, Environmental Research Institute, 1989, pp 15-23.

Engelmaier, W., "Surface Mount Solder Joint Long-Term Reliability: Design, Testing, Prediction," *Soldering and Surface Mount Technology*, 1, 1989, pp. 14-22.

Evans, A.G., et.al, "Proof Testing of Ceramic Materials - An Analytical Basis for Failure Prediction," *International Journal of Fracture*, Vol. 10, pp. 379-392, 1974.

Georgia Tech Continuing Education Course, "Infrared Technology and Applications," Washington, D.C., April 12-14, 1994.

Harris, A.P., "Reliability in the Dormant Condition," *Microelectronics and Reliability*, Vol. 20, (1980).

Howard, T.W., "Stockpile Reliability Program," Army Research, Development, and Engineering Center Briefing, 14 Dec 1994.

Johnson, T.H., "Lead Salt Detectors and Arrays," *Infrared Detectors - Proceedings of the SPIE*, Volume 443, pp. 60-94, 1983.

Jowett, C.E. *Electronics and Environments*, New York, John Wiley and Sons, (1973).

Klocek, P, et al., "Optical Properties of GaAs, GaP, and CVD Diamond," *Tactical Infrared Systems*, Proc. SPIE, 1498, pp 148.

Kuster, H., and Ebert, J., "Pyroelectric Measurement of Absorption in Oxide Layers and Correlation to Damage Threshold," *Laser Induced Damage in Optical Materials: 1979*, NBS Spec. Pub. 568, 1980.

McMillan, R.W., "MMW Solid-State Sources" in book titled, "Principles and Applications of Millimeter-Wave Radar," Artech House, Inc., Norwood, MA, 1987.

Melmed, M., "Long-Term Inactive Storage Effects on Electronic Devices and Assemblies in Support of SADARM," (ARFSD-TR-90015) U.S. Army Armament Research, (1991). Development, and Engineering Center, Picatinny Arsenal, NJ (November 1990).

Norris, K.C., and Landzberg, A.H., "Reliability Of Controlled Collapse Interconnections", IBM J. Res Dev.(USA), Vol.13, No.3, May 1969.

Palmer, J.R., "Hostile High Energy Visible Laser Environment Providing Destruction of Optical Signal in Imaging Systems," Optical Devices in Adverse Environments, Proc. of the SPIE, Vol. 867, 1987.

Pecht Associates, Inc. "Effect of Long-Term Storage on Electronic Devices," Final Technical Report, DAAA21-91-C-0023, Phase-I study submitted to U.S. Army ARDEC, August 1991.

Pecht, J. and Pecht, M., *Long-term Non-operating Reliability of Electronic Products*, CRC Press, Boca Raton, FL, July 1995.

Pecht, M., *Handbook of Electronic Package Design*, Marcel Dekker, 1991.

Pompei, D., "Climatological Conditions and Effects on Storage at Selected Conus Army Ammunition Depots," (QAR-R-018) AMCCOM, Dover, NJ 1985.

Pruszyński, C.J., "Overpressure Proof Testing of Large Infrared Windows for Aircraft Applications," Tactical Infrared Systems, Proceedings of the SPIE, Volume 1498, May 1991.

II-VI Inc., "Optics Catalog and Optical Material Properties Sheet," Saxonburg, PA 16056

Resnick, M. and Riedinger, V.T. "Munitions Testing at Proving Grounds and in Desert, Arctic, and Tropical Environments," *Technical Memorandum 1607*, Picatinny Arsenal, NJ (1965).

Rode, J.P., "Hybrid HgCdTe Arrays," Infrared Detectors - Proceedings of the SPIE Volume 443, pp 120-130, 1983.

Shibata, K., Nakamura, H., Fujii, A., "Ceramics for 3-5 micron IR Transmission," *Infrared Technology XV*, Proc. of SPIE, 11517, pp 296, 1989.

Sim, S.P., "The Reliability of Laser diodes and Laser Transmitter Modules," *Microelectronics Reliability*, Vol. 33, No. 7, pp 1011-1030, 1993.

Sim, S.P., Skeats, A.P., Skrimshire, C.P. and Collins, J.V., "Reliability Testing of Optoelectronic Components," *British Telecom Technological Journal*, Vol. 4, No.2, pp. 104-113, April, 1986.

Skolnik, M.I., "Introduction to Radar Systems," McGraw-Hill Book Company, New York, 1980.

Vincent, J.D., "Fundamentals of Infrared Detector Operation and Testing," John Wiley & Sons, New York, 1990.

Wolfe, W.L. and Zissis, G.J., "Infrared Handbook", ERIM-Michigan, 1989.

**APPENDIX A**  
**QUESTIONNAIRE AND RESPONSE SUMMARY**



DEPARTMENT OF THE ARMY  
U.S. ARMY ARMAMENT RESEARCH, DEVELOPMENT AND ENGINEERING CENTER  
PICATINNY ARSENAL, NJ 07806-5000



REPLY TO  
ATTENTION OF

Electronics and Producibility  
Branch

SUBJECT: Effects of Long-Term Storage on Electronic Devices

Pecht Associates Incorporated, Hyattsville, MD is presently under contract to the US Army Armament Research, Development and Engineering Center (ARDEC) to evaluate the effects of long-term inactive storage on the various sensor electronics used in SMART MUNITIONS.

Electronic components and devices used in one-shot SMART MUNITIONS experience a completely different life-cycle than most electronic components. They will be stored for long periods, sometimes up to 20 years, in an inactive state and then must operate reliably over a short, active lifetime.

Little is known about the failure modes and the failure mechanisms that act on these electronic components during long-term storage. Pecht Associates, Inc., is involved in developing physics-of-failure based storage reliability models to address this problem.

As a company with valuable experience in developing and testing electronic components, you can assist in evaluating the effects of long-term storage on SMART MUNITIONS sensor electronics by completing the attached questionnaire. Any other pertinent information you may have that could benefit our endeavor would also be appreciated. Please return any/all information to: Ms. Judy Pecht, Pecht Associates, Inc., 7027 Hunter Lane, Hyattsville, MD 20782. To assure adequate time for review of your response, please return the completed questionnaire at your earliest convenience.

Your assistance in this effort is greatly valued by the Army. If you have any questions, please contact Ms. Judy Pecht at 301-927-4567.

It is understood that this letter is not intended to be a commitment by the Government which could form the basis of a claim for compensation. A contracting officer is the only individual authorized to incur legal obligations on behalf of the Government.

Sincerely,

Chief, ~~Electronics~~ and  
Producibility Branch

Enclosures



## QUESTIONNAIRE

1. Please provide the following information about yourself

Name \_\_\_\_\_  
Organization \_\_\_\_\_  
Job Title \_\_\_\_\_  
Years Experience \_\_\_\_\_  
Address \_\_\_\_\_  
\_\_\_\_\_  
Phone Number \_\_\_\_\_  
Fax Number \_\_\_\_\_  
E-mail \_\_\_\_\_

After completing this questionnaire, please mail it in the attached envelope to :  
Ms. Judy Pecht, Pecht Associates, Inc., 7027, Hunter Lane, Hyattsville, MD 20782

## QUESTIONNAIRE

We are interested in assessing the storage reliability of the following components that are connected with infrared and millimeter-wave sensors and other smart munition electronics.

Infrared Sensor	Millimeter-wave Sensor	Signal Processing Electronics
<p>a) detectors</p> <ul style="list-style-type: none"> <li>◦ photovoltaic               <ul style="list-style-type: none"> <li><input type="checkbox"/> HgCdTe (3-5 <math>\mu\text{m}</math>, 8-12 <math>\mu</math>)</li> <li><input type="checkbox"/> InSb (3-5 <math>\mu\text{m}</math>)</li> <li><input type="checkbox"/> Ge (1-1.9 <math>\mu</math>)</li> <li><input type="checkbox"/> Si (0.3-1.1 <math>\mu\text{m}</math>)</li> <li><input type="checkbox"/> CdSe (0.2-0.7 <math>\mu\text{m}</math>)</li> <li><input type="checkbox"/> InAs (1.8-2.7 <math>\mu\text{m}</math>)</li> </ul> </li> <li>◦ photoconductive (intrinsic)               <ul style="list-style-type: none"> <li><input type="checkbox"/> HgCdTe (3-5, 8-12 <math>\mu\text{m}</math>)</li> <li><input type="checkbox"/> InSb (3-5 <math>\mu\text{m}</math>)</li> <li><input type="checkbox"/> PbS (1-4.5 <math>\mu\text{m}</math>)</li> <li><input type="checkbox"/> PbSe (1-7 <math>\mu\text{m}</math>)</li> <li><input type="checkbox"/> Si (0.2-0.7 <math>\mu\text{m}</math>)</li> <li><input type="checkbox"/> Ge (0.5-1.8 <math>\mu\text{m}</math>)</li> </ul> </li> <li>◦ schottky barrier               <ul style="list-style-type: none"> <li><input type="checkbox"/> PtSi</li> <li><input type="checkbox"/> IrSi</li> <li><input type="checkbox"/> CdS</li> </ul> </li> </ul> <p>b) coolers</p> <ul style="list-style-type: none"> <li><input type="checkbox"/> thermoelectric</li> <li><input type="checkbox"/> cryogenic</li> </ul> <p>c) optics</p> <ul style="list-style-type: none"> <li><input type="checkbox"/> lens</li> <li><input type="checkbox"/> mirror</li> <li><input type="checkbox"/> coating</li> <li><input type="checkbox"/> filter</li> </ul> <p>d) <input type="checkbox"/> focal plane arrays and header assembly</p>	<p>a) technology</p> <ul style="list-style-type: none"> <li><input type="checkbox"/> MIMIC</li> <li>MICs</li> <li>microstrip               <ul style="list-style-type: none"> <li><input type="checkbox"/>- soft substrate</li> <li><input type="checkbox"/>- hard substrate</li> </ul> </li> <li><input type="checkbox"/> wave guide technologies</li> </ul> <p>b) components</p> <ul style="list-style-type: none"> <li>◦ gunn diode               <ul style="list-style-type: none"> <li><input type="checkbox"/> GaAs</li> <li><input type="checkbox"/> InP</li> <li><input type="checkbox"/> Si</li> </ul> </li> <li><input type="checkbox"/> varactor diode</li> <li><input type="checkbox"/> IMPATT diode</li> <li><input type="checkbox"/> injection locked amplifier</li> <li><input type="checkbox"/> magnetrons</li> <li><input type="checkbox"/> klystrons</li> <li><input type="checkbox"/> gyrotrons</li> <li><input type="checkbox"/> travelling wave tubes (TWT)</li> <li><input type="checkbox"/> crossed fields amplifiers (CFA)</li> <li><input type="checkbox"/> extended interaction amplifiers (EIA)</li> <li><input type="checkbox"/> extended interaction amplifiers (EIA)</li> <li><input type="checkbox"/> power grid tubes</li> <li><input type="checkbox"/> circulators</li> <li><input type="checkbox"/> low noise amplifier (LNA)</li> <li><input type="checkbox"/> duplexer</li> <li><input type="checkbox"/> RF switch</li> <li><input type="checkbox"/> mixers</li> <li><input type="checkbox"/> mixer diodes</li> <li><input type="checkbox"/> IF amplifiers</li> <li><input type="checkbox"/> pin diodes</li> <li><input type="checkbox"/> feedthroughs (contact and non-contact)</li> <li><input type="checkbox"/> microstrip antenna</li> </ul>	<p>a) memories</p> <ul style="list-style-type: none"> <li><input type="checkbox"/> EPROM</li> <li><input type="checkbox"/> EEPROM</li> <li><input type="checkbox"/> RAM</li> <li><input type="checkbox"/> ROM</li> </ul> <p>b) PWB</p> <ul style="list-style-type: none"> <li><input type="checkbox"/> multilayer</li> <li><input type="checkbox"/> flex boards</li> <li><input type="checkbox"/> kapton</li> </ul> <p>c) programmable devices</p> <ul style="list-style-type: none"> <li><input type="checkbox"/> FPGAs</li> <li><input type="checkbox"/> PALs</li> <li><input type="checkbox"/> VLSI</li> <li><input type="checkbox"/> LSI</li> </ul> <p>d) ASIC technology digital analog and mix signal</p> <ul style="list-style-type: none"> <li><input type="checkbox"/> CMOS</li> <li><input type="checkbox"/> BIMOS</li> <li><input type="checkbox"/> bipolar</li> <li><input type="checkbox"/> HCMOS</li> <li><input type="checkbox"/> CBIP</li> <li><input type="checkbox"/> CBICMOS</li> <li><input type="checkbox"/> GaAs</li> </ul> <p>e) packages</p> <ul style="list-style-type: none"> <li><input type="checkbox"/> LCC</li> <li><input type="checkbox"/> DIPS</li> <li><input type="checkbox"/> TAB</li> <li><input type="checkbox"/> SMT</li> <li><input type="checkbox"/> flip chip</li> <li><input type="checkbox"/> EP/TAB</li> <li><input type="checkbox"/> CANS</li> <li><input type="checkbox"/> QUAD</li> <li><input type="checkbox"/> SIP</li> <li><input type="checkbox"/> SOIC</li> <li><input type="checkbox"/> SOT</li> <li><input type="checkbox"/> ball grid array</li> <li><input type="checkbox"/> thin film hybrids</li> <li><input type="checkbox"/> chip on board</li> <li><input type="checkbox"/> thick film hybrids</li> </ul> <p>f) crystals</p> <ul style="list-style-type: none"> <li><input type="checkbox"/> tuning fork</li> <li><input type="checkbox"/> quartz</li> </ul>

1. Please check those components that your Company manufactures/tests/utilizes or that you are familiar with ?
2. Have you conducted reliability assessment (operational or storage) on any of these components? If yes, please circle the relevant components and provide details and results of the assessment and any data obtained.

3. In your opinion what are the predominant failure mechanisms in these components under long-term storage conditions ? Also, please mention any failure mechanism models that you might be aware of.

4. Are you aware of other personnel who might be able to provide more information on the above questions ? If yes, please provide names and phone numbers.

## RESPONSE TO QUESTIONNAIRE

<p>Edward Abraham R &amp; QA Manager Motorola, Inc. 5005 E. McDowell Road Phoenix, AZ 85008</p>	<p>05/21/94 sent 01/10/95 resent</p>
<p>Harris Adams Coast Magnetics 1207 N. La Brea Avenue Inglewood, CA 90302 (213) 673-3254</p>	<p>05/21/94 sent 01/10/95 resent</p>
<p>David H. Alexander Hughes Aircraft Company MS EO/EO1/A183 P.O.Box 902 El Segundo, CA 90245 (310) 616-4812</p>	<p>05/21/94 sent 01/10/95 resent</p>
<p>Joel Askinazi Hughes Danbury Optical Systems, Inc. 100 Wooster Heights Road Danbury, CT 06810-7589</p>	<p>05/21/94 sent 01/10/95 resent</p>
<p>Robert W. Astheimer Barnes Engineering Company 44 Commerce Road Stamford, CT 06904</p>	<p>05/21/94 sent 01/10/95 resent</p>
<p>Dr. Richard Augeri AIL Systems, Inc. Commack road Deer Park, NY 11729 (516) 595-3286</p>	<p>Unable to forward as addressed Returned 10/26/94</p>
<p>Shankar B. Bagliga Servo Corporation of America 111 New South Road Hicksville, NY 11802-1490 (516) 938-9700 x314</p>	<p>Response Received 9/15/94 Data asked for is not available</p>

<p>M. Baker  Allied Signal, Inc.  101 Columbia Road  Morristown, NJ 07962-1021  (201) 455-5149</p>	<p>05/21/94 sent  01/10/95 resent</p>
<p>J. Barrett  Allied Signal, Inc.  101 Columbia Road  Morristown, NJ 07962-1021  (201) 455-5164</p>	<p>05/21/94 sent  01/10/95 resent</p>
<p>Randy Bass  Honeywell  10701 Lyndale Avenue, S.  Bloomington, MN 55420  (612) 956-4565</p>	<p>05/21/94 sent  01/10/95 resent</p>
<p>Tom Beiree  Raytheon Company  Missile Systems Laboratories  P.O.Box 1201  50 Apple Hill Road  Tewksbury, MA 01876-0901  (508) 858-1995</p>	<p>05/21/94 sent  01/10/95 resent</p>
<p>Curtis Birnbach  Hudson Research, Inc.  P.O. Box C  New Rocherelle, NY 10804-0122  (914) 576-7990</p>	<p>05/21/94 sent  01/10/95 resent</p>
<p>E. Scott Blackwell  OPTO MECHANIK, Inc.  425 N. Drive  P.O. Box 361907  Melbourne, FL 32935  (407) 254-1212</p>	<p>05/21/94 sent  01/10/95 resent</p>
<p>Dr. Mark Greiner  Cincinnati Electronics Corp.  7500 Innovation Way  Mason, OH 45050-9699  (513)573-6188</p>	<p>Response received 7/22/94 (from Mr. Tom Wisnewski). "PbS detectors are sensitive to light exposure and to humidity over long term conditions"</p>

<p>Barry Breindel Aerojet 1025 Connecticut Avenue, N.W. Suite 1107 Washington, DC 20036 (202) 828-6865</p>	<p>05/21/94 sent 01/10/95 resent</p>
<p>Joe Carcone Sanyo Electronics, Inc. 200 Risen Road Little Ferry, NJ 07643</p>	<p>Response received 7/27/94 (from by Mr. Akifumi Goto). They are not manufacturers but distributors.</p>
<p>Dr. Lewis T. Claiborne Loral Vought Systems Incorporated P.O. Box 650003 Dallas, TX 75265-0003 (214) 603-9052</p>	<p>05/21/94 sent 01/10/95 resent</p>
<p>Dr. William Clark Army Research Laboratory AMSRL-EP-EH Fort Belvoir, VA 22060-5838 (703) 704-2039</p>	<p>05/21/94 sent 01/10/95 resent</p>
<p>Robert Decaro Irvine Sensors Corporation 3001 Redhill Avenue, Building III Costa Mesa, CA 92626 (714) 549-8211</p>	<p>05/21/94 sent 01/10/95 resent</p>
<p>Dennis F. Dillon EMCORE Corporation 35 Elizabeth Avenue Somerset, NJ 08873 (908) 271-9686</p>	<p>Response received 7/22/94 (from Mr. Gary S. Tompa) They have not conducted reliability assessment on these components. He has provided names of other companies.</p>
<p>Alan Doctor Servo Corporation of America 111 New South Road Hicksville, NY 11802-1490 (516) 938-9700x328</p>	<p>05/21/94 sent 01/10/95 resent</p>
<p>Jim Douglass XL Vision 10300 102nd Terrace Sebastian, FL 32958</p>	<p>05/21/94 sent 01/10/95 resent</p>

<p>George Eardian M/A-COM Semiconductor Products, Inc. Bldg.1, South Avenue Burlington, MA 01803</p>	<p>Undeliverable as addressed Returned 02/06/95</p>
<p>W.S. Ewing Rome Air Development Center Hanscom AFB, MA 01731-5000</p>	<p>Response received 04/03/95 (from Mr. Freeman D. Shepherd) Do not recommend use of IrSi in Infrared Sensor. For PtSi, no failure has ever been observed. Many devices have been destroyed by overvoltage and other abuse. Also saw no significant parameter drift over camera lifetime up to 5 years.</p>
<p>James Fawcett Westinghouse Electric Corporation E-O Systems Department Baltimore, MD 21203</p>	<p>05/21/94 sent 01/10/95 resent</p>
<p>Glenn S. Fields GE Corporate R&amp;D P.O. Box 8 (KW-C258) Schenectady, NY 12301 (518) 387-6570</p>	<p>05/21/94 sent 01/10/95 resent</p>
<p>Paul Fileger Teledyne Brown Engineering 300 Sparkman Drive, N.W. P.O. Box 070007, MS 200 Huntsville, AL 35807-7007 (205) 726-2425</p>	<p>Response received 8/2/94 (from Mr. Bruce Peters) They have not conducted reliability assessment on any of these components and they are unaware of any failure mechanisms under long-term storage</p>
<p>J.J. Forsthoefel Cincinnati Electronics Corp. Detector and Microcircuit Laboratory 7500 Innovation Way Mason, OH 45040-9699</p>	<p>05/21/94 sent 01/10/95 resent</p>
<p>Dean Frew Texas Instruments Technology Programs 1745 Jefferson Davis Highway Suite 605 Arlington, VA 22202 (703) 413-3033</p>	<p>05/21/94 sent 01/10/95 resent</p>



<p>Jim Gates  FLIR Systems, Inc.  16505 SW 72nd Avenue  Portland, OR 97224  (503) 684-3731</p>	<p>05/21/94 sent  02/06/95 resent</p>
<p>Michael V. Geraci  Antenna and Radome Research Associates  15-T Harold Court  Bay Shore, NY 11706  (516) 231-8400</p>	<p>05/21/94 sent  02/06/95 resent</p>
<p>M.D. Gibbons  Infrared Group, Electronics Laboratory  General Electric Co.  B3-260  Syracuse, NY 13221</p>	<p>05/21/94 sent  02/06/95 resent  04/03/95 returned due to Mr. Gibbons left  04/06/95 resent</p>
<p>Dr. Richard E. Gillespie  Recon/Optical, Inc.  1911 N. Fort Myer Drive  Suite 809  Arlington, VA 22209  (703) 525-2590</p>	<p>05/21/94 sent  02/06/95 resent</p>
<p>Blaise Gomes  National Semiconductor  Semiconductor Drive  Santa Clara, CA 95051  (408) 721-5526</p>	<p>05/21/94 sent  02/06/95 resent</p>
<p>Denys Gontard  Martin Marietta Electronics and Missiles  Group,  Orlando, FL 32855-5837</p>	<p>05/21/94 sent  02/06/95 resent</p>
<p>Merle Gordon  SEMICON Components, Inc.  10 North Ave.  Burlington, MA 01803  (617) 272-9015</p>	<p>They mainly deal with Si Gunn Diodes; canned devices such as DO4, DO5, TO3 rectifiers and transistors; and uni-polar and bipolar voltage suppressors in DO13 packages. Under long-term storage, process contaminants cause degradation of material layers. Carbonic acid (CO<sub>2</sub> + H<sub>2</sub>O) is one such contaminant. Moisture in packages serves to enhance intermolecular reactions over time.</p>

<p>Dr. Richard A. Gudmundsen Perceptrix Inc. 12052 Larchwood Lane Santa Ana, CA 92705 (714) 544-5181</p>	<p>Response received 7/11/94 Solid-state diffusion/chemical reactions are predominant failure mechanisms under long-term storage.</p>
<p>Dr. John T. Hall Huges Aircraft Company 1100 Wilson Blvd., 19th Floor Arlington, VA 22209 (703) 284-4246</p>	<p>05/21/94 sent 02/06/95 resent</p>
<p>Joel Hazlett Opto Mechanik, Inc. XL Vision 10300 102nd Terrace Sebastian, FL 32958 (407) 589-7331</p>	<p>05/21/94 sent 02/06/95 resent</p>
<p>J.M. Hilkert Texas Instruments, Inc. Defense Systems and Electronics Group P.O.Box 660246 Dallas, TX 75266</p>	<p>Response received 04/03/95 (From Mr. Buf Slay) No long term storage data. Failure mechanisms include corrosion, continuity failures, delaminations and assembly related problems.</p>
<p>Steve Hopkins National Semiconductor Corp. 5901 South Calle Santa Cruz Tucson, AZ 85749</p>	<p>05/21/94 sent 02/06/95 resent 04/03/95 returned 04/06/95 resent</p>
<p>Ms. Paula Jevelle OFC Corporation 2 Mercer Road Natick, MA 01760 (508) 655-1650</p>	<p>05/21/94 sent 02/06/95 resent</p>
<p>Mike I. Jones General Dynamics/Fort Worth Division P.O.Box 748 Fort Worth, TX 76101 MZ 2615</p>	<p>05/21/94 sent 03/21/95 resent</p>

<p>T.H. Johnson  Santa Barbara Research Center  75 Coromar Drive  Goleta, CA 93117</p>	<p>05/21/94 sent  03/21/95 resent</p>
<p>R. Barry Johnson  Optical E.T.C., Inc.  3077 Leeman Ferry Road  Huntsville, AL 35801  (205) 880-8207</p>	<p>05/21/94 sent  03/21/95 resent</p>
<p>W. Keith Kahl  Oak Ridge National Laboratory  P.O. Box 2009, MS 8039  Bldg. 9102-2  Oak Ridge, TN 37831-8039  (615) 574-0372</p>	<p>05/21/94 sent  03/21/95 resent</p>
<p>Bill Kincaid  Teledyne Energy Systems  110 West Timonium Road  Timonium, MD 21093  (301) 252-8220</p>	<p>05/21/94 sent  03/21/95 resent  04/19/95 returned</p>
<p>Stuart H. Klapper  Hughes Aircraft Company  MS EO/EO1/B122  P.O. Box 902  El Segundo, CA 90245  (310) 616-9047</p>	<p>05/21/94 sent  03/21/95 resent</p>
<p>P. Klocek  Texas Instruments Inc.  Optical Materials Laboratory  P.O. Box 655012, MS 55  Dallas, TX 75265</p>	<p>05/21/94 sent  03/21/95 resent</p>
<p>Jerry Kneifel  Dale Electronics, Inc.  P.O. Box 609  Columbus, NE 68601  (402) 563-6449</p>	<p>Reponse received 6/30/94  They manufacture passive electronics and  have conducted reliability assessment only  on resistors and inductors</p>

<p>Dr. Robert Kogan Westinghouse Electric Corporation Aerospace Division Box 746 Baltimore, MD 21203</p>	<p>05/21/94 sent 03/21/95 resent</p>
<p>Dale K. Kotter Westinghouse Idaho Nuclear Company P.O. Box 4000 MS 2202 Idaho Falls, ID 83415 (208) 526-1954</p>	<p>05/21/94 sent 03/21/95 resent</p>
<p>Dr. Juan F. Lam Hughes Research Laboratories 3011 Malibu Canyon Road Malibu, CA 90265 (310) 317-5929</p>	<p>05/21/94 sent 03/21/95 resent</p>
<p>Dale Lehmann Cincinnati Electronics Corporation 7500 Innovation Way Mason, OH 45040-9699 (513) 573-6188</p>	<p>05/21/94 sent 03/21/95 resent</p>
<p>Barry Lindenfelser Magnavox Electronic Systems Company 46 Industrial Avenue Mahwah, NJ 07430 (201) 529-1700</p>	<p>05/21/94 sent 03/21/95 resent</p>
<p>Nels (Bud) Magnuson Sandia National Laboratories Division 7222 Albuquerque, NM 87185 (505) 844-4749</p>	<p>Response received 6/31/94. Most failures associated with mechanical problems (packages, wire bonds, foreign particles) and solder interaction with gold plating to form brittle intermetallics leading to separation of components from substrate.</p>
<p>George Beningo Loral 2 Forbes Road Lexington, MA 02173 (617) 863-3670</p>	<p>Response received 08/27/94. All test results for FPA's have shown very limited performance loss (all test articles continue to meet specifications) and no catastrophic failures.</p>

David McCann Westinghouse Electric Company Aerospace Division Box 746 Baltimore, MD 21203	05/21/94 sent 03/21/95 resent 04/06/95 resent
Robert W. McMillan (MMW SENSORS) Georgia Institute of Technology Georgia Tech Research Institute Atlanta, GA 30332	05/21/94 sent 03/21/95 resent 04/06/95 resent 04/19/95 returned
Dr. David B. Medveo MERET, Inc. 1815 24th Street Santa Monica, CA 90404-4988 (213) 828-7496	05/21/94 sent 03/21/95 resent 04/06/95 resent 04/19/95 returned, moved not forwardable
James Miller Aerodyne Controls Corp. 30 Haynes Court Ronkonkoma, NY 11729 (516) 737-1900	05/21/94 sent 03/21/95 resent 04/06/95 resent
A.F. Milton Naval Research Laboratory Washington, D.C. 20375	05/21/94 sent 03/21/95 resent 04/06/95 resent
G.H. Olsen EPITAXX, Inc. 3490 U.S. Route 1 Princeton, NJ 08540	05/21/94 sent 03/21/95 resent 04/06/95 resent 04/19/95 returned
William J. Parrish Amber Engineering, Inc. 5756 Thornwood Dr. Goleta, CA 93117-3802	05/21/94 sent 03/21/95 resent 04/06/95 resent
Fred Perry Boston Electronics Corp. 72-T Kent Street Boston, MA 01730 (617) 566-3821	05/21/94 sent 03/21/95 resent 04/06/95 resent

<p>D.H. Pommerrenig  Electro-optic Systems Department  SI&amp;SSD, Rockwell International  Corporation  Mail Code SJ70,  12214 Lakewood Blvd.  Downey, CA 90241</p>	<p>05/21/94 sent  03/21/95 resent  04/06/95 resent</p>
<p>Thomas E. Potter  Texas Instruments, Inc.  34 Forest St., M.S. 12-33  Attleboro, MA 02730  (508) 699-1769</p>	<p>05/21/94 sent  03/21/95 resent  04/06/95 resent</p>
<p>Don Prillaman  ITT Electro-Optical Products  7635 Plantation Road  Roanoke, VA 24019</p>	<p>Response received 6/27/94  They do not manufacture or use any of  these components</p>
<p>J.P. Rode  Rockwell International Science Center  1049 Camino Dos Rios  Thousand Oaks, CA 91360</p>	<p>05/21/94 sent  03/21/95 resent  04/06/95 resent</p>
<p>Larry Rystrom  Boeing Electronics  P.O. Box 24969, M/S 9J-07  Seattle, WA 98124</p>	<p>05/21/94 sent  03/21/95 resent  04/06/95 resent  04/19/95 returned</p>
<p>Nathan Sclar  Electro-optics Department  Rockwell International Science Center  3370 Miraloma Avenue  Anaheim, CA 92803</p>	<p>05/21/94 sent  03/21/95 resent  04/06/95 resent</p>
<p>John L. Snyder  Electrooptics and Infrared Consultant  501 Glen Canyon  Garland, TX 75040</p>	<p>05/21/94 sent  03/21/95 resent  04/06/95 resent</p>
<p>Paul P. Suni  Loral Fairchild Imaging Sensors  1801 McCarthy Blvd.  Milpitas, CA 95035  (408) 433-2417</p>	<p>05/21/94 sent  03/21/95 resent  04/06/95 resent</p>

Tom Venable  
Cincinnati Electronics Corp.  
7500 Innovation Way  
Mason, OH 45040-9699  
(513) 573-6330  
(513) 573-6290 - FAX

Thomas S. Wein  
Raytheon Company  
Missile Systems Division  
Hartwell Road  
Bedford, MA 01730  
(508) 671-9144

Don Winton  
Infrared Industries, Inc.  
12151-T Research Parkway  
Orlando, FL 32826  
(407) 282-7700

David Willits  
Alliant Techsystems  
M/S MN11-2961  
600 2nd St. N.E.  
Hopkins, MN 55343

Telephonic conversation in June 1994.  
The helium in cooling dewars has a life of  
1 year or 2000 hours. Some flash  
memories (EPROMs) in IR devices might  
have to be reprogrammed after long-term  
storage

Response received 6/27/94.  
They have conducted reliability assessment  
on some of the components, but cannot  
provide results without compensation.

Response received 03/26/95.  
When stored in 0°C - 40°C  
nitrogen/atmosphere sealed reliability  
exceed 11yrs. In standard atmosphere -  
60%RH PbS/PbSe will deteriorate in 6mos  
to 2yrs. Failure is due to condensed water  
contamination - mineral deposits from  
water vapor.

Response received 04/19/95.  
The company used to do a fair amount of  
the test, but in recent years it has relied on  
outside sources for data.

**APPENDIX B**  
**CADMP-IIe MODELS AND ATTRIBUTES**



Symbol	Description (units)	Location	Model/Type & Value
<b>Shattering of Windows</b>			
Rupture_wind	Modulus of rupture for window material (psi)	Material Library	Mechanism: Shattering of Windows CADMP-IIe Name: Window_Shatter Model Type: Overstress Units: °C  $\frac{\text{Rupture\_wind} * .8}{\text{Young\_wind} * \text{Alpha\_wind}} - \Delta T$
Young_wind	Young's modulus of window material (psi)	Material Library	
Alpha_wind	Coefficient of thermal expansion for window (°C)	Material Library	
ΔT	Environmental temperature range (°C)	Environment or Test/Screen Library	
<b>REFERENCES:</b> Palmer, J.R., "Hostile High Energy Visible Laser Environment Providing Destruction of Optical Signal in Imaging Systems," Proc of SPIE, Vol. 867, 1987.			

Symbol	Description (units)	Location	Model/Type & Value
<b>Dewar Heat Leakage</b>			
W_cryogen	Weight of cryogenic material (lb)	Package Designer: Case	Mechanism: Heat Leakage from Dewar Packages CADMP-IIe Name: Dewar_Miss_Time Model Type: Wearout Units: hours to failure  $\left[ \frac{W\_cryogen * DM\_cryogen^2}{36 \pi} \right]^{1/3} * 1.714 * 10^{-9} * .9 [TH\_dewar^4 - TH\_cryogen^4]$
DM_cryogen	Density of cryogenic material (lb/ft <sub>3</sub> )	Material Library	
HC_cryogen	Latent heat of cryogenic material (Btu/lb)	Material Library	
TH_dewar	Temperature of dewar (K)	Package Designer: Case	
TH_cryogen	Temperature of cryogen (K)	Package Designer: Case	
<i>notes:</i> 1.714 x 10 <sup>-9</sup> is Boltzmann's constant (Btuh <sup>-1</sup> ft <sup>-2</sup> °R <sup>-4</sup> ) .9 is the effective emissivity, taken as a constant			
<b>REFERENCES:</b> Breckenridge, R., "A Solid Cryogen Cooler for an X-Ray Spectrometer," presented at the NASA Cryogenic Workshop, Marshall Space Flight Center, Huntsville, AL, March 29-30, 1973.			

Symbol	Description (units)	Location	Model/Type & Value
<b>Dewar Outgassing</b>			
PR_dewar	Pressure the dewar is required to maintain (torr)	Package Designer: Case	Mechanism: Dewar Outgassing (Leakage) CADMP-IIe Name: Dewar_outgas Model Type: Wearout Units: Hours to failure
V_dewar	Dewar volume (liters)	Package Designer: Case	$\frac{PR\_dewar}{V\_dewar * Leak\_case * 3600}$
Leak_case	Leak rate of the dewar package (torr·liters/sec)	Package Designer: Case	
<b>REFERENCES:</b> Vincent, J.D., "Fundamentals of Infrared Detector Operation and Testing," John Wiley & Sons, New Yorkm 1990.			

Symbol	Description (units)	Location	Model/Type & Value
<b>Fatigue Failure of Indium Bumps</b>			
Cfd_sol_flp	Fatigue ductility coefficient of the solder (dimensionless)	Material Library	Mechanism: Fatigue in Flip-Chip Indium Bumps in Hybrid Detectors CADMP-IIe Name: Hybrid_Flip_Chip_Model Model Type: Wearout Units: hours to failure
Tavg	Average environmental temperature (°C)	Environment Library	
ΔT	Change in environmental temperature (°C)	Environment Library	$\frac{1}{2} \left( \frac{HYBRID\_DELTA\_GAMMA}{2 Cfd\_sol\_flp} \right)^{COFFIN\_MANSON\_EXP\_sto}$
DI_die_flp	Distance of bumps from neutral axis (mils)	Package Designer: Case	
α_die_flp	Coefficient of thermal expansion of die (°C)	Material Library	$COFFIN\_MANSON\_EXP\_sto = -.442 - .0006(Tavg) + .0174 * \ln \left( 1 + \frac{360}{TI\_d} \right)$
α_hybrid	Coefficient of thermal expansion of hybrid (°C)	Material Library	

Symbol	Description (units)	Location	Model/Type & Value
SJH_die_flp	Height of solder joint (mils)	Package Designer: Case	$HYBRID\_DELTA\_GAMMA = \frac{DI\_die\_flp - \alpha\_hybrid) \Delta T}{SJH\_die\_flp}$
TI_d	Half cycle dwell time (hours)	Environment Library	
			<b>REFERENCES:</b> Engelmaier, W., "Functional Cycling and Surface Mounting Attachment Reliability," ISHM Technical Monograph Series 6984-002 Oct 1984, pp 87-114.

Symbol	Description (units)	Location	Model/Type & Value
<b>Stress Corrosion Cracking of Windows</b>			
Fractough_lidwind	Fracture toughness of window material (psi · in <sup>1/2</sup> )	Material Library	Mechanism: Window Cracking CADMP-IIe Name: Stress_Corr_Crack_Windows Model Type: Overstress Units: psi in <sup>1/2</sup>
Poisson_lidwind	Poisson ratio of window material	Material Library	$\text{Fractough\_lidwind} - \frac{3(3 + \text{Poisson\_lidwind})\text{Press\_lidwind} * \text{Radius\_lidwind}}{8 * \text{Thick\_lidwind}}$
Press_lidwind	Static pressure load on window (psi)	Package Designer: Lid	$(\pi * \text{Flaw\_lidwind})^{1/2}$
Radius_lidwind	Radius of window (mils)	Package Designer: Lid	
Thick_lidwind	Thickness of window (mils)	Package Designer: Lid	
Flaw_lidwind	Depth of largest flaw from top surface of window (mils)	Package Designer: Lid	
<b>REFERENCES:</b> Pruszynski, C.J., "Overpressure Proof Testing of Large Infrared Windows for Aircraft Application," tactical Infrared Systems, Proc of SPIE, Vol. 1498, May 1991.			

## DISTRIBUTION LIST

Commander  
Armament Research, Development and Engineering Center  
U.S. Army Tank-automotive and Armaments Command  
ATTN: AMSTA-AR-IMC (3)  
AMSTA-AR-GCL  
Picatinny Arsenal, NJ 07806-5000

Defense Technical Information Center (DTIC)  
ATTN: Accessions Division (12)  
8725 John J. Kingman Road, Ste 0944  
Fort Belvoir, VA 22060-6218

Director  
U.S. Army Materiel Systems Analysis Activity  
ATTN: AMXSY-MP  
Aberdeen Proving Ground, MD 21005-5066

Commander  
Chemical/Biological Defense Agency  
U.S. Army Armament, Munitions and Chemical Command  
ATTN: AMSCB-CII, Library  
Aberdeen Proving Ground, MD 21010-5423

Director  
U.S. Army Edgewood Research, Development and Engineering Center  
ATTN: SCBRD-RTB (Aerodynamics Technology Team)  
Aberdeen Proving Ground, MD 21010-5423

Director  
U.S. Army Research Laboratory  
ATTN: AMSRL-OP-CI-B, Technical Library  
Aberdeen Proving Ground, MD 21005-5066

Chief  
Benet Weapons Laboratory, CCAC  
Armament Research, Development and Engineering Center  
U.S. Army Armament, Munitions and Chemical Command  
ATTN: SMCAR-CCB-TL  
Watervliet, NY 12189-5000

Director  
U.S. Army TRADOC Analysis Command-WSMR  
ATTN: ATRC-WSS-R  
White Sands Missile Range, NM 88002

COMMANDER  
ARMAMENT RESEARCH, DEVELOPMENT AND ENGINEERING CENTER  
U.S. ARMY TANK-AUTOMOTIVE AND ARMAMENTS COMMAND  
ATTN: AMSTA-AR-IMC (3)  
AMSTA-AR-GCL  
AMSTA-AR-FSP-E (6)  
PICATINNY ARSENAL, NJ 07806-5000